SYNTHESIS AND STUDIES ON BRANCHED AND 2',5'-LINKED OLIGONUCLEOTIDES.

by

André Hameed Uddin

A thesis submitted to the Faculty of Graduate Studies
and Research of McGill University in partial fulfilment of the requirements
for the Degree of Doctor of Philosophy

Department of Chemistry
McGill University
May 1996

ISBN 0-612-19779-4

Dedication

To my fiancée Gina Catena, and my parents: Inge Ahsan-Uddin and the late Syed Khaja Ahsan-Uddin.

As Shakespeare wrote,
"*I cannot but remember such things were, that were more precious to me.*"

Abstract

The first example of a stable triple-stranded helix consisting of exclusively T•AT (reverse-Hoogsteen•Watson/Crick) base triplets is reported. This approach to induce and stabilize the anti-parallel triplex involves the use of a branched oligonucleotide with two parallel dT_{10} strands joined to riboadenosine via 2'-5' and 3'-5' phosphodiester linkages, *i.e.*, $rA^{[2'\text{-}5'\text{-}dT10]}{}_{[3'\text{-}5'\text{-}dT10]}$ (**2.1**). Triple helix formation by branched oligonucleotide **2.1** and dA_{10} was investigated by thermal denaturation analysis, circular dichroism spectroscopy, PAGE retardation assays and fluorescent studies. A linear oligonucleotide with a loop made of four dC residues between two dT_{10} strands, and with a 5'-5'-phosphodiester linkage at one of the C/T_{10} junctions, i.e., 3'-$dT_{10}C_4$-5'-5'-dT_{10}-3' did not form a similar triple helical structure. This result shows that the conformational rigidity imparted to the pyrimidine strands, by the branch point in **2.1**, serves to pre-organize and stabilize the complex.

A fibre optic sensor was designed and constructed for the fluorimetric detection of TAT triple-helical DNA hybridization. Fluorescent studies were then conducted and showed unequivocal hybridization of support bound oligomer with complementary oligonucleotides from the solution phase, as inferred by ethidium bromide staining.

A thymidine nucleoside containing a flexible linker at the N^3 position served as a replacement for nucleotide loops in triplex forming DNA. Moreover, a new solid-phase methodology for constructing "Y" branched nucleic acids having a flexible linker was developed. This branched oligonucleotide contains two binding domains, one involving Watson-Crick base pairing, and the other involving triplex formation via Hoogsteen base pairing.

The synthesis of a 2',5'-linked antisense oligoribonucleotide (RNA) containing the four natural bases (Ad, Gu, Cy, Ur) and that is complementary to HIV-1 genomic RNA is reported for the first time. This oligomer exhibited remarkable hybridization properties,

binding more strongly to 3',5'-linked RNA than single stranded 3',5'-linked DNA. This oligomer was capable of inhibiting reverse transcription *in vitro* and HIV-1 replication in cell cultures. N^6-Benzoyl-5'-O-dimethoxyltrityl-3'-O-methyl-2'-O-N,N'-diisopropyl(β-cyanoethyl)adenosine phosphoramidite was prepared via methylation of the 2'-O-silylated monomer and subsequently incorporation into an oligodeoxynucleotide to afford the first oligomer containing a 3'-O-methyl nucleoside. Finally, a 2',5'-linked oligoribonucleotide built from unnatural L-adenosine was synthesized and was found to hybridize better to poly (rU) and (dT) than either of the corresponding 2',5' and 3',5'-linked oligomers built from D-adenosine.

Resume

Le premier exemple d'une triple hélice stable constituée à partir des triplets T•AT (pairage Hoogsteen•Watson/Crick) est présenté. L'approche utilisée afin d'induire et de stabiliser la triple hélice anti-parallèlle implique l'utilisation d'un oligonucléotide branché avec deux brins parallèlles dT_{10} qui sont joints à la riboadénosine *via* une liaison phosphodiester 2'-5' et 3'-5' ,i.e., $rA^{[2'\text{-}5'\text{-}dT10]}{}_{[3'\text{-}5'\text{-}dT10]}$ (**2.1**). La formation de la triple hélice par l'oligonucléotide branché **2.1** et dA_{10} a été étudiée par dissociation thermique, spectroscopie dichroisme circulaire, électrophorèse et étude de fluorescence. Un oligonucléotide linéaire avec une portion faite de quatre résidus dC entre deux brins dT_{10} et avec une liaison phosphodiester 5'-5'à une liaison C/T, i.e., 3'-$dT_{10}C_4$-5'-5'-dT_{10}-3', n'a pas formé une triple hélice similaire. Ce résultat indique que la rigidité conformationnelle inférée par le point de branchement de **2.1** sur les brins pyrimidines permet une pré-organisation et stabilise le complexe.

Un senseur basé sur une fibre optique a été construit afin de détecter par fluorométrie la formation d'une triple hélice d'ADN. Des études de fluorescence ont ensuite été réalisées et ont montrées de façon non équivoque par un marquage au bromhydrate d'éthidium l'hybridation de l'oligomère lié au support avec un oligonuclétide complémentaire en solution.

Un nucléoside thymidine renfermant une lien flexible à la position N^3 a servi pour former une triple hélice. De plus, une nouvelle méthodologie pour la synthèse en phase solide d'acide nucléique branché "Y" incorporant une liaison flexible a été dévelloppé. Cet oligonucléotide branché contient deux domaines, un premier pouvant former un pairage de type Watson-Crick et un autre impliquant la formation de la triple hélice via un pairage Hoogsteen.

La synthèse d'oligonucléotides antisens liés de façon 2'-5' et contenant les quatres bases naturelles (Ad, Gu, Cy,Ur) a été réalisée pour la première fois. L'oligomère synthétisé présentedes propriétés remarkable car il se lie plus fortement à un ARN 3'-5' qu'à un ADN 3'-5'. L'oligomère complémentaire à l'ARN génomique du virus VIH-1 a démontré la possibilité d'inhiber l'enzyme "transcriptase inverse" *in vitro* et la réplication du VIH-1 dans des cultures de cellules. Le phosphoramidite N^6-benzoyl-5'-O-diméthoxytrityl-3'-O-méthyl-2'-O-(N,N'-diisopropyl(ß-cyanoéthyl))adénosine a été préparé via la méthylation du monomère sylilé en 2' et son insertion subséquente dans un oligonuclétide a donné le premier oligomère contenant un nucléoside méthylé au 3'-O. Finalement, un oligoribonucléotide construit à partir du nucléotide non naturel L-adénosine a été synthétisé. Il a été démontré que cet oligomère s'appariait, comparativement aux oligomères correspondants 3'-5' et 2'-5' synthétisés à partir de la D-adénosine, plus fortement avec poly(rU) et poly(dT).

Acknowledgements

Dr. Masad Damha for his support, enthusiasm, guidance and encouragment. I especially appreciated the motivation Dr. Damha provided during the course of my studies. I would also like to express my thanks to Dr. Damha for his inspiration and cooperation throughout my work at McGill University. I would particularly like to commend Dr. Damha for the insight he provided with regard to the writing of my thesis. Also for all of the interesting nucleic acid discussions we had during our luncheons at Basha.

I would like to thank Dr. Sandeep Raha and Dr. Robert H.E. Hudson for helping me making a wise decision to work for Dr. Damha. Dr. Hudson deserves special gratitude and commendation for his exceptional guidance and general assistance with my studies. I would also like to thank Dr. Hudson for his friendship, for the invitation to visit "Rob's resort" in Pasadena, and for all of the insight he provided, particularly with regard to "column chromatography."

I would like to thank Dr. Ulrich Krull for giving me the opportunity to work in his laboratory at the University of Toronto, for the Toronto to Montreal travel allowance, and for the excellent Judo lessons. It was a priviledge to collaborate on the triple helix assay with two high calibre scientists: Paul A. Piunno and Dr. Krull. Kind thanks to Paul Piunno for providing Figure 2.15 and 2.13, as well as the digitization of the gels. A special thanks to Rob Hudson, Paul Piunno and M.K. for making work so enjoyable in the lab. Also - Vive le Ontario-Quebec Exchange Travel Allowance!

Dr. R. Bruce Lennox and Louis Cuccia for their insightful biotechnology discussions. A special thanks to Louis for help with several experiments, and for criticially proofreading of the biotechnology articles.

Dr. Michael Parniak, Gadi Borkow, and Dominique Arion of the McGill AIDS Centre for the H.I.V. reverse transciptase assays.

Dr. Richard T. Pon (U. of Calgary) for providing certain oligodeoxynucleotide sequences.

Dr. Joanne Turnbull (Concordia University) for assistance with the CD experiments.

Dr. François Sauriol for teaching me n.m.r.

Dr. Orval Mamer and Dr. Daniel Boismenu for running the electron spray mass and Dr. Hamed for FAB mass spec.

Dr. Claude Hélène (Muséum National d'Histoire Naturelle) for his gift of the triplex specific ligand BePI.

Dr. Anna Garbesi (IcoCEA-CNR) for a sample of L-adenosine.

Sebastien Robidoux for translation of the abstract, as well as the exceptional hospitality of both him and his wife Linda. As well as my colleagues in lab 207 for their helpful discussions and proofreading of this thesis: Anne Noronha, Christopher Wilds, and Sebastien.

René Lévesque and Ewa Morawska for their introduction to the exciting world of business. I am particularly indebted to René for his business tutorials, and helping me advance my future career as a biotechnology analyst.

I would like to acknowledge Sensei Takashi Kimeda for teaching me the importance of focusing my mind and perserverance.

Both my late father and the late Dr. Roop Lal Chaudhary for their words of wisdom which I shall remember.

I would like to thank Ms. Gina Catena for her patience, everlasting love and support throughout the course of my studies.

Table of Contents

Abbreviations and Symbols

A	adenosine
A_{260}	UV absorbance measured at 260 nm
Ad	adenine
AIDS	acquired immunodeficiency syndrome
AON	antisense oligonucleotide(s)
APS	ammonium persulphate
b	broad
bDNA	branched DNA
BIS	N,N'-methylene-bis(acrylamide)
bNA	branched nucleic acid
BPB	bromophenol blue
Bz	benzoyl
C	cytidine
CE	capillary electrophoresis
CEO-	2-cyanoethoxy (or β-cyanoethyl)
COSY	correlated spectroscopy
Cy	cytosine
D	deuterium
d	doublet (n.m.r.)
DCE	1,2-dichloroethane
DCM	dichloromethane
dd	doublet of doublets (n.m.r.)
DIPEA	diisopropylethylamine
4-DMAP	4-dimethylaminopyridine
DMF	N,N-dimethylformamide
DMT	dimethoxytrityl
dN	2'-deoxynucleotides
DNA	2'-deoxyribonucleic acid

EDTA	disodium ethylenediaminetetraacetate dihydrate
EtOH	ethanol
eq	equivalents
FAB-MAS	fast atom bombardment mass spectrometry
G	guanosine
GOPS	3-glycidopropyltrimethylsilane
Gu	guanine
%H	percent hyperchromicity
HIV	human immunodeficiency virus
HOAc	glacial acetic acid
HMQC	heteronuclear multiple quantum coherence spectra
HPLC	high performance liquid chromotography
Hz	Hertz
i-	iso
J	coupling constant
λ	wavelength
LCAA-CPG	long-chain alkylamine controlled pore glass
LvOH	levulinic acid
M	molar
m	multiplet (n.m.r.)
max	maximum
m/c	mass to charge ratio
MeOH	methanol
Me	methyl
min	minute
mL	millilitre
mM	millimolar
μM	micromolar
mol	mole

nm	nanometer
NMR	nuclear magnetic resonance
nt	nucleotides
OD	optical density
OPC	oligonucleotide purification cartridge
PAC	phenoxyacetyl
PAGE	polyacrylamide gel eiectrophoresis
PEG	pentaethylene glycol
PBS	primer binding site of HIV genome
ppm	parts per million
Pu	purine
Py	pyrimidine
py	pyridine
R	repeat region of the HIV genome
®	registered trademark
R_f	retardation factor (TLC mobility)
RNA	ribonucleic acid
RNase	ribonuclease
RT	reverse transcriptase
rt	room temperature
s	singlet
sec	second
SEM	2-trimethylsilylethoxymethyl
SVPDE	snake venom phosphodiesterase
t-	tertiary
T	thymidine
T*AT	parallel (or Hoogsteen) TAT triple-helix
T•AT	antiparallel (or reverse Hoogsteen) TAT triple-helix
TBAF	tetra-*n*-butylammonium fluoride
tBDMS	*t*-butyldimethylsilyl

TBE	TRIS/boric acid/EDTA buffer
TCA	trichloroacetic acid
TEMED	N,N,N'N'-tetramethylethylenediamine
TMS	trimethylsilyl
Th	thymine
THF	tetrahydrofuran
TLC	thin layer chromotography
T_m	thermal melt transition temperature (melting temperature)
t	triplet (n.m.r.)
Tris	2-amino-2-(hydroxymethyl)-1,3-propanediol
U	uridine
Ur	uracil
UV-vis	ultraviolet-visible
v/v	volume by volume
w/v	weight by volume
XC	xylene cyanol

Chapter 1 Introduction.

1.1 Importance of Nucleic Acids.

"*Nothing of what is nobly done can ever be lost*", only after dwelling upon this Charles Dickens' quotation can one truly appreciate how remarkable it was when Watson and Crick elucidated the double helical structure of DNA.[1] This incredible discovery made more than forty years ago led to the central dogma of molecular biology, whereby genetic information flows from DNA to RNA to proteins.[2] With ensuing findings concerning the nature and capabilities of nucleic acids, the amount of research directed at understanding and manipulating them has grown exponentially. Most of the progress made in the field of nucleic acids should be directly attributed to the advances made in chemical synthesis of both RNA and DNA.

1.2 Structural Aspects of DNA and RNA.

Before discussion of DNA and RNA synthesis, it is vital to examine the structure of DNA and RNA. DNA and RNA are polymers made up with a large number of deoxyribonucleotides or ribonucleotides units, respectively, each composed of a pentose sugar, a nitrogen heterocyclic base and a phosphate moiety (Figure 1.1). The bases found typically in nature are bicyclic purines (adenine **1.3** or guanine **1.4**) or monocyclic pyrimidines (uracil **1.5**, cytosine **1.6**, and thymidine **1.7**). The five purine and pyrimidine bases found in nucleic acids are shown in Figure 1.1. Nucleosides consist of a purine or pyrimidine base bound to the C-1' position of the sugar ring by a β-N-glycosidic linkage. The purines are linked by the N-9 position to form adenosine and guanosine, and the pyrimidines are linked by the N-1 position to form cytidine, thymidine and uridine. Molecules of DNA consist of two polynucleotide strands held together by Watson-Crick hydrogen bonds between adenine and thymine, as well as between cytosine and guanine. These strands typically form right-handed double-helices, oriented with an antiparallel directionality.

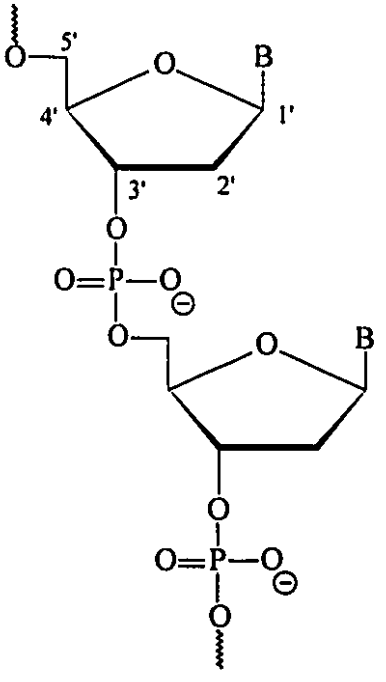

1.1, DNA

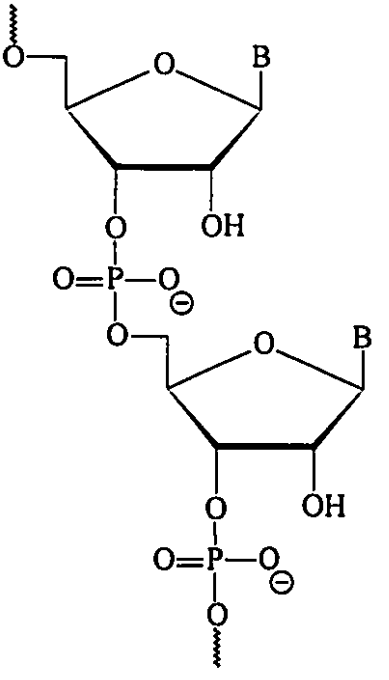

1.2, RNA

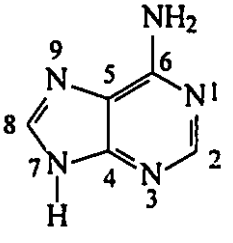

1.3, Adenine

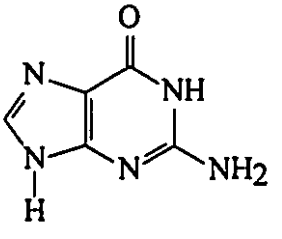

1.4, Guanine

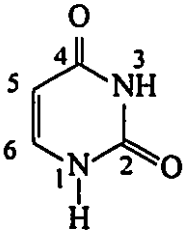

1.5, Uracil

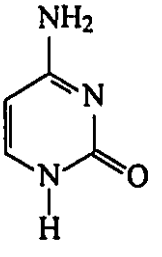

1.6, Cytosine

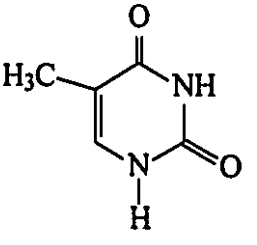

1.7, Thymine

Figure 1.1. The primary structure of DNA, RNA and their heterocyclic bases.

It is the dynamic equilibrium that exists between the two conformations of the furanose sugar which ultimately dictates which conformation the oligonucleotide will adopt. As illustrated in Figure 1.2, the furanose rings are puckered in order to minimize non-bonding interactions between their substituents. The pentose ring preferentially adopts two envelope conformations a C2' endo (^{2}E, or S pucker) and C3'-endo (^{3}E, N pucker). This twisting out of the plane for the 2' and 3' carbons is relative to the plane of the C1'-O4'-C4'. For example, an S puckering occurs when the C2' carbon puckers on the same side as the ring as the C5' and the base. In solution, A-DNA's sugar equilibrium lies toward C-3' endo conformation, whereas B-DNA has primarily C2'-endo sugars. It should be noted that double stranded RNA and RNA-DNA hybrids generally adopt an A-conformation (C3' endo) as a result of the 2'-hydroxyl being sterically unable to fit into the B-conformation. In addition to differences in sugar conformation, there are differences in the types of helices they adopt. For example, A-DNA and B-DNA have 11 and 10.4 base pairs per turn of the helix, respectively, as a result of the A helix being more compressed from dehydration. Also, A-DNA and B-DNA have a 19° and 1° tilt of base pairs from the normal to helix axis, respectively. However, these conformational properties between RNA and DNA are not their only differences.

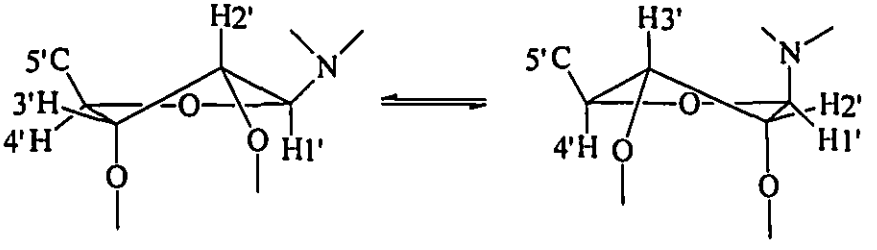

C2' endo (S) C3' endo (N)

Figure 1.2. The C2' and C3'-endo conformations of the furanose ring in dynamic equilibrium.

DNA is essentially the "storage house" for genetic information, whereas RNA translates this coded information to the production of proteins. There are three main differences between RNA and DNA, that being: (i) the sugar units in DNA and RNA are 2'-deoxy-D-ribose and D-ribose, respectively, (ii) DNA has thymine as a base whereas RNA has uracil, and (iii) DNA is typically double stranded and RNA is primarily found as a single stranded species.

Another feature of double helical nucleic acids is the presence of a major and a minor groove. Both grooves, are lined by potential hydrogen-bond acceptor and donor atoms from the bases (Figure 1.3). The major groove of A-DNA is both narrow and very deep, relative, to B-DNA's groove which is wide and quite deep. The minor groove of A-DNA is very broad and shallow compared to B-DNA's groove which is narrow and quite deep. It is the major groove which permits a third strand of DNA or RNA to hydrogen bond to form a triple-helical complex.

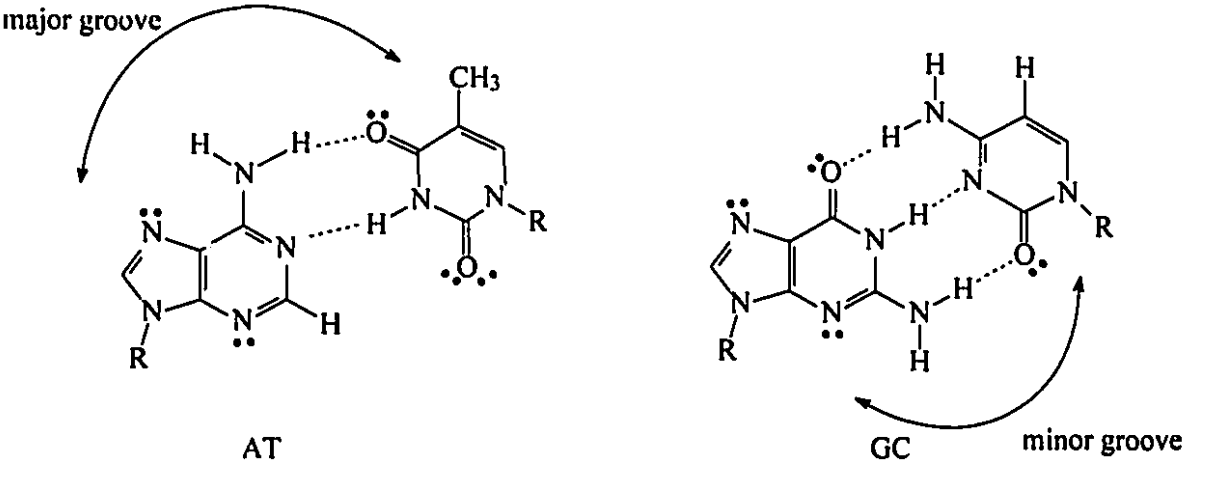

Figure 1.3. Recognition of Double Stranded DNA. This illustration depicts the potential hydrogen bond acceptor and donor atoms of the major and minor grooves of DNA.

1.3 Triple-helical Nucleic Acids.

Triple-stranded helical nucleic acids were first recognized nearly 40 years ago, shortly after the elucidation of the structure of double-stranded DNA[3]. Even so, triplexes remained a structural curiosity until recently, when it was shown that small synthetic oligonucleotides were able to bind to duplex DNA in a sequence-specific manner.[4] The discovery of triplex-containing structures that may exist *in vivo* and may play a role in mediating cellular events has further stimulated interest in triple-helical DNA.[5] With the advent of NMR spectroscopic techniques as well as in-depth thermodynamic and molecular dynamic studies, a much better understanding of the structure and properties of these molecules is being realized.[6] Undoubtedly, a major factor contributing to these developments is the facility with which synthetic oligonucleotides and their analogs are available today.[7] Oligonucleotide-directed triple helix formation offers the possibility of developing therapeutic agents capable of site-specific inhibition of transcription *in vivo*, and remains an active area of research ("antigene" strategy).[8] Another area that has received significant experimental attention is the sequence-specific recognition of single stranded DNA[9] and RNA[10] by triple-helix formation. This more recent and general strategy offers the opportunity to design new diagnostic probes, biochemical tools and potential therapeutic agents that target (viral) messenger RNA ("antisense" strategy).

Several DNA triple helices have been characterized, which fall into two distinct classes depending on the mode of binding of the third strand to duplex DNA.[11] One of the most studied triplexes are those consisting of T*AT and C+*GC triplets,[4a,12] in which the third (T or C+) strand is oriented parallel to the purine strand of the Watson-Crick duplex. In this case, the third strand lies within the DNA major groove and is held in place by Hoogsteen hydrogen bonds[13] to the purine strand. In the alternative motif, the third (purine-rich) strand binds anti-parallel to the purine strand of the duplex through a reverse-Hoogsteen base-pairing scheme.[14] The best characterized triplets within this "anti-parallel" motif are T•AT, G•GC, and A•AT (Figure 1.4).

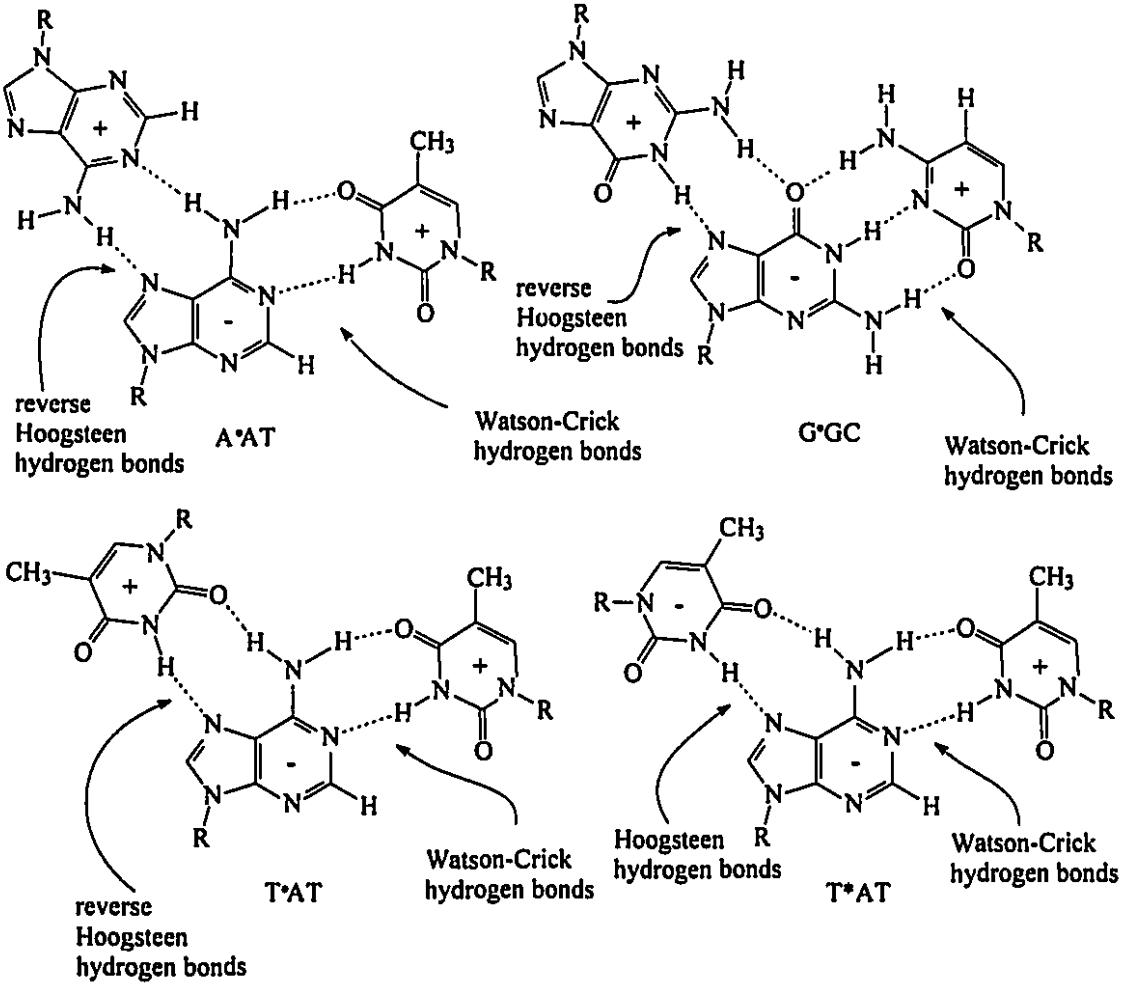

Figure 1.4. The three types of base triplets found in the antiparallel motif (A•AT, G•GC, and T•AT). Configurations for the parallel and antiparallel T-A-T triplex motifs are also shown. The (+) and (-) signs within the bases represent strand polarity. The T*AT triplet on the bottom right represents the more common motif wherein the third strand lies in the major groove parallel to the purine strand. The representation on the bottom left corresponds to the antiparallel motif, whereby the third strand of poly (T) lies antiparallel to the purine strand of the duplex.

Thymidine residues in the third strand (T) can be accommodated in both contexts, either in the "parallel" (T*AT, Hoogsteen) and "anti-parallel" (T•AT, reverse Hoogsteen) motifs (Figure 1.4).

The Damha group has been involved in investigation of the TAT antiparallel and parallel triplexes. *Ab initio* calculations predict that the energies of T*AT (parallel) and T•AT (anti-parallel) base triplets differ by only 0.1 kcal/mol, in favor of the latter.[15] However, in oligonucleotides, additional stereochemical constraints and hydrophobic interactions favor the T*AT (parallel) bonding scheme.[6b,16] For example, dT_{10} binds to duplex dT_{10}/dA_{10} in the parallel (T*AT) scheme rather than the anti-parallel (T•AT) orientation.[17] Furthermore, work originating from the laboratory of Fox and co-workers[18] and others[19] have elegantly demonstrated that antiparallel oriented T•AT triplets can form only when a few of such triplets are interdispersed between G•GC triplets. A stretch of contiguous antiparallel T•AT triplets has been detected recently, however, its formation necessitated adjacent G•GC stretches, magnesium ions, and further stabilization by an acridine ligand.[18b] The location of the acridine intercalator was also critical, exerting its stabilizing effect only when positioned immediately adjacent to the G•GC stretch. In the absence of either the G•GC stretch, magnesium ions, or the acridine ligand, the complexes were not detected. This was explained by the suggestion that the acridine or the stretch of G•GC triplets alone does not provide a nucleation center strong enough to generate a stable T•AT stretch. The requirement of high G•GC content[19a] and divalent cations[20] for the stabilization of anti-parallel (G•GC and T•AT) helices has also been recognized by others. In chapter 2, branched nucleic acids are discussed in terms of their ability to stabilize antiparallel T•AT triplexes.

1.4 Progress made in synthesis of DNA/RNA.

Without the advances made in the synthesis of oligonucleotides, structural and biological studies of nucleic acids would never have met with so much success. One of the major hurdles in the development of chemical synthesis of nucleic acid synthesis was the creation of compatible protecting groups for the hydroxyl groups of the ribose and deoxyribose sugar units, the exocyclic amine functionalities on the bases, and the cyanoethyl group[21] for phosphates. The bases of nucleosides have amino groups that are susceptible to coupling reagents, and must be derivatized to avoid possible side reactions.

The acyl protecting groups for the exocyclic amines: benzoyl[22] (Bz) for adenine and cytosine and the isobutyryl (iBu) for guanine, were chosen since they remain stable under mildly basic or acidic conditions but could be removed in one step upon treatment of concentrated ammonia. Moreover, these protecting groups increase the solubility of nucleosides in organic solvents, thereby facilitating their purification during chromatography.

In order to ensure the formation of a 3',5'nucleotide linkage rather than 5',5' or 3',3' linkages during the condensation of two nucleosides, the 5'-hydroxyl must be selectively protected. The 5' hydroxyl protecting agent typically used is the dimethoxytrityl and monomethoxytrityl group, both introduced to nucleic acid synthesis by Khorana and coworkers.[23] In addition to conferring greater solubility in organic solvents, these protecting groups are acid labile and their removal can be easily monitored by spectrophotometric methods. RNA synthesis is further complicated by the presence of an extra 2'-hydroxyl, which must also be protected in order to avoid the undesired 2',5'-linkages. For the 2' and 3'-hydroxyl moieties, the preferred protecting group is the *t*-butyldimethylsilyl (*t*BDMS) protecting group, popularized by Corey,[24] but developed for RNA synthesis (Figure 1.5) by Ogilvie and coworkers.[25] The tBMDS group is not cleaved under the acidic conditions required for the removal of 5'-trityl groups and is stable to the steps of automated oligonucleotide synthesis. Furthermore, the *t*-butyldimethylsilyl group can be easily removed upon treatment with triethylamine tris(hydrogen fluoride) or tetra-*n*-butylammonium fluoride.

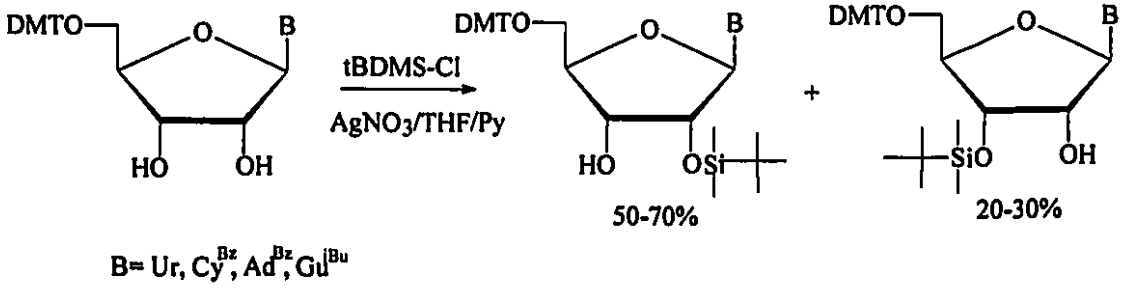

Figure 1.5. Selective 2'silylation of ribonucleosides.

In 1975, Lestinger and coworkers made a tremendous contribution to the chemical synthesis of oligonucleotides through the development of the "phosphite-triester" methodology.[7a] Based upon Letsinger's original work, Caruthers and Beaucage introduced deoxyribonucleoside phosphoramidites for synthesizing oligonucleotides.[26] As illustrated in Figure 1.6, the phosphoramidite approach entailed using a nucleoside 3'-O-N,N-dialkylphosphoramidite in the presence of a weak acid such as tetrazole (pKa 4.9) to couple a protected nucleoside quickly and efficiently. The impact of this method is that these phosphoramidites can be stored for extended periods of time as stable powders, could be isolated easily, and are insensitive to water.

Automated chemical synthesis of nucleic acids was made possible by solid phase methodologies, essentially developed by Letsinger.[27] As illustrated in Figure 1.7, the essence of solid-phase synthesis is the coupling reaction between a nucleotide phosphoramidite and a derivatized nucleoside anchored to a solid support. By using an excess of the nucleoside phosphoramidite derivative, the reaction can be forced to produce high coupling yields. Moreover, the reagents used during each step of the synthesis cycle can easily be washed off from the support-bound oligomer, by avoiding the labour intensive problems of coupling and purification characteristic of solution synthesis. There are essentially four steps in the solid-phase synthesis of oligonucleotides which can be automated: (i) derivatization or attachment of a nucleoside to the support, (ii) assembly of the oligomer in the 3' to 5'-direction (employing conventional 3' phosphoramidites), (iii) deprotection of the protecting groups and concomitant removal of the oligomer from the support and (iv) purification of the oligonucleotide. This highly efficient chemistry, combined with the development of DNA synthesizers ("gene machines") by Ogilvie and co-workers[7c] to assemble genes, has made a major impact on the scientific community. Today, the manufacturing of synthetic oligonucleotides has decreased dramatically from millions of dollars per gram in the late 1970's, to *ca.* $5,000 per gram in 1990, to Hybridon's cost of $300 per gram in 1996.[28] Without all of the

progress made in the chemical synthesis of oligonucleotides, it would have never been possible to have nucleic acid therapeutics undergoing clinical trials.

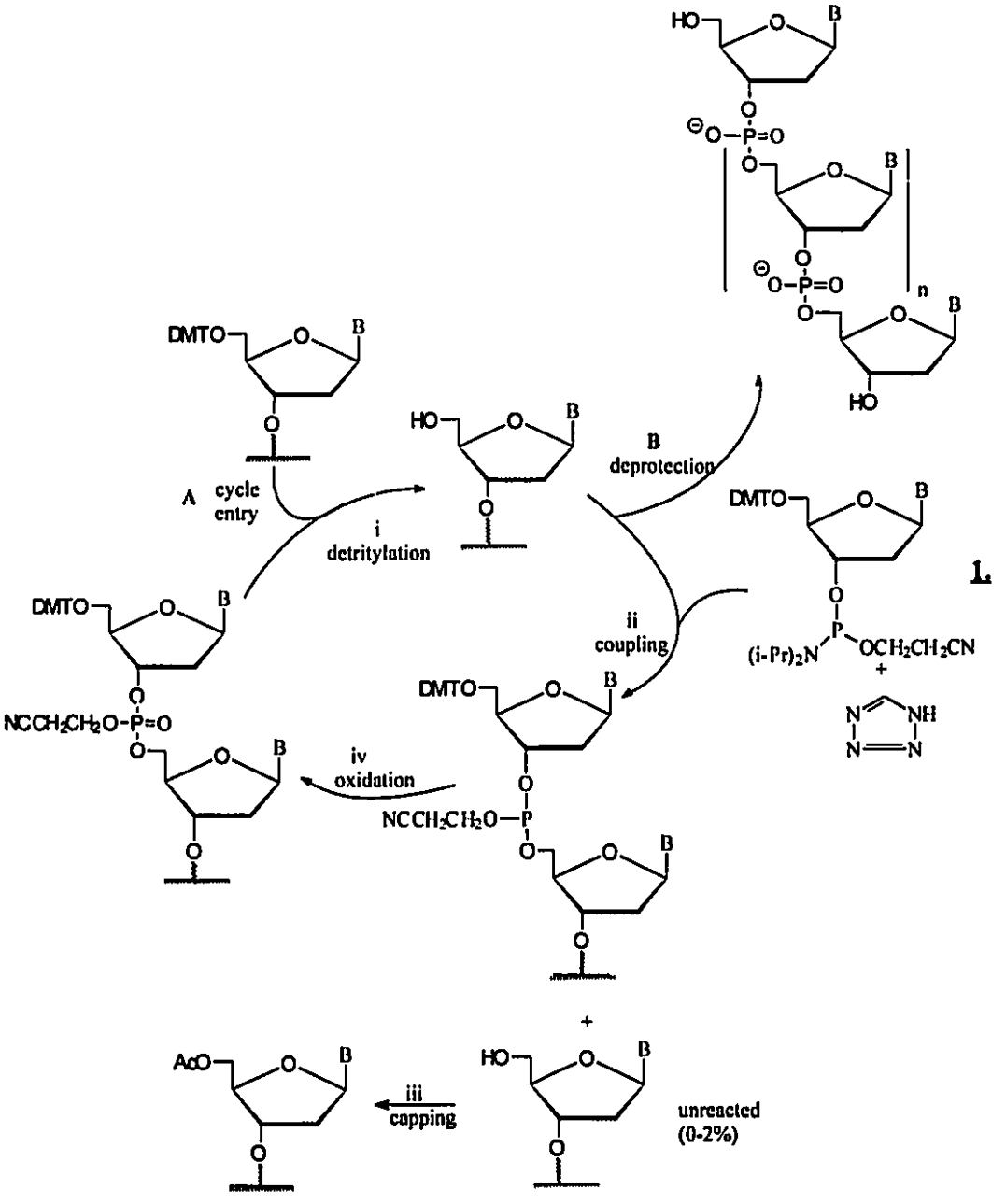

Figure 1.7. Schematic of automated solid-phase synthesis cycle using nucleoside phosphoramidites. (A) Cycle entry with a solid support derivatized nucleoside. (i) Detritylation: trichloroacetic acid in dichloroethane (ii) Coupling: nucleoside-3'-phosphoramidite and tetrazole. (iii) Capping: acetic anhydride, N-methylimidazole and collidine in THF. (iv) Oxidation: iodine, pyridine, and water in THF. (B) Cycle exit: Deprotection: the support bound oligomer is deprotected and cleaved from the support in one step employing concentrated ammonia in ethanol.

1.5 Nucleic Acid Based Therapeutics.

As the famous science fiction author Arthur C. Clarke wrote, *"any sufficiently advanced technology is greater than magic."* When antibiotics were originally discovered they were termed "magic bullets" for their ability to kill bacteria. Today, with the recent surge in biotechnology, the question remains of what will be the next "magic bullet." Conventional drugs typically affect cellular functions by interacting with proteins. Nucleic acids are increasingly being considered as therapeutics, either by interfering with the function of RNA or DNA, or by binding to specific proteins. That is, there has been considerable progress made in recent years in the development of nucleic acid-based drugs (oligonucleotides) such as antisense: compounds which bind to RNA; triplex forming (antigene) compounds: which bind to double stranded DNA; aptmers[29]: compounds which bind specific proteins; and ribozymes[30] (catalytic RNA): which bind to and cleave RNA targets. There has also been a growing interest in other fields using nucleic acids: gene therapy,[31] the human genome project,[32] and genetic manipulation of food. However, due to the large scope of this growing field, only a brief overview of the more relevant antisense and antigene strategies will be discussed.

1.5.1 Antisense Strategy.

A new class therapeutics whose sole purpose is "to seek out and impede" the function of viral (or cancer) messenger RNA has been labeled the "antisense strategy". Antisense oligonucleotides were first shown to inhibit viral replication (Rous Sarcoma Virus) by Zamecnik and Stephenson in 1978.[33] Antisense oligonucleotides consisting of modified DNA/RNA to prevent cellular degradation, are designed to specifically bind to selected messenger RNAs (the "sense" strand) to block translation. By binding to the messenger RNA in a very sequence specific manner, "harmful" proteins can no longer be produced. The power of this strategy is that as long as the genetic sequence is known, an antisense molecule can be designed to target them (Figure 1.7).

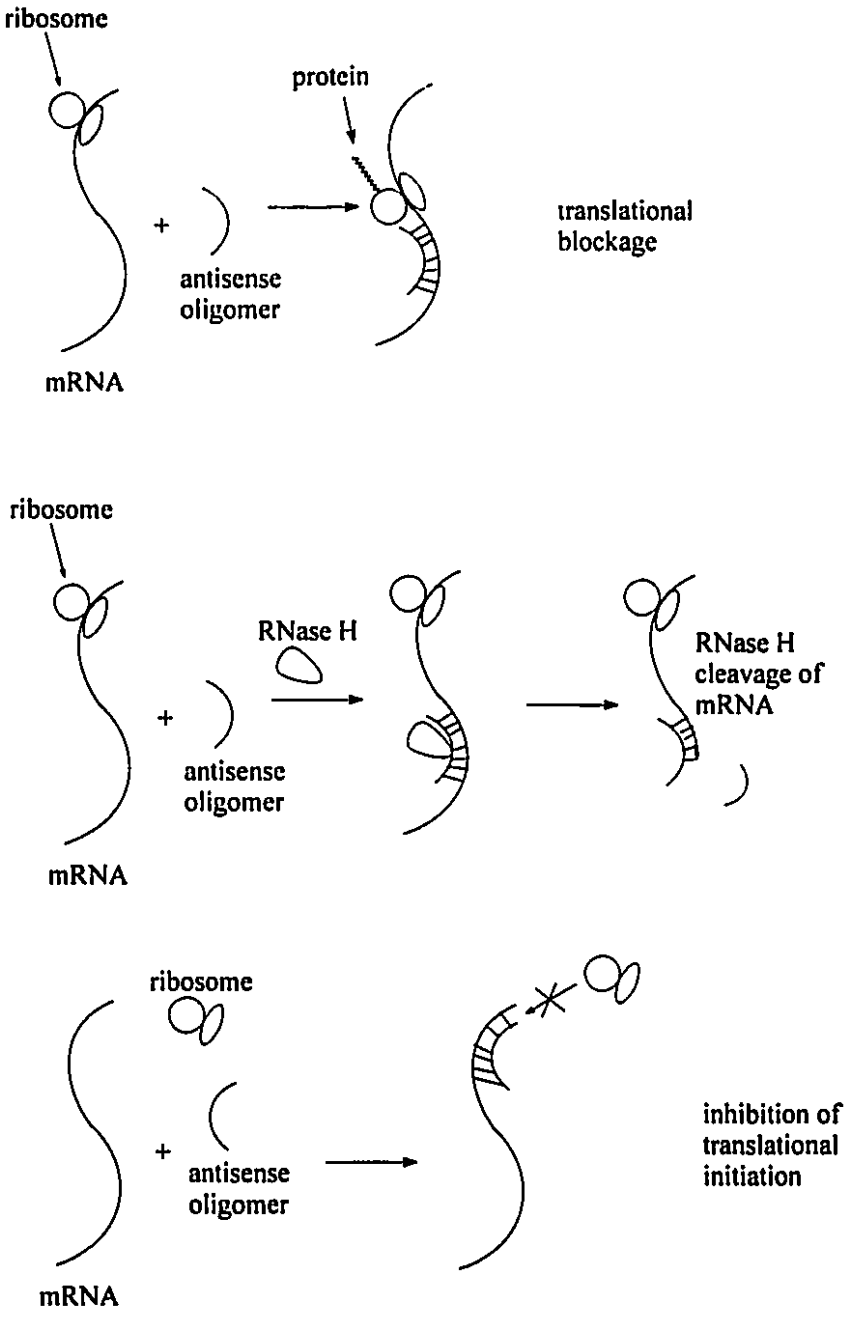

Figure 1.7. The antisense modes of action. Translational blockage prevents the ribosomes from completing the synthesis of the protein encoded by the mRNA. RNase H cleavage activated by antisense oligomer binding, ultimately causes incomplete protein synthesis. Inhibition of ribosome binding results in the prevention of protein synthesis.

Antisense oligomers offer the prospect of safe and effective treatments for a broad range of diseases. However, before an antisense oligonucleotide can be used therapeutically it must satisfy a demanding set of design requirements, including: high efficacy; high

specificity; good stability in the body; effective delivery into the subcellular compartments containing the targeted genetic sequences; and affordable cost.

Some of the problems of using unmodified oligodeoxynucleotides as antisense agents are that they are degraded rapidly in serum and cross the membrane poorly. Therefore, a dominant objective in the design of an effective antisense oligonucleotide is to have a modification which provides resistance to nucleases yet still permits binding to nucleic acids with both a high affinity and specificity. Chemical modifications have been made to the bases, sugar and phosphate moieties. Since the phosphodiester linkage is the major target of degradation by nucleases, one of the main strategies to improve degradation and bioavailability of antisense oligomers has been to chemically modify or replace this moiety. Backbone modifications (Figure 1.8) that have received considerable interest are the phosphorothioates,[34] the methylphosphonates,[35] and the phosphoramidates.[36] Phosphorothioates bind to mRNA complement with a relatively high affinity, have better pharmokinetics, elicit RNase H activity and are nuclease resistant. However, there are certain problems associated with the phosphorothioates such as: non-specific binding to proteins, and an existence of diastereomeric mixtures by virtue of introducing a chiral centre with each phosphorothioate linkage.

Many other hurdles lie in the way of antisense oligonucleotides, such as development of better routes of administration, and an improved understanding of their mode of action. Synthetic oligonucleotides do not always work by "antisense mechanisms" since their polyanionic charge allows these compounds to hybridize to proteins in a non-specific manner.[37] In addition, antisense oligonucleotides tend to accumulate in the liver, kidneys, and bone marrow of animals, and it is yet to be determined what the long term affect will be for this deposition.[38] The clinical trials presently underway for antisense therapeutics should shed some light into this very active area.

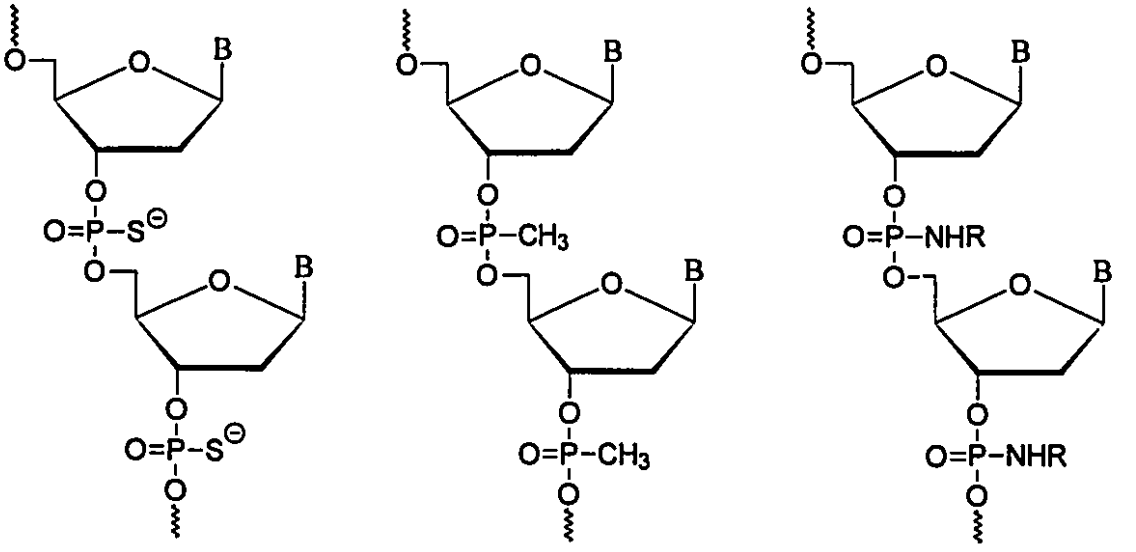

1.9 1.10 1.11

Figure 1.8. The first generation of backbone modified antisense oligomers: the phosphorothioates (1.9), the methylphosphonates (1.10) and the phosphoramidates (1.11).

One of the major challenges which lies ahead in the field of antisense chemistry will be how to effectively deliver these compounds to specific cells. The success of antisense chemotherapy depends on their efficient delivery to the cytoplasm and/or nucleus. Letsinger[39] has investigated the conjugating of cholesterol moieties to antisense oligomers for increasing their cellular uptake. Encapsulation of oligonucleotides into liposomes is another exciting area of research as it would protect the antisense oligomer from nucleases, and would thus serve as an effective method of delivery.[40] In addition, by having virus-derived fusion peptides and receptor binding carbohydrates at the surface of the liposomes,[41] antisense oligomers could be targeted to specific cells and subsequently be delivered to the cytoplasm. Another area of antisense delivery which looks very promising is nanoparticle delivery, presently being investigated by Hélène and coworkers.[42]

Viruses are an obvious target for antisense therapy due to the difficulty in treatment with conventional drugs and because viral genes differ significantly from human genes. For example, there is a great need for anti-viral therapy that can interfere with HIV gene and protein expression at times after viral integration has already occurred. Therapeutics such as protease inhibitors, which can accomplish this aim, have been plagued by problems of drug resistance, due to mutations in the viral genes. This problem of mutagenesis also occurs with both nucleoside and non-nucleoside inhibitors of reverse transcriptase. For these reasons, antisense strategies that target conserved regions of the HIV genome should certainly be investigated. Presently, there are a number of antisense researchers developing antisense agents with the purpose of inhibiting the HIV virus.[43]

Recently, there is great expressed interest by pharmaceutical companies to work in collaboration with antisense companies to discover novel and more specific drugs. The pharmaceutical industry is driven to develop innovative drugs in order to have the lowest cost, life-saving treatments. Biotechnology offers expertise and several tools, *e.g.*, catalytic antibodies, gene cloning and subsequent protein expression, combinatorial chemistry, and rational drug design to identify novel therapeutics compared to the massive screening often used by the traditional pharmaceutical industry. One of the newest techniques that is being employed by biotechnology companies to add to its drug discovery capability involves the use of antisense agents.

Only upon the understanding the current problems encountered with the pharmaceutical companies does one realize the requirement for biotechnology to spoon-feed new ideas to this industry. With the ongoing discussion of price controls, the pharmaceutical industry has to a certain extent, been driven to decrease research spending in order to maximize profits. Furthermore, pharmaceutical companies are facing considerable pressure due to products finishing their patent protection. Ultimately, the pharmaceutical industry must reduce costs while sustaining an efficient drug development program. Biotechnology firms clearly offer an unquestionable source of innovative therapeutics. Having antisense

agents as a new "biotech tool", one more dimension to the vast drug discovery capability of this industry has been added.

There are two main methods which can be employed to uncover potential drug targets. The first being - finding out which molecular target corresponds to the diseased phenotype. Another approach involves using antisense oligomers to study molecular diseases having multiple factors contributing to the diseased state, that is, antisense agents can be used to "turn on and off" a selected gene for a disorder caused by family of genes. In conjunction with conventional drug discovery, antisense agents should aid in finding solutions to treat a wide range of diseases. As written in the January 1990 issue of *Scientific American*, Harold M. Weintraub described the field of antisense nucleic acids as follows, "*Molecules that bind with specific messenger RNAs can selectively turn off genes. Eventually certain diseases may be treated with them; today antisense molecules are valuable research tools.*"

1.5.2 The 2-5A System and its uses as Potential Antisense Agents.

In mammals, the interferon system provides a universal antiviral response. For example, *in vitro* studies involving pretreatment of various mammalian cell lines with interferon can confer resistance to subsequent viral infection.[44] Interferons can induce the synthesis of enzymes called 2-5A synthetases, which upon stimulation with double-stranded RNA can produce oligoadenylates with 2',5' linkages (known as 2-5A or $ppp(A2'p)_{[2\ to>4]}$) by polymerization of adenosine triphosphate (ATP). These oligoadenylates in turn activate an endoribonuclease (RNase L) which degrades viral and cellular mRNA and are subsequently degraded by a cellular 2' phosphodiesterase. A number of studies to prevent phosphodiesterase degradation of the 2-5A oligos has focused on modifications of either the sugar or phosphodiester backbone. In addition, there have been a number of efforts attempting to capitalize on the 2-5A system for development of a potent antiviral agent, either directly or through the use of chimeric 2-5A antisense agents.[45]

Originating from the 2-5 A system, has blossomed a field of antisense research directed at oligonucleotides containing 2',5' linkages. This interest in 2',5'-linked oligomers arises from the fact that natural 3',5'-linked RNA is quickly degraded by nucleases. In utilizing RNA and RNA analogs as antisense agents, during oligonucleotide assembly it is necessary to selectively couple either the 2' or 3' hydroxyl group. This is typically achieved by masking either hydroxyl moiety with an appropriate protecting group *e.g.* the t-BMDS.[25] Recent work done in the Damha laboratory has been most encouraging. This group has demonstrated that 2',5'-linked oligonucleotides may be effective antisense agents since they bind to RNA selectively (over DNA) and are more nuclease resistant than natural RNA. These oligomers form the basis of studies described in chapter 4.

1.5.3 Antigene Strategy.

The sequence specific recognition of double-helical DNA is a requirement for various cellular functions including transcription, replication and cell division. The antigene strategy is based upon the sequence specific recognition of double stranded DNA, and has also potential therapeutic implications for the treatment of a variety of genetic, viral and oncogenic diseases.

The antigene strategy made real advances in 1988 when Hogan *et al.* demonstrated for the first time, in a cell free assay, that a triplex forming oligomer was capable of inhibiting transcription of the oncogene *c-myc*.[14a] Independently, the Dervan group working under similar cell free conditions, showed that antigene oligomers could selectively prevent transcription of viral genes.[46] Adding to these encouraging results, Hélène provided *in vitro* evidence that triplex forming oligomers could inhibit expression of the interleukin-2 receptor.[47] Hogan's laboratory went on to demonstrate that the *c-myc* gene could be inhibited by *in vitro* triple-helix formation.[48] Currently, there are no antigene compounds in clinical trials, which may be attributed to several problems associated with this approach. One of the major limitations of the antigene strategy is a result of the limitation of the available code, which is restricted to recognizing only homopurine tracts

by pyrimidine tracts. That is, sequences of 15-18 purines within the DNA are required for a target site, which occur only rarely within genes. As discussed in chapter 2, the "branched strategy" being pursued by our research group offers a partial solution to this problem.

Another problem of the antigene strategy is a result of the inability of triplexes to form under physiological pH levels. That is, in the pyrimidine motif, the cytosine of the C^+GC triplet are essentially unprotonated at physiological pH. Dervan's group has taken a different approach, whereby they can recognize all four bases pairs with a limited degree of specificity double-helical DNA using nonnatural deoxyribonucleosides.[49] Their laboratory has demonstrated that substitution of a cytosine in a pyrimidine sequence with an N^7 glycosylated guanine base,[50] or with a 5-methylcytosine alleviates the requirement for a protonated cytosine. The recent studies by Glazer and coworkers indicate that triplex forming oligonucleotides can have unexpected mutagenic effects.[51] Once these problems have been addressed adequately, it may be plausible for the antigene strategy to enter clinical trials.

1.6 Some Techniques used to investigate Nucleic Acid Struture.

1.6.1 Melting Temperatures - A Technique used to investigate Complex Formation.

One of the most convenient ways to study the association of nucleic acids in solution is through the use of the UV spectroscopy *i.e.* melting temperature studies.[52] The heterocyclic bases of nucleic acids are flat aromatic chromophores which display characteristic UV absorption spectra (λ_{max} *ca.* 260nm). It is the stacking interactions of the adjacent bases in a single stranded nucleic acid which causes the overall UV absorption to be less than the individual nucleotide components.[53] It is the chromophore-chromophore interactions of double-stranded complexes which in turn decreases the UV-absorption, relative to the individual strands.

Upon heating a double stranded complex, both the hydrogen bonds and the base stacking of the double helix is disrupted, causing the dissociation into single strands. The unwinding of the double helix is referred to as "melting" since it typically occurs abruptly at a certain temperature. This dissociation or melting of the double helix into single strands can be measured by UV spectroscopy at 260nm. Typically, a distinct S-shaped curve is obtained when absorbance is followed as a function of temperature. The melting temperature, or T_m, is defined as the temperature at which half of the complex has dissociated into its single-stranded form. Besides the melting temperature, the degree of base-stacking/hydrogen bonding can be inferred from the hyperchromicity. The hyperchromicity is commonly calculated using the equation $\%H=(A_f-A_i)/A_f \times 100\%$, whereby A_f is the final absorbance after melting of the complex, and A_i is the initial absorbance prior to melting. Melt profiles (or melt curves) are simply a plot of absorbance versus temperature and are run by mixing the complementary strands in aqueous buffer, cooling the solution, and then slowly raising the temperature until the complex is melted.

1.6.2 Circular Dichroism.

Circular dichroism is another powerful technique commonly used to study the structure of nucleic acids. Nucleic acids, being chiral molecules, rotate the plane of polarized light. CD experiments can quantitate the differential absorbance of left- and right-handed circularly polarized light only in the intervals where absorption occurs, which is reported in molar ellipticity [θ].[54]

What makes CD such a powerful tool is its sensitivity to small perturbations in the secondary structure of nucleic acids. For example, CD spectroscopy is sensitive to aspects such as base tilt, base stacking and nearest-neighbour interactions.[55] However, there are limitations with CD, the most important being that it is strongly dependent on the base composition and the sequence.[56] This stresses the importance of not making

general conclusions without comparing CD spectra of nucleic acids of known conformation. Despite this minor limitation, CD is an excellent method to study both the conformation and the structure of nucleic acids.

1.6.3 Fluorescence.

One more technique which can be utilized for studying nucleic acid structure involves the use of fluorescent DNA-binding ligands several compounds. For example, there are a number of fluorophores which bind either to the major or minor grooves of DNA, and/or intercalate between the bases. In addition, there are certain fluorescent ligands which can bind more specifically to certain complexes *i.e.* duplexes over triplexes, and vice versa. Without question, fluorescence is one of the more valuable tools which can be used for probing the structure and detecting complex formation as a result of its high sensitivity.[57] The fluorophore being sensitive to perturbations in its local environment can then be used to probe the association of nucleic acids and the resulting structure.

Fluorescence as with the other methods employed for studying nucleic acid structure and function, has its disadvantages. One of the essential problems is that, the DNA-ligand must not only be capable of binding to the complex, but it must have wavelengths of excitation and emissions which would not damage the nucleic acids being probed. Another disadvantage is the amount of nucleic acid material that is required in order to obtain an adequate signal to noise ratio.

1.7 Plan of Study.

Recently, a new type of nucleic acid analogue, the "branched" oligonucleotides, where parallel strands are joined to a branchcore adenosine via 2',5'- and 3',5'-phosphodiester linkages were synthesized by our research group. Preliminary physiochemical analysis of these compounds suggested that they form remarkably stable triple-helical complexes having the unusual TAT (reverse Hoogsteen/Watson-Crick) configuration (Figure 1.4). The

triple inducing capacity of branched oligonucleotides prompted us to study this complex in much more detail and to evaluate these compounds as potential antisense agents. Further investigations into the use of branched nucleic acids as molecular probes and as potential chemotherapeutic agents, led us to design "Y"-shaped oligonucleotides that are linked at one branch through a flexible aliphatic linker. These analogues are expected to have an advantage in recognizing substrates via "duplex/triplex" formation by providing structural flexibility.

Oligoribonucleotides containing exclusively 2',5'-phosphodiester linkages were also synthesized with the intention to study their antisense properties in *in vitro* cell culture systems infected with HIV-1. Of special interest are the selective hybridization properties of 2',5'-linked oligonucleotides, binding more tightly to ssRNA than to ssDNA. Sequence-specific duplex formation and RNA binding selectivity by 2',5'-oligomers containing all four bases has not been reported. Thus, a study was undertaken to investigate the extent to which these oligomers and other 2',5'-linked analogues, can discriminate between DNA and RNA strands - a property which makes these oligomers specific antisense agents and selective nucleic acid probes.

Chapter 2. Association of Branched Nucleic Acids: Structural and Physicochemical Analysis of Antiparallel T•AT Triple-Helical DNA.

2.1 Introduction.

Recent studies in the Damha laboratory proposed the use of synthetic branched ("V" and "Y") oligonucleotides to: (i) study the structure and role of naturally occurring branched RNA intermediates,[58] and (ii) exploit their unique "forked" architecture to stabilize triple helical structures.[59,60] Initial studies by Hudson and Damha suggested that a branched oligonucleotide with identical oligo(thymidine) chains linked to the 2' and 3'-positions of a ribose branch-point nucleoside, i.e., $rA^{[2'\text{-}5'\text{-}dT10]}_{[3'\text{-}5'\text{-}dT10]}$ binds to dA_{10} to yield a triple-stranded complex containing only T•AT (reverse Hoogsteen•Watson/Crick) base triplets (see section 1.3, Introduction).[59,61] In this study, this novel triplex was further investigated both from a structural and physiochemical viewpoint. Specifically, the factors that affect the stability of this complex were investigated. Using buffers containing magnesium or sodium, it was shown that the antiparallel triplex could form, or be inhibited with potassium. It was demonstrated that the adenylate strand can bind cooperatively to the branched structure and for the first time, the circular dichroism spectral "signature" of the T•AT triplex was obtained. Also, the structure of the T•AT triple helix was probed with both intercalating and minor groove binding DNA ligands. In collaboration with Dr. Krull and co-workers (Erindale College, University of Toronto), a biosensor for detecting the formation of both "parallel" and "antiparallel" TAT triplexes was developed. This technique makes use of a highly sensitive optical fibre technology which had been previously proven to detect duplex formation.[62]

2.1.1 Structure Considerations.

The branched nucleic acid **2.1** was studied due to its relative simplicity, its ease of synthesis,[58a,b] and unique structural features. Recent studies on small branched RNA fragments, e.g., the trinucleoside diphosphate $A^{[2'\text{-}5'dT]}_{3'\text{-}5'dT}$, indicate that the sugar-

phosphate framework of the adenosine residue is rigid, a result of the strong base stacking between the adenine at the branchpoint and the adjacent 2'-thymine.[58d,63] The 2'-5' and 3'-5'-phosphodiester linkages of $A^{[2'\text{-}5'dT]}_{3'\text{-}5'dT}$ are nearly parallel to one another and display significant preference for the ε^- and $\varepsilon^{\cdot\cdot}$ conformation about the C2'-O2 and C3'-O3' bonds (Figure 2.1).[58d] Also, the furanose ring of the adenosine residue shows a high preference for the C2'-endo pucker conformation ($^2E/^3E = 0.80$) , a common feature of purine sugars linked to a pyrimidine via a 2',5'-linkage.[64] These properties are also retained in larger branched molecules.[63] Thus the branched nucleic acids **2.1** or **2.2** can be regarded topologically as a "V"-like or "Y"-like structure, respectively, with the two dT_{10} strands oriented at a slight angle with respect to each other. The polarity of both dT_{10} strands is identical being 5'→ 3' (from top to bottom, Figure 2.1) and is a consequence of the solid-phase convergent synthetic methodology developed by Damha *et al.* (Figure 2.2).

This characteristic makes **2.1** a highly attractive candidate for stabilizing the antiparallel T•AT triplex as it has the necessary parallel orientation for the dT strands found in this complex (see Section 1.3). Furthermore, the branched adenosine nucleotide provides a semi-rigid core that would favor a bimolecular triplex upon binding of **2.1** to dA_{10}. This is an important structural feature since the linear analogue 3'-$dT_{10}dC_4$-5'-5'-dT_{10}-3' does not form a triplex with dA_{10}.

A

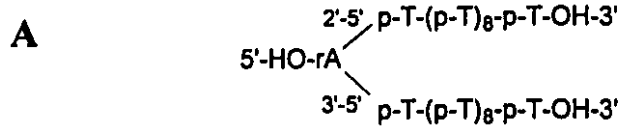

"V" Compound (2.1)

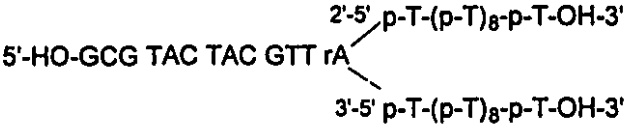

"Y" Compound (2.2)

B

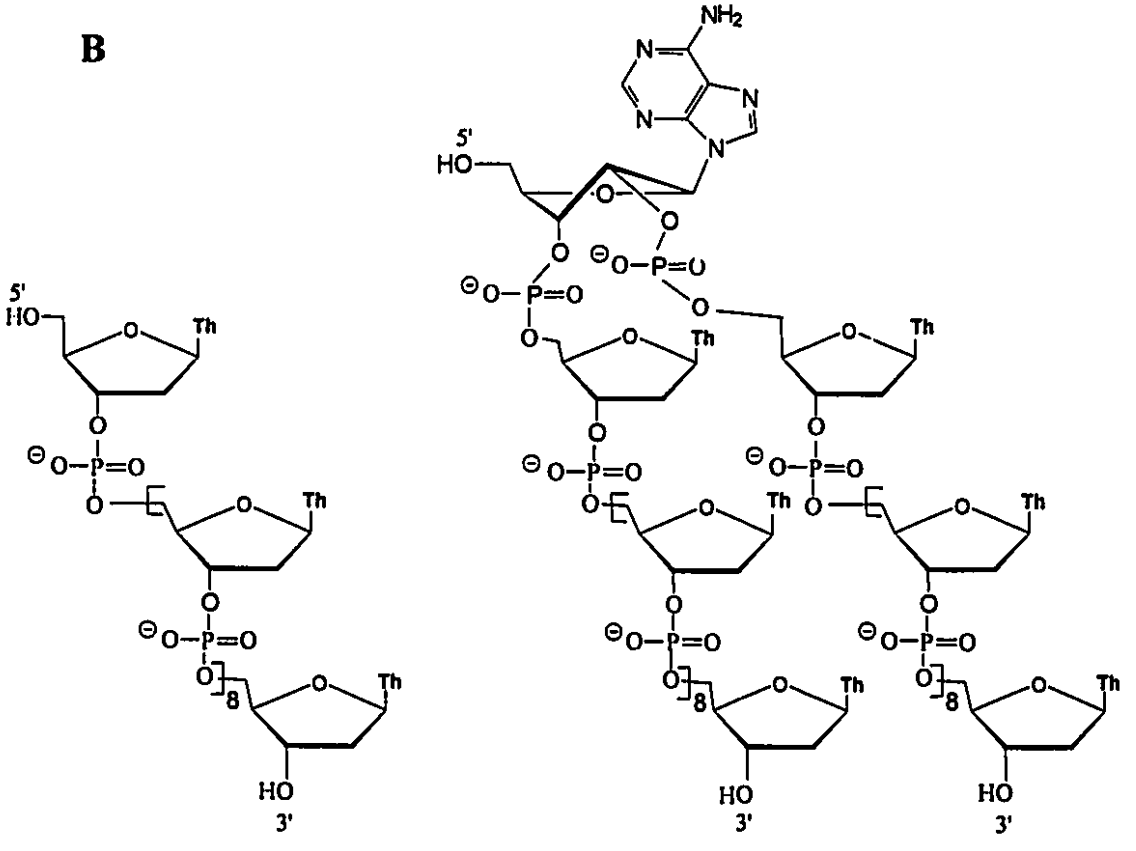

dT_{10} "V" Compound (2.1)

Figure 2.1. A. The branched nucleic acids 2.1 and 2.2 can be topologically regarded as "V" and "Y"-like structures, respectively. B. Primary structure of dT_{10} and the branched oligomer 2.1 showing the conformation of the branch-point adenosine unit as found in solution.

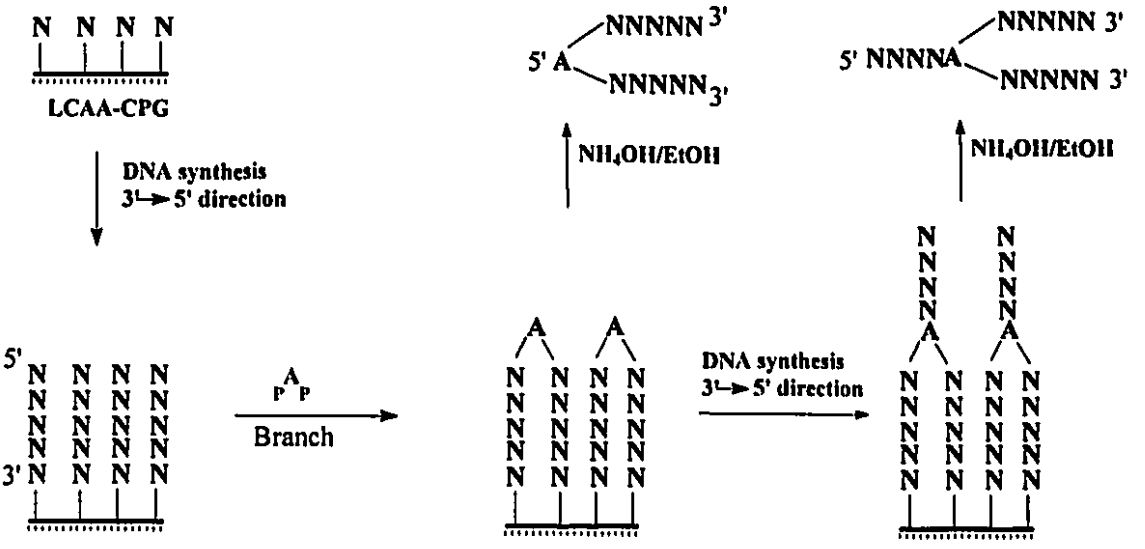

Figure 2.2 The solid-phase convergent synthetic methodology for bNA's, developed by Damha *et al.*[58a-c] The branching monomer A^{P}_{p} is N^{6}-benzoyl-5'-O-(dimethoxytrityl)adenosine-2',3'-O-bis(2-cyanoethyl-N,N-diisopropylphosphoramidite).

2.2 Results and Discussion

2.2.1 Stoichiometry between 2.1 and dA_{10}.

Studies by Hudson and Damha showed that the melt curve at 260 nm for the complex formed between compound **2.1** and dA_{10} showed a monophasic, cooperative transition at 35.3 °C involving a hyperchromicity of 25% (50 mM $MgCl_2$, 10 mM Tris, pH 7.3). Similar results were obtained when the complex was studied in a Na^+ buffer system of high ionic strength (1 M NaCl, 10 mM Na_2HPO_4, pH 7.0), having a melting temperature of 32.8 with a hyperchromicity of 20%. Of note, the melting profile of **2.1**/dA_{10} showed a significantly greater hyperchromic rise than the melting of the dT_{10}:dA_{10} duplex under either Na^+ (%H=16) or Mg^{2+} (%H=20) conditions. This is attributed to the greater stacking interaction involved in a possible triple-stranded **2.1**/dA_{10} complex as compared to the double-stranded dT_{10}:dA_{10} complex. Hudson and Damha went on to demonstrate

that the addition of more dA_{10} to complex **2.1**/dA_{10} did not cause any change to the thermal denaturation profile suggesting that **2.1** and dA_{10} interact in a 1:1 stoichiometry.

Hudson and Damha verified independently the stoichiometry of interaction of **2.1** with dA_{10} by titrating the branched oligomer with complement in the method of continuous variation.[65] The Job plots or mixing curves demonstrate that **2.1** and dA_{10} bind with 1:1 stoichiometry, regardless of the direction of titration for oligomer **2.1** and dA_{10}. This provides evidence that the complex involves both dT_{10} strands and is thus triple-helical. If only Watson-Crick interactions were involved, compound **2.1** would be expected to bind to two equivalents of dA_{10}. However, because of the monophasic nature of the melt curve, it may be argued that the branched molecule is sterically inhibited and simply cannot simultaneously use both dT_{10} "arms" for hybridization. That is, the branched molecule is only capable of forming a duplex with one "arm" while the other "arm" remains a "spectator" (Figure 2.3). However, several lines of evidence obtained in the present study render this explanation improbable.[1]

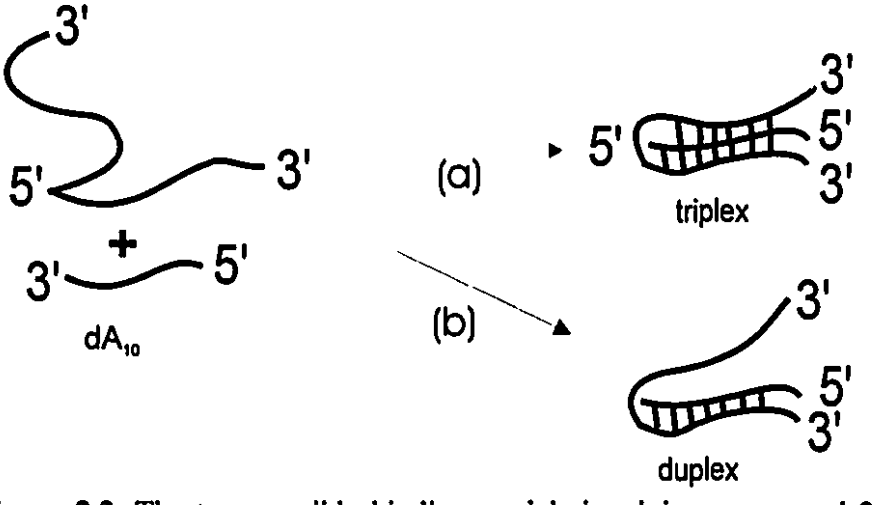

Figure 2.3. The two possible binding models involving compound **2.1** and dA_{10}. The "V" molecule is capable of (a) forming a triplex or (b) compound **2.1** forms a duplex containing a dangling (or "spectator") strand.

[1] Previously it was necessary to clarify what was done by Hudson, from this point onwards all work up to section 2.4.3 was done by Uddin.

2.2.2 Monitoring T•AT Triplex Transitions at 284 nm.

It is well documented that A-T Watson-Crick duplexes do not display changes in absorbance when their melting transition are monitored at 284 nm since, at this wavelength, they share a (virtual) isosbestic point with the melted duplex (i.e., single stranded dA_{10} and dT_{10})[9c,9e,17,66-70] Triplex transitions, on the other hand, display changes in absorbance at both 260 and 284 nm, e.g., triplex → single strands,[9c,9e,69,71] or triplex → duplex + single strand.[17, 68-70] Thus, by measuring melting profiles at 284 nm it is possible to observe a triplex transition independently from a A-T duplex transition. This is demonstrated by the UV absorbance spectrum at three temperatures proved that there indeed was an isosbestic point for the dAT_{10}:dA_{10} (1:1) and **2.1**:dA_{10} complexes (Figure 2.4).

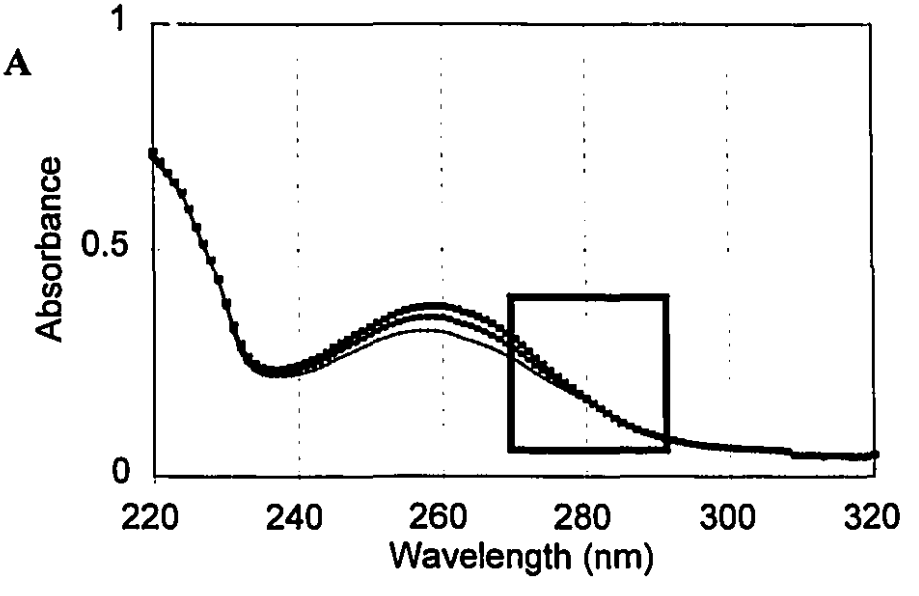

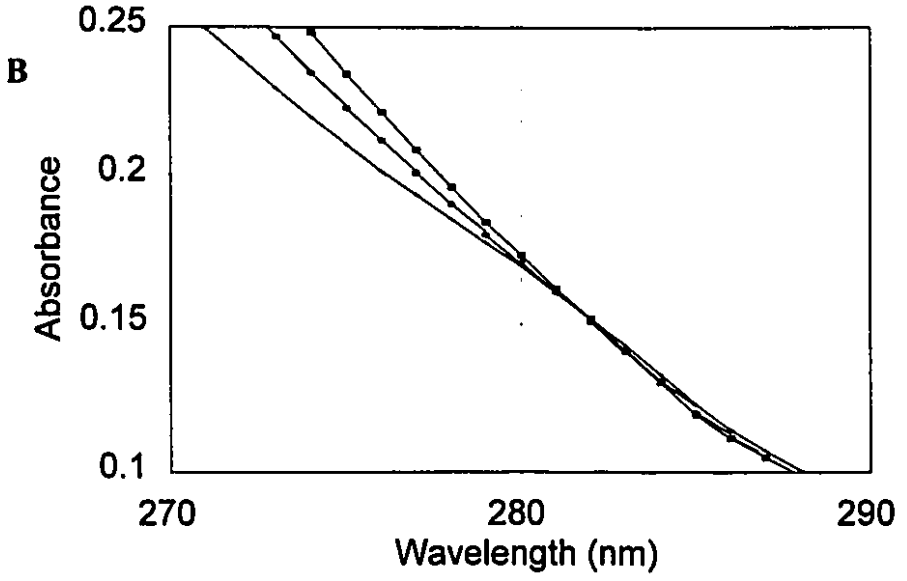

Figure 2.4 A. UV spectra of dAT_{10} complexed with dA_{10}, the scans were done at three temperatures 5 °C (+), 35 °C (●), and 70 °C (■). **B.** This graph shows that the 282nm region is an isosbestic point for the (1:1) AT_{10}/dA_{10} duplex. Conditions were: 10mM Tris, 50mM $MgCl_2$, pH 7.3.

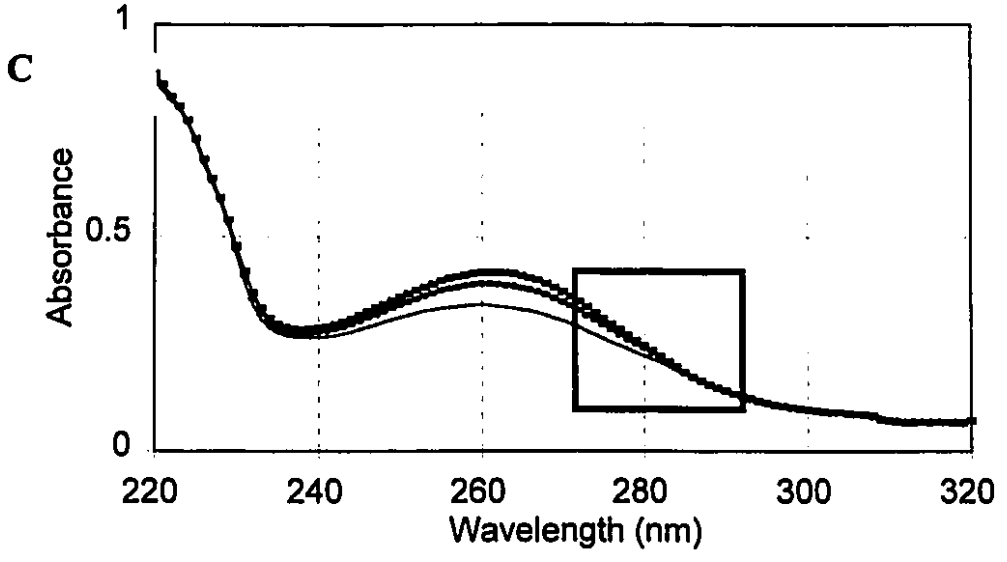

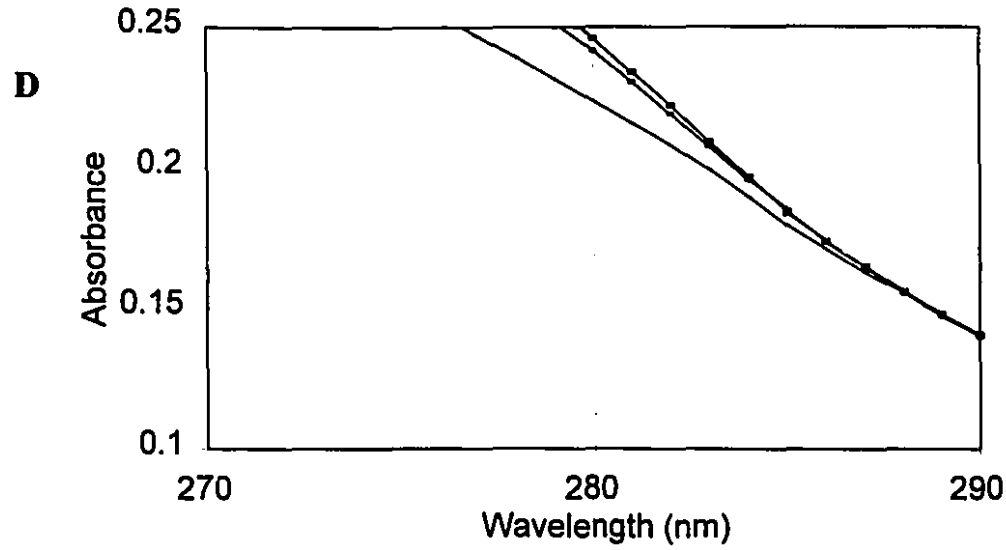

Figure 2.4 C. Absorbance versus Wavelength of "V" (**2.1**) complexed with dA_{10}, the scans were done at three temperatures 5 °C (+), 35 °C (•), and 70 °C (■). **D.** This graph shows that the 284nm region is not an isosbestic point for the **2.1**/dA_{10} complex.

In contrast, a 1:1 mixture of dA_{10} and dT_{10} exhibited a monophasic helix-coil transition at 260 nm and no observable transition at 284 nm.[17,69] Monitoring complex **2.1**/dA_{10} at 284 nm in either Na^+ or Mg^{2+} buffers shows clear melting transitions of small but significant hyperchromicity and confirms that, under these conditions, both the 2'- and 3'-dT_{10} "arms" in **2.1**, are involved in the binding of a dA_{10} single strand.

2.2.3 Nature of the Triplex to Coil Transition.

Commonly, triplex dissociation occurs through a two step mechanism, i.e., dissociation of the triplex to a duplex and single strand, followed by dissociation of the duplex to single strands. Each process may show a separate transition in the thermal melt profile when resolved by sufficiently differing T_m 's. For example, for the canonical dT_{10}*dA_{10}:dT_{10} (parallel) triplex, melting or displacement of the Hoogsteen third strand was observed as a separate event (T_m 18 °C) to the melting of the underlying duplex (T_m

32 °C) (50mM Mg^{+2}, 10 mM Tris).[17, 68] However, both Hudson and Uddin have been unable to observe a clear biphasic profile for **2.1**/dA_{10} that would suggest an intermediate dissociation step (50 mM Mg^{+2} or 0.2-1 M Na^{+}). This behavior most likely arises in part from the intramolecular nature of the triplex, *i.e.*, following the binding of one dT-"arm" to the target (Watson-Crick pairing), the effective local concentration of the other dT-"arm" is increased as to promote (reverse-Hoogsteen) binding to the adjoining duplex. The sharpness of the transition observed at 260 (and 284) nm indicates cooperativity between these two processes, e.g., via a "nucleation-zipping" mechanism.[72] Similar (one-step) cooperative transitions were observed for the "fold-back" oligomer 5'-dT_{10}-$dCTC_2$-dT_{10}-3',[73] for circular,[9b,c,f,10a] and other structurally altered nucleic acids.[9e,69] It is noteworthy that whatever the type of ion, Mg^{+2} or Na^{+}, the T_m value for complex **2.1**/dA_{10} is *ca.* 3 °C higher than that for the dT_{10}:dA_{10} duplex, which models the Watson-Crick duplex that can form in **2.1**/dA_{10}. In addition to providing further evidence that both dT_{10} strands in **2.1** are involved in base pairing interactions, this result shows that binding of one dT_{10} arm appears to enhance the thermal stability of the underlying duplex. A strikingly similar melting behavior has been observed for the intermolecular [$d(G_3A_4G_3)$•$d(C_3T_4C_3)$:$d(G_3A_4G_3)$] "anti-parallel" triplex.[14e]

2.2.4 Circular Dichroism Studies.

Triplex-formation between **2.1** and dA_{10} was further supported by circular dichroism (CD) measurements. The CD spectra of **2.1**, dA_{10}, and the control oligomer dT_{10} are shown in Figure 2.5A. Compound **2.1** (5 °C) shows a CD spectrum qualitatively similar to dT_{10} with a strong positive long wavelength Cotton effect at 287 nm and a weaker negative effect at 244 nm, and a cross-over at 257 nm, which occurs near the maximum of the UV absorbance. The position of the major positive CD band at 288 nm is considerably red-shifted relative to that of dT_{10} (281 nm) and linear 11-mer dAT_{10} (279 nm, not shown). Complex formation is readily monitored by changes in both the amplitude and position of the CD bands. The CD spectrum of a 1:1 mixture of dA_{10} and

dT_{10} at 5 °C (i.e., below duplex T_m) is characterized by maxima at 226, 263, and 284 nm as well as two minima at 247 and 268 nm (Figure 2.5C-g). The spectrum of dT_{10}*dT_{10}:dA_{10} at 5 °C is similar and characterized with a broader and smaller positive band at 227 nm (Figure 2.5C-f). This feature is believed to be indicative of triplex formation for this particular sequence.[68,69,74]

The 1:1 mixture **2.1**/dA_{10} in Mg^{+2} (60 °C) displays a spectrum that is similar to a superimposition of the spectra of the free, single stranded **2.1** and dA_{10} (Figure 2.5B-d) When the temperature is decreased from 60 °C to 5 °C (**2.1**/dA_{10} in triplex form), the Cotton effects show a marked amplitude decrease with a slight red shift for the band at 287 nm (Figure 2.5B-e). The 5 °C spectrum of this complex is different from the CD spectra for dT_{10}:dA_{10} duplex (Figure 2.5C-g) and parallel dT_{10}*dT_{10}:dA_{10} (Figure 2.5C-f) and [5'-dT_{10}-$dCTC_2$-dT_{10}-3']:dA_{10} triplexes, and cannot be assigned to any canonical form of DNA. Furthermore, it cannot be explained as the sum of the spectra of dT_{10}:dA_{10} duplex and dT_{10} at 5 °C. This was considered to be strong evidence in favor of the **2.1**/ dA_{10} complex being a triple helix and having a conformation with respect to base pair stacking and third strand orientation that is different to that of the canonical T*AT triplex.[6b]

As shown in Figure 2.5D, the CD spectra of 3'-$dT_{10}dC_4$5'-5'dT_{10}-3'/dA_{10} (Mg^{+2}) and **2.1**/dA_{10} (K^+) are similar to that of dT_{10}:dA_{10} duplex (Mg^{+2}) indicating that a duplex-stranded helix was formed in both instances, as determined by their thermal denaturation profiles.

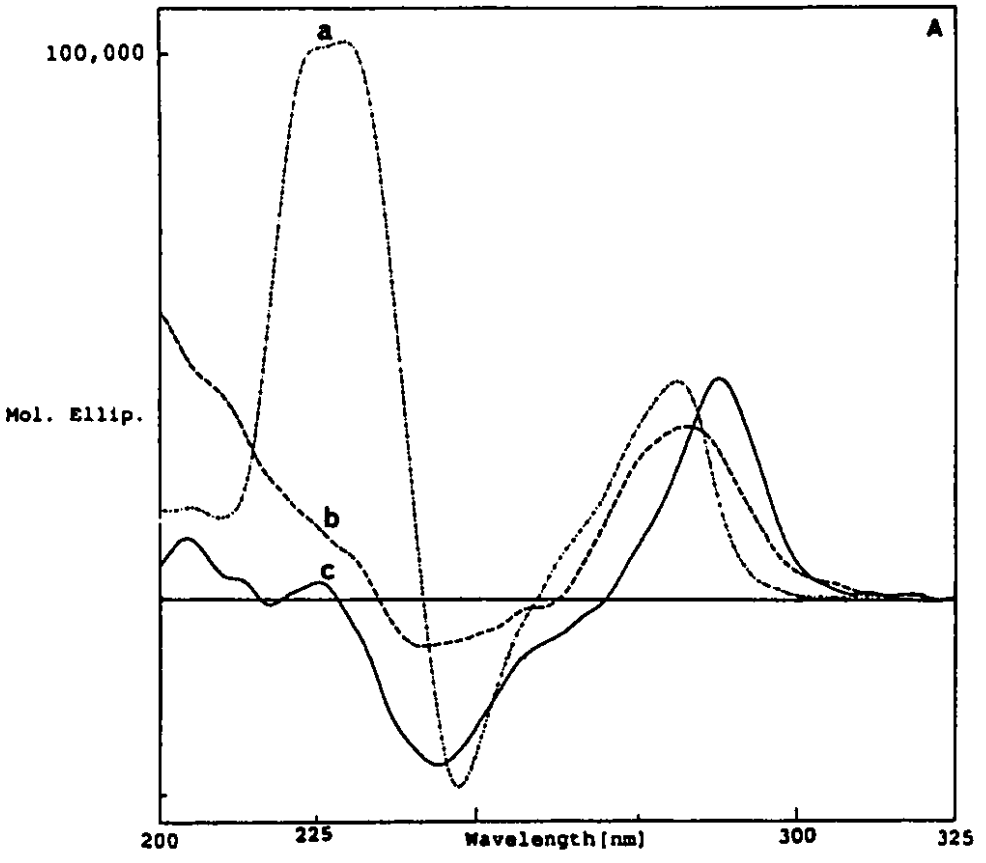

Figure 2.5 A. CD spectra of (a) dA_{10} (5 °C), (b) dT_{10} (5 °C), (c) (**2.1**) (5 °C). Conditions: 50 mM $MgCl_2$, 10 mM Tris, pH. 7.3.

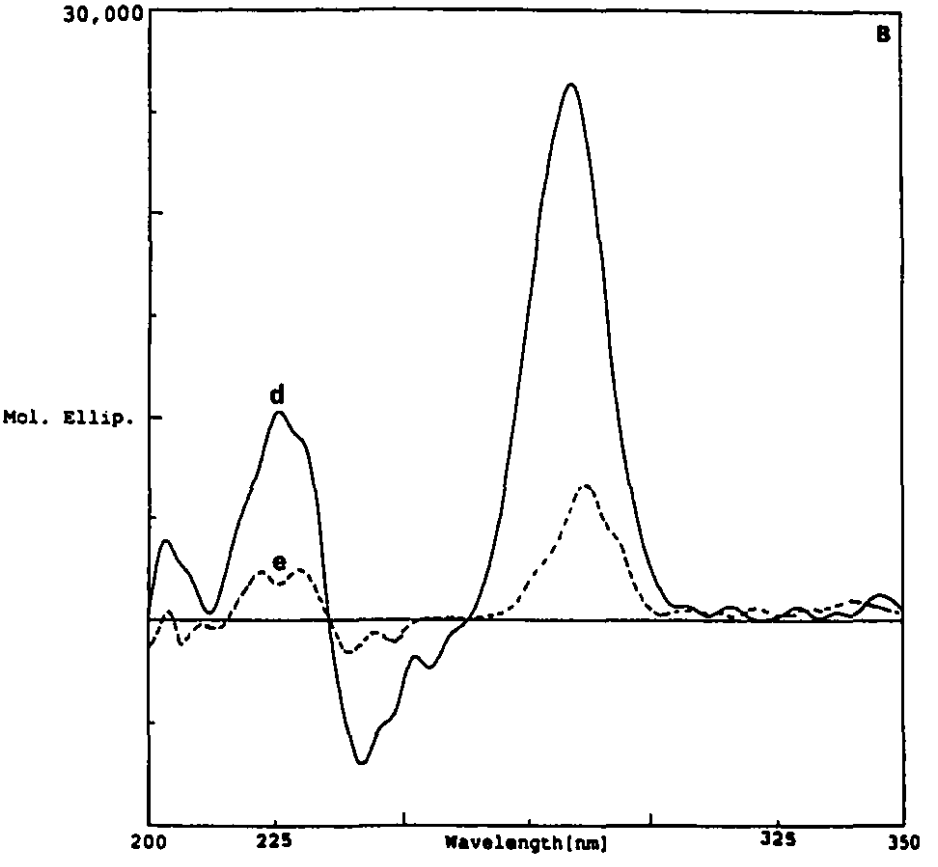

Figure 2.5 B. CD spectra of: (d) 1:1 (2.1)/dA_{10} (60 °C), (e) 1:1 (2.1)/dA_{10} (5 °C). Conditions: 50 mM $MgCl_2$, 10 mM Tris, pH. 7.3.

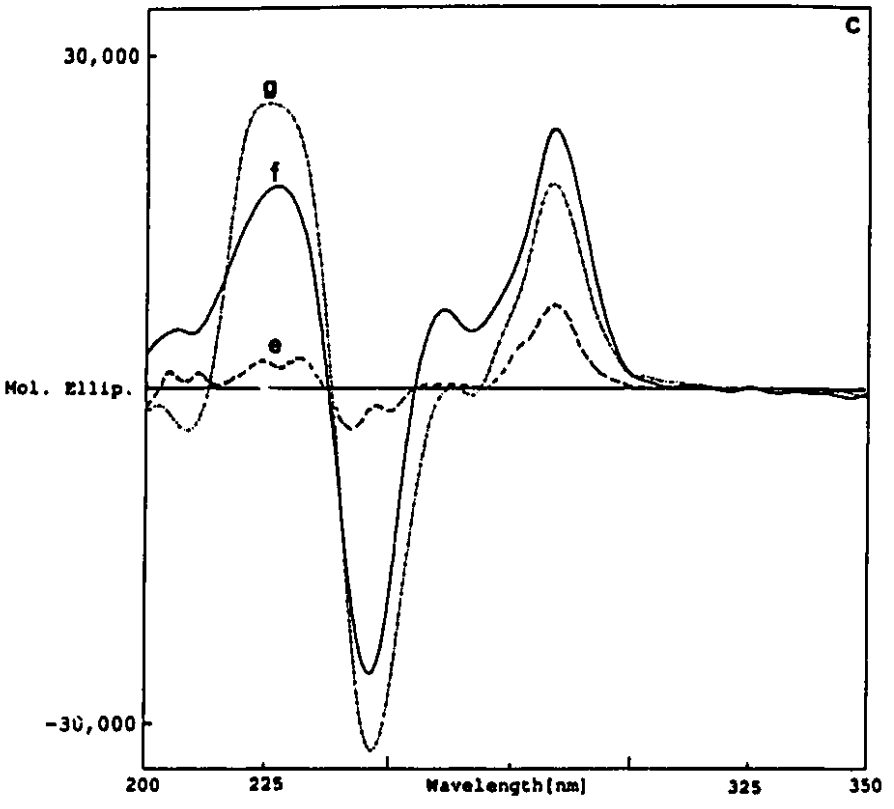

Figure 2.5 C. CD spectra of (e) 1:1 (2.1)/dA_{10} (5 °C), (f) triplex dT_{10}*dA_{10}:dT_{10} (5 °C), (g) duplex dT_{10}:dA_{10} (5 °C). Conditions: 50 mM $MgCl_2$, 10 mM Tris, pH. 7.3.

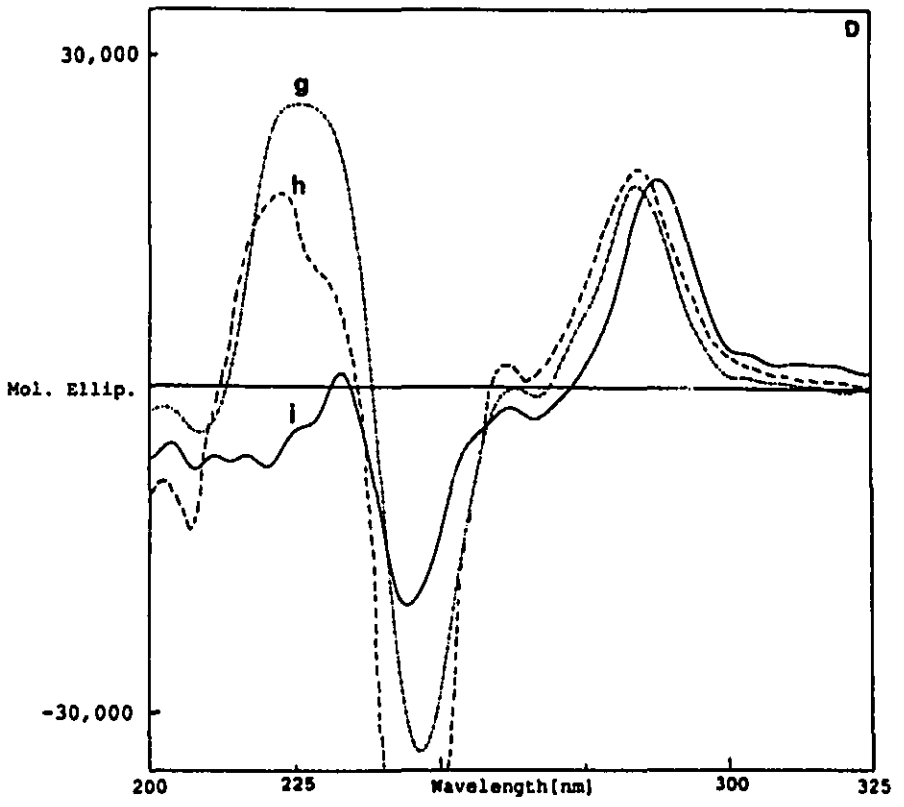

Figure 2.5 D. CD spectra of: (g) duplex dT_{10}:dA_{10} (5 °C), (h) 1:1 3'-$dT_{10}dC_4$5'-5'dT_{10}-3':dA_{10} (5 °C), (i) 1:1 (**2.1**)/dA_{10} (5 °C) in K^+ buffer. Conditions for (g)-(h): 50 mM $MgCl_2$, 10 mM Tris, pH. 7.3; (i) 140 mM KCl, 5 mM Na_2HPO_4, 1 mM $MgCl_2$, pH 7.2.

2.2.5 Effect of cation.

It has been recently found that moderate concentrations of potassium cations, such as those present under physiological conditions (140 mM), inhibit the formation of "anti-parallel" triple-stranded DNA.[20] Therefore, it was determined whether it was possible to observe under these conditions two separate transitions during the melting of **2.1**/dA_{10}, or perhaps, a single melt transition that was consistent with duplex melting. Mixtures of **2.1** and dA_{10} (1:1), and dT_{10} and dA_{10} (1:1), were incubated in a buffer containing 140 mM

KCl, 5 mM Na_2HPO_4, and 1 mM $MgCl_2$ (pH 7.2), ionic concentrations known to inhibit triple-helix formation[20] and which are representative of intracellular conditions.[75] Complex formation was monitored by measuring melting profiles at 260 and 284 nm. Both complexes exhibited similar monophasic helix-coil transitions at 260 nm (*ca.* T_m 19.0 °C, %H= 8) and no observable transition at 284 nm, indicating that a duplex formed in both instances (**2.1**/dA_{10}, Figure 2.6). These results, together with the CD studies described above, support the "spectator" T-strand model for the interaction of **2.1** and dA_{10} under these conditions (Figure 2.3).

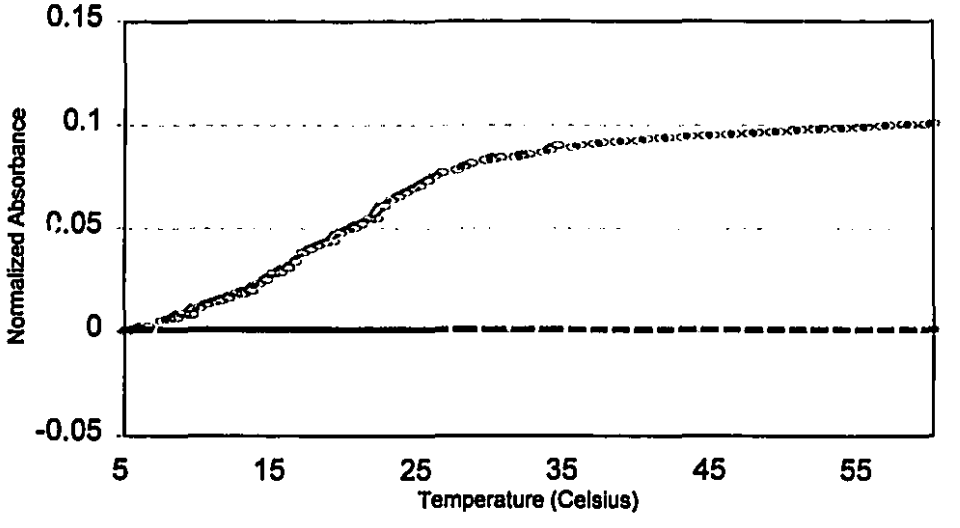

Figure 2.6. UV absorbance melting profile for the complex formed between **2.1** and dA_{10} monitored at 260 nm (-O-) and 284 nm (-■-) in physiological buffer (140 mM KCl, 5 mM Na_2HPO_4, 1 mM $MgCl_2$, pH 7.2). Normalized change in absorbance was calculated by $[(A_t - A_o)/(A_f)]$ where A_t = absorbance at any temperature; A_o= initial absorbance; A_f = final absorbance.

2.2.6 Effect of Target Chain Length and Sequence.

Further evidence for compound **2.1** forming a triple helical structure comes from measurements of complex stability with oligoadenylates of different chain lengths (dA_n). Figure 2.7 lists the melting temperatures of several **2.1**/dA_n complexes as well as those for the model dAT_{10}:dA_n duplexes. The melting curves of all complexes involving **2.1** showed a single inflection at 284 nm, indicating that bimolecular triplexes are formed.

Examination of the data leads to the following conclusions: For complexes involving the branched oligomer **2.1** and dA_n, the T_m is linearly dependent on the target chain length (n) over a limited range. With regard to the melting of the duplexes, the changes in T_m are less sensitive to n. Note that at n=10, both lines change slopes, which corresponds to the number of thymines present in dAT_{10}, and in each of compound **2.1**'s dT "arms". Beyond this value, the T_m's of the complexes remain linearly dependent on n ($10 \leq n \leq 20$), although the "V" line is still the most steep. This most likely reflects differences in the stability of the complexes, and supports the idea that in the case of **2.1**/dA_n, the adenylate strand is held to one dT_{10} strand by Watson-Crick bonding and to the other strand by reverse- Hoogsteen bonding. The increasingly higher T_m values beyond n=10, is most

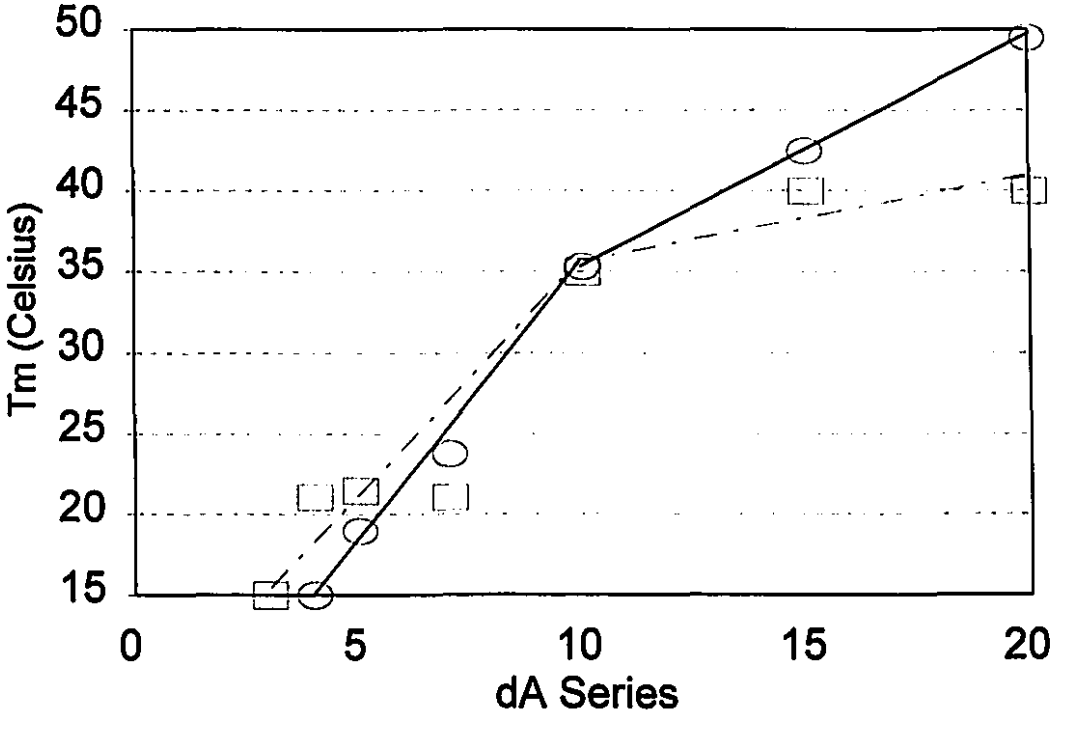

Figure 2.7. The effects of varying the adenylate chain length (n) on the melting temperature of complexes **2.1**/dA_n (-O-), and dAT_{10}/dA_n (-□-). Conditions: 50 mM $MgCl_2$, 10 mM Tris, pH 7.3.

likely the effect of stability as a result of reduced "fraying" at the ends of the complexes.[76] Another possible source of enhanced affinity as the dA_n segment increases, is the expected effect of "sliding degeneracy". This refers to the possibility of multiple positions of binding of **2.1** on an dA_n template (n>10), or of dA_n on a **2.1** template (n<10).

Below n=5, the thermal stability of the duplexes exceeds that of the branched triplexes. For example, the melting curve of a 1:1 mixture of linear dAT_{10} and dA_4 showed a sharp single transition at 21 °C, however, the first sharp transition detected with compound **2.1** was with dA_5. Thus, five base triplets are the minimum requirement for triple helix formation, in agreement with recent studies with parallel triplexes.[72]

Binding to dA_5 (1 eq.) results in branched and linear complexes with comparable thermal stability (T_m 19 and 21.5 °C, respectively; Figure 2.8). Addition of another molar equivalent of dA_5 gives a considerably stronger branched complex, with a T_m which is 6 ° C higher than the one formed with only one equivalent (Figure 2.8B). This cooperative interaction may be attributed to be caused by the propagation of a conformational change (e.g., base stacking) between adjacent sites of the terminal adenosine residues. The high cooperative nature of the melt profile (Figure 2.8B) suggests that binding of the first dA_5 oligomer provides a strong nucleation center for, and enhances, binding of the other. This behavior is in contrast to that observed for the duplex, in which no significant change in the T_m is observed upon further addition of dA_5 (Figure 2.8A). However, for both duplex and triplex, the hyperchromicity associated with the 2x dA_5 cases is significantly greater than for the 1x dA_5 cases, consistent with the involvement of more bases in these complexes. Cooperative effects such as the one observed for the **2.1**/(2x dA_5) complex are well documented in the literature,[8b,77,78] but have not been reported for triplexes conforming to the antiparallel (or "purine") motif.

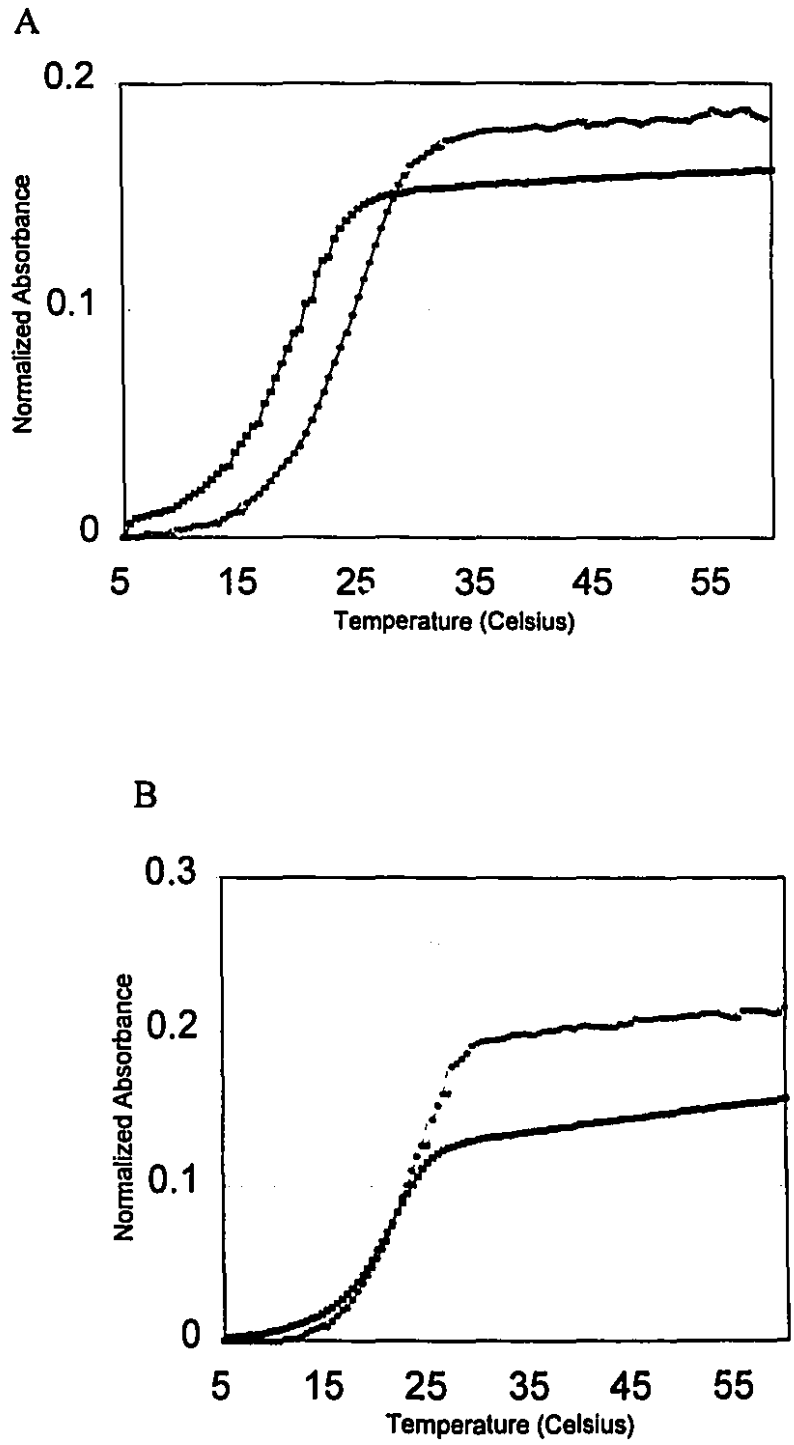

Figure 2.8. UV absorbance melting curves (260 nm) for "V" (2.1) (Figure A) and dAT_{10} (Figure B), complexed with 1 equivalent (-■-) and 2 equivalents (-O-) of dA_5. Conditions: 50 mM $MgCl_2$, 10 mM Tris, pH 7.3.

Table 2.1. Melting Temperatures (T_m)[a] and Hyperchromicities (%H) for Fully Paired and Mismatched Complexes.

	Target	T_m (°C)	%H
ATTTTTTTTTT	AAAAAAAAAA	34.7	17.4
	AAAA I AAAAA	17.7	16.9
	AAAA G AAAAA	17.8	15.4
A / TTTTTTTTTT \ TTTTTTTTTT	AAAAAAAAAA	35.3	22.8
	AAAA I AAAAA	24.1	16.4
	AAAA G AAAAA	21.5	18.5

[a]Conditions: 50mM $MgCl_2$, 10mM Tris, pH 7.3.

Proper base-pairing is important in the antiparallel T•AT triplex as shown by the experiments with "V" (**2.1**) and the mismatch targets dAAAAXAAAAA (X= T or G) (Table 2.1). A single mismatch resulting from substitution of dA by dT (or dG), leads to a decrease in T_m of 11-13 °C. Of note, the TTT "mismatch" is less destabilizing than the TGT "mismatch". Also, the hyperchromicity associated with dissociation in the fully complementary case is 25%, while in the mismatch cases it is 16-18%, consistent with the involvement of fewer bases in the complex. Interestingly, the corresponding decreases in T_m for the mismatch duplexes are more significant (*ca.* 17 °C) compared to the mismatched triplexes (Table 2.1). This was not expected since a mismatch in the purine strand of a triplex structure would disrupt not only the Watson-Crick interaction but also the reverse-Hoogsteen interaction. Based upon the T_m results obtained with compounds **3.3** and **3.4** (see chapter three), it was found that having one mismatch does not have a significant effect on triplex destabilization. Mismatch studies involving parallel T*AT triplexes (circular-DNA[9c] and other conformationally restricted triplexes[9c]) have a more pronounced destabilization since these cases involved more than one base triad disruption. Further mismatch studies with the antiparallel triplex structure (**2.1**:dA_{10}) are required to determine how stringent and specific these base-base interactions are.

2.2.7 Effect of the Branch-Point.

Interestingly, the linear oligomer 3'-$dT_{10}dC_4$-5'-5'-dT_{10}-3', having also the appropriate polarity of dT strands but lacking the rigid branched framework, did not form a triplex, as judged by its circular dichroism spectrum (vide infra) and "flat" melt curve at 284 nm (data not shown). This result suggests that the rigidity of the branched core in **2.1** contributes significantly to the stabilization of the triplex. A related phenomenon is the remarkable stability of parallel Py*Pu:Py complexes formed between single stranded purine oligonucleotides and triple-helix forming oligonucleotides containing a rigid terephthalamide unit.[9c]

A question that arises in this study is whether all ten T residues in **2.1** are involved in base pairing interactions, or whether the branch-point prevents base pairing near it. These questions were addressed by comparing the melting temperatures of the complexes **2.1**:dA_{10} and **2.1**:dA_7 (complexes I and II, Figure 2.9). The significantly greater thermal stability of the former, combined with the slope-change observed at n=10 in the T_m vs dA_n plot (Figure 2.7), indicates that near full-length base pairing can occur with dA_{10} complement. In addition, this result suggest that the branch-point does not limit the "tails" ability to hybridize with complementary nucleic acids.

Comparison of the thermal stability of complexes I (T_m 35.3 °C) and III (T_m 32.8 °C), confirms the proposition that the branch-point does not present a significant deleterious steric or structural barrier. In addition, the branched residue can base-pair with a complementary residue in the target sequence, as suggested by the melting experiments with complexes III and IV (Figure 2.9). The complex containing a rA/dC mismatch (III) has a T_m which is 3-4 °C lower than that of the fully complementary complex (IV). This result indicates that interactions between the branchpoint residue and nucleotides of the target strand can in fact contribute to the stabilization of these triplexes. This observation is related to one described recently by Noll et al. in which a dT residue within a dT_4 loop

connecting two homopyrimidine binding strands interacts with an dA residue in the target sequence.[79]

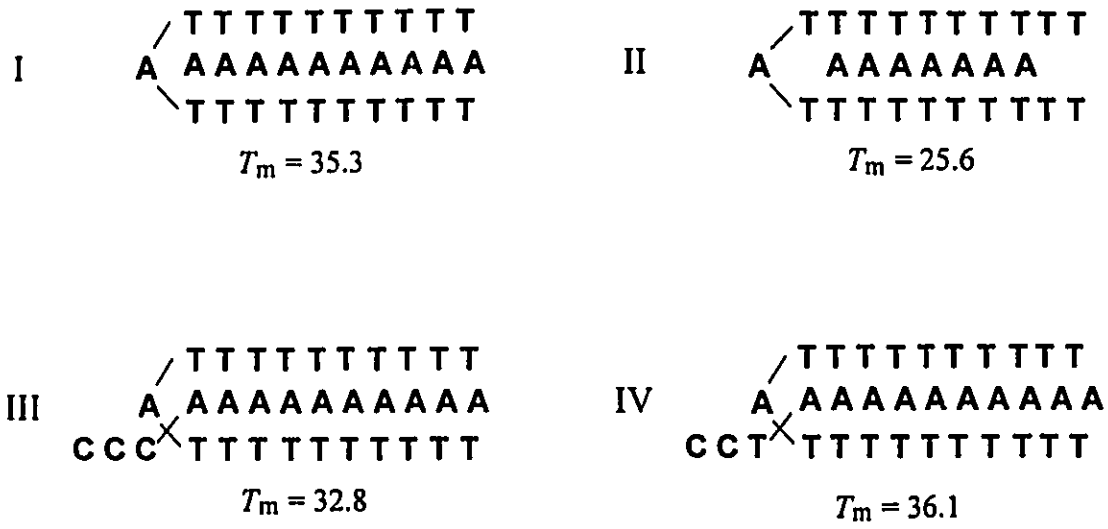

Figure 2.9. Effect on the target chain length and sequence on the T_m of branched complexes. Conditions: 50 mM $MgCl_2$, 10 mM Tris, pH 7.3.

2.2.8 Relative thermal stability of (parallel) T*AT versus (antiparallel) T•AT triplexes.

In order to compare more quantitatively the relative stability of parallel and antiparallel TAT triplexes, the melting temperatures of the "antiparallel" complex **2.1**:dA_{10} (T_m= 35 °C) and the bimolecular "parallel" complex [5'-dT_{10}-$dCTC_2$-dT_{10}-3']:dA_{10} (T_m 47 °C) was measured in 50 mM $MgCl_2$, 10 mM Tris, pH 7.3 buffer. The significantly lower melting temperature of the **2.1**:dA_{10} complex (ΔT_m= 12 °C) is consistent with the general understanding of antiparallel py-pu-py triplexes that are not very stable and usually hard to observe.

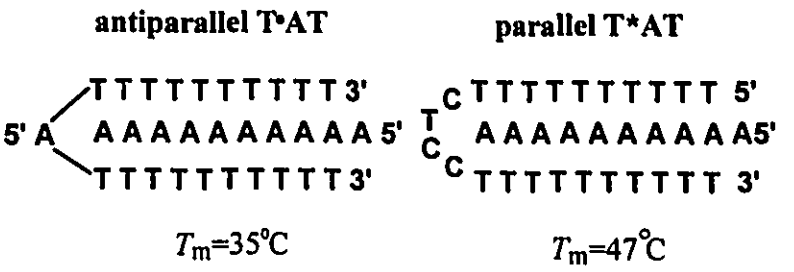

Figure 2.10. Relative stabilities of parallel and antiparallel TAT triple-helical complexes. Conditions: 10mM Tris, 50mM $MgCl_2$, pH 7.3.

2.2.9 Targeting polypyrimidine tracts adjacent to regions of mixed base composition.

Triplex formation has practical limitations due to the inherent problem of being only capable of targeting oligopurine tracts. Dervan *et al.* and others have addressed this issue by designing molecules that can recognize mixed sequence duplexes by alternate strand triplex formation.[80] Another way to circumvent this requirement is by synthesizing oligonucleotides with two binding motifs, capable of forming both Watson-Crick and Hoogsteen hydrogen bonds.[81]

Continuing with the theme of designing and constructing novel branched nucleic acids, a second generation "Y" compound was synthesized. A branched molecule with three domains was constructed having a "guide" sequence containing all four naturally occuring bases (Th, Ad, Gu, Cy), and two poly (dT) sequences of the same polarity. The function of the "guide" sequence and the poly (dT) strand would be to capture the complementary target strand via Watson-Crick hydrogen bonds and the role of the second poly (dT) strand would fold over and form the antiparallel triplex. The benefit of using a branched molcule to capture a single-stranded target is that the compound would be recognized twice, once by the "guide" portion (duplex formation) and then again by the third branch poly (dT) strand in triplex formation.

To delineate the properties of these branched oligonucleotide probes, the "Y" molecule (**2.2**) 5'-dGCGTACTACGTT-rA$^{[2'\text{-}5'\text{-}dT10]}_{[3'\text{-}5'\text{-}dT10]}$ was synthesized. The complex strengths were then compared for dA_{10} binding to the "V" (**2.1**) and "Y" (**2.2**) sequences. The resulting complex with the "Y" oligomer has a T_m which is 3.5 degrees higher than with the "V" oligomer, establishing that its 5'-"arm" has a small but decisive stabilizing effect. The 5'-arm would be expected to reduce the overall degrees of freedom of the 2' and 3'-dT_{10} strands and thus lead to enhanced stability (or reduced "breathing") of the triplex. The Damha group is currently investigating the influence of both the 5'-arm length and base sequence on the strength of binding with dA_{10} and other target sequences.

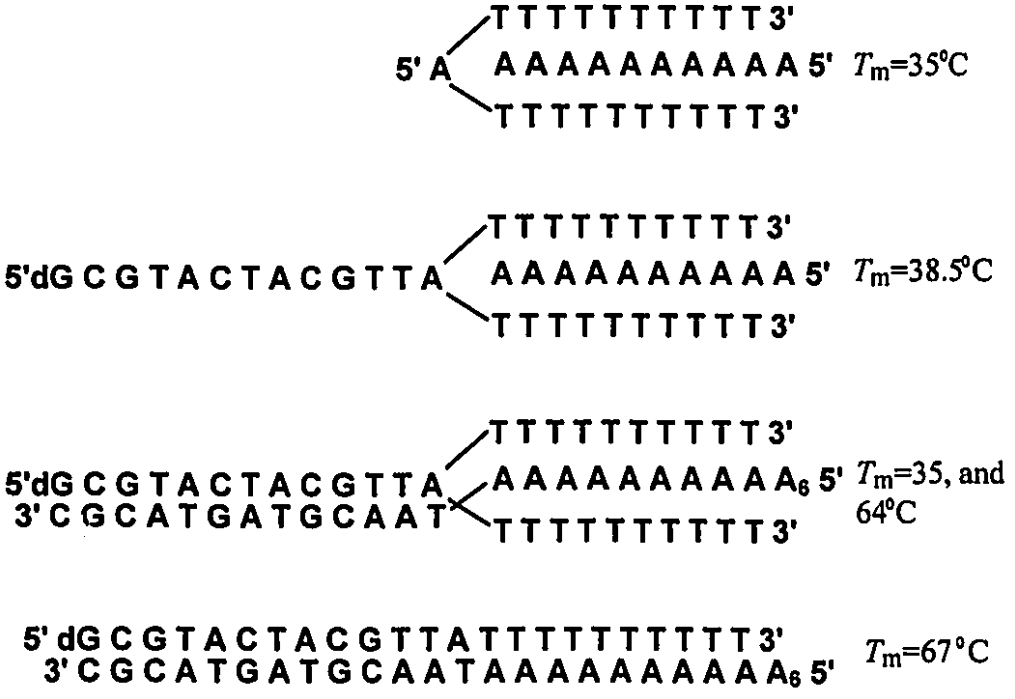

Figure 2.11. Branched "Y" Compound **2.2** with Two Binding Motifs: An Antiparallel T•AT Triplex and a Mixed Base Composition Duplex. The thermal stability of compound **2.2** was compared to a linear oligomer and compound **2.1**. Conditions: 50mM $MgCl_2$, 10mM Tris, pH 7.3.

The branched molecule **2.2** has two different binding motifs which can hybridize to a dA tract via reverse Hoogsteen triplex and to a mixed base sequence via duplex formation. As illustrated in Figure 2.12, thermal denaturation of **2.2**/dA_{10} gave a biphasic transition. The two transitions are well separated, due to the difference in thermal stability between

the duplex and triplex regions. Thus using this branched system, target molecules may be recognized twice once by duplex formation and then again by triplex formation via the branch strand. Branched compounds which have the ability to form chimeric "duplex-triplex" complexes with one molecule may have important implications for the development of novel nucleic acid based diagnostics.

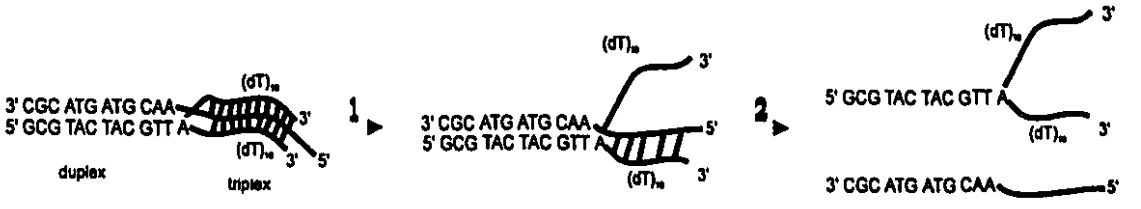

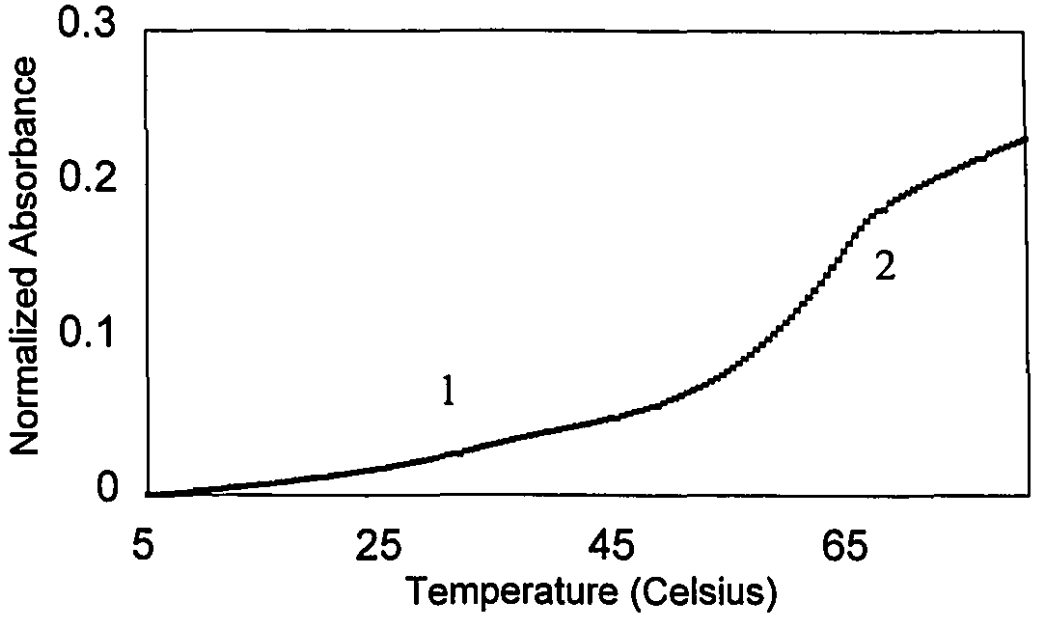

Figure 2.12. UV absorbance melting profile for the complex formed between **2.2** and dCGCATGATGCAATA$_{15}$ monitored at 260 nm in magnesium buffer (50 mM $MgCl_2$, 10 mM Tris, pH 7.3). Normalized change in absorbance was calculated by $[(A_t - A_o)/(A_f)]$ where A_t = absorbance at any temperature; A_o= initial absorbance; A_f = final absorbance.

2.3 Investigations of DNA binding ligands that stabilize (parallel) T*AT and (antiparallel) T•AT triplexes.

2.3.1 Background of DNA-Binding Ligands.

DNA structures and morphology are conveniently probed by nucleic acid binding ligands. Many ligands are known to interact in a noncovalent manner with the target oligonucleotide. Binding modes can be characterized as: (i) intercalation of the ligand, in which typically a planar aromatic moiety slides between the DNA bases - stabilized by π-π stacking and dipole interactions, or (ii) either minor or major groove interaction which is stabilized by hydrogen bonding, hydrophobic and/or electrostatic interactions[82]. Recently, a considerable amount of progress has been made with regard to probing and stabilizing triplexes with specific DNA-binding ligands. For example, Fox *et al.* have shown that 2,6-disubstituted anthraquinones selectively interact and stabilize triple-stranded DNA over duplex DNA.[83] Hélène and co-workers have recently demonstrated that a benzo[e]pyridoindole derivative (BePI) {3-methoxy-7H-8-methyl-11-[(3'-amino)propylamino]-benzo[e]pyrido[4,3-b]indole} (Figure 2.13) showed preferential binding to triple helical structures rather than to duplexes.[84] BePI having four planar rings can optimize stacking between the dye and the triplets upon intercalation. Hélène *et al.* have diligently characterized the ligand BePI, with regard to investigating its specific mode of binding to parallel T*AT triplexes.[85] BePI has been found to strongly stabilize triplexes having reverse-Hoogsteen G•GC and T•AT triplets.[86] Ethidium bromide binding to poly (dA)•poly(dT) has been found to preferentially stabilize these triplexes via an intercalative mechanism.[87] For parallel triplexes of mixed pyrimidine base composition, it has been shown that ethidium bromide destabilizes triple helical formation.[88] The minor groove binder, Hoescht 33258 has been widely utilized as a chromosome stain and it also has antibiotic and certain anticancer activity.[89] The benzimidazole rings of Hoescht 33258 fit tightly into the minor groove in A:T region similar to the pyrrole rings of netropsin and distamycin. It should be noted that both

Hoescht 33258[90] and a related minor groove ligand: netropsin, were shown to destabilize parallel T*AT triplexes.[91]

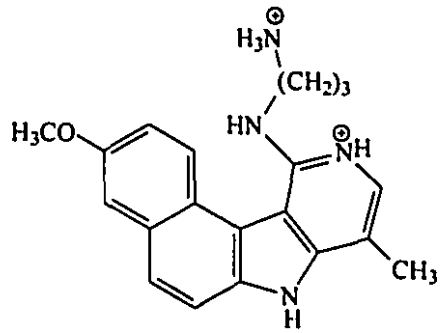

BePI

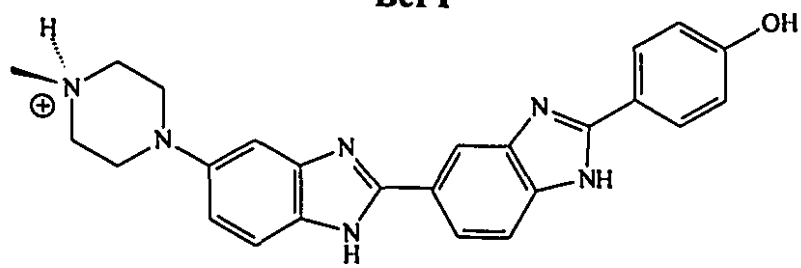

Hoescht 33258
(bisbenzimide)

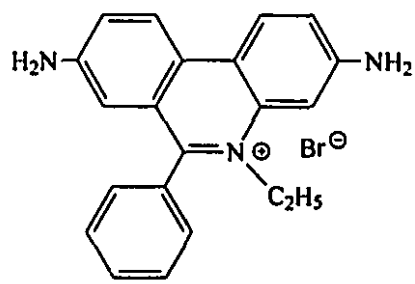

Ethidium bromide

Figure 2.13. The Structures of the DNA-Binding Ligands: BePI, Hoescht 33258, & Ethidium bromide.

Ligands have also been used to induce the formation of triplexes that would otherwise not form.[92] Triplexes, particularly the antiparallel T•AT triplex cannot be formed easily. For this reason, various DNA-binding agents were used in this study to dramatically enhance the triple helix stability of the antiparallel T•AT triplex. Specifically, the ligand binding of ethidium bromide, Hoescht 33258, and BePI to this triplex was investigated (Figure 2.11).

2.3.2 Thermal Melt Data of Ligand-DNA Interactions.

In order to measure the effects the ligands have on triplex and duplex stability, thermal denaturation experiments were conducted. As can be inferred from Table 2.3, the stabilization of the duplex or triplex upon binding of the ligand was calculated by the melting temperature difference between the complex with 10μM of the ligand and the complex alone.

Consistent with what has been previously observed by Hélène and co-workers for parallel triplexes, BePI stabilized both the parallel and antiparallel triplexes to a greater extent relative to the duplex control. In comparison to the duplex and the two triplexes, BePI stabilized the complexes in the order of: antiparallel triplex>parallel triplex>duplex.

Referring to Table 2.3, one will note that with ethidium bromide there were small differences with regard to the thermal stability of the complexes. The order of stability by binding of ethidium bromide was found to be: antiparallel triplex>parallel triplex >duplex. However, the thermal stability was not as profoundly affected as compared to using the BePI ligand.

It has been shown that the minor groove binder Hoescht 33258 selectively binds to TA tracts. Probing the structure of the AT duplex and parallel/antiparallel triplexes, using Hoescht 33258, it was found that this ligand preferentially stabilized the duplex relative

to the triplexes. This is consistent with what has been previously reported, however, the triplexes were also stabilized. This triplex stabilization may be attributed to unique structure of branched oligonucleotides. Triplex studies involving Hoescht were reported for sequences that bound to their complement strand in a two step dissociation proccess (*ie.* triplex to duplex to single strands).[91] Thus, for these triplex systems, it can be concluded that Hoescht may be utilized to stabilize these particular complexes which melt cooperatively as one transition.

Table 2.3. Thermal Melt with DNA-binding Ligands and AT duplexes and TAT antiparallel and parallel triplexes.

Complex	Ligand [¶]	T_m (°C)	%H	ΔT_m (°C)
antiparallel triplex				
"V" (**2.1**) + dA_{10}	-	35.3	22.8	-
"V" (**2.1**) + dA_{10}	Hoescht 33258	45.0	27.2	9.7
"V" (**2.1**) + dA_{10}	BePI	45.1	17.3	9.8
"V" (**2.1**) + dA_{10}	EtBr	38.7	14.6	3.4
Parallel Triplex				
$T_{10}CTC_2T_{10}$ + dA_{10}	-	47.1	21.0	-
$T_{10}CTC_2T_{10}$ + dA_{10}	Hoescht 33258	55.6	27.5	8.5
$T_{10}CTC_2T_{10}$ + dA_{10}	BePI	55.5	18.1	8.4
$T_{10}CTC_2T_{10}$ + dA_{10}	EtBr	50.0	11.3	2.9
duplex				
AT_{10} + dA_{10}	-	34.7	17.4	-
AT_{10} + dA_{10}	Hoescht 33258	49.0	23.2	14.3
AT_{10} + dA_{10}	BePI	40.0	15.9	5.3
AT_{10} + dA_{10}	EtBr	34.8	11.4	0.1

[¶]Ligand concentrations were 10μM. $\Delta T_m = T_{m(duplex+ligand)} - T_{m(duplex)}$ or $T_m = T_{m(triplex+ligand)} - T_{m(triplex)}$

Making a general comparison of the melting temperature changes observed for the various complexes, it should be noted that the antiparallel triplex showed a greater sensitivity to ligand binding relative to the parallel triplex. That is, the reverse Hoogsteen (antiparallel) triplex was stabilized to a greater extent than the Hoogsteen (parallel) triplex.

2.3.3 PAGE Retardation Assay

The electrophoretic mobility of both the Watson-Crick base paired dT_{10}:dA_{10} duplex, the Hoogsteen dT_{10}:dA_{10} triplex and reverse Hoogsteen **2.1**:dA_{10} triplex was studied in the presence of magnesium. In order to show the relative mobilities of the complexes and that ethidium bromide intercalates into both duplexes and parallel/antiparallel triplexes, a gel shift assay was run (Figure 2.14A) and stained with EtBr (Figure 2.14B).

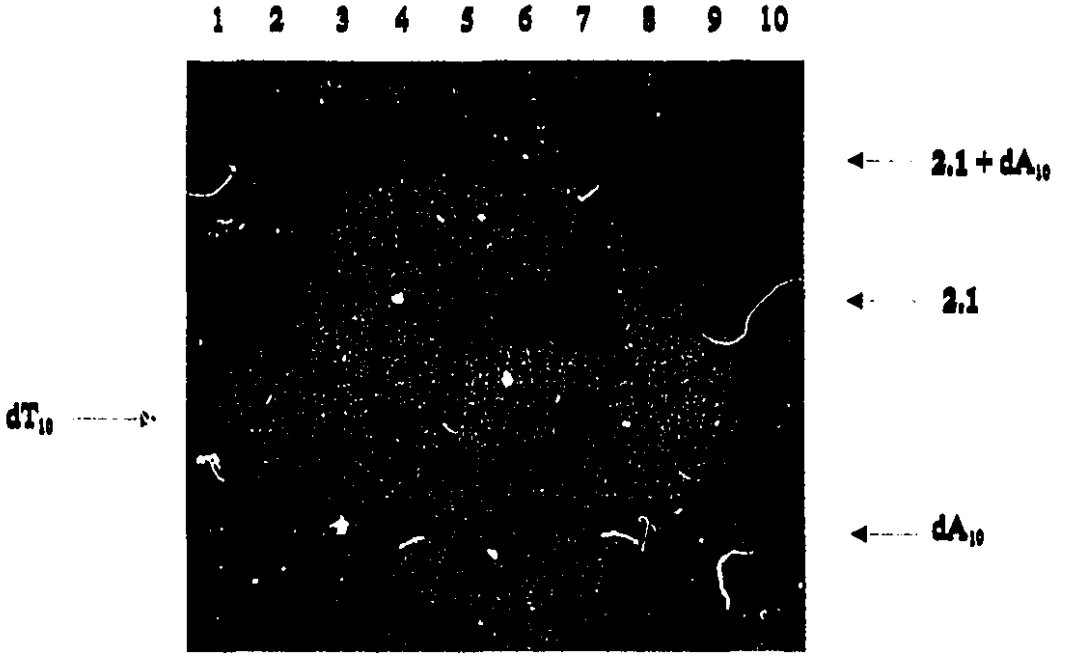

Figure 2.14 A. Photograph of a UV-shadowed native polyacrylamide gel containing single strands, duplex and triple helical complexes of branched and linear controls. DNA samples were loaded in 50mM $MgCl_2$, and 30% sucrose. Lanes 4-10 are dT_{10}, dT_{10}:dA_{10} (1:1),. dT_{10}:dA_{10} (2.5:1), dT_{10}:dA_{10}(4:1), dA_{10}, **2.1** + dA_{10}, and **2.1**, respectively. As can be noted the dT_{10}:dA_{10} triplex (lane 7) showed a greater retardation in the mobility relative to the corresponding duplex (lanes 5 and 6). The slowest mobility was observed in lane 9 for **2.1**:dA_{10}.

This PAGE retardation assay (Figure 2.14A) shows that the reverse Hoogsteen branch triplex has a slower mobility than the control linear dT_{10}*$dA_{10}dT_{10}$ Hoogsteen triple helix. The triple helix migrates more slowly than the duplex due to the presence of an additional pyrimidine strand. As the ratio of T_{10} to dA_{10} was increased, first only duplex was observed, finally only triplex was observed. Association of the **2.1** :dA_{10} was quantitative as evidenced by the complete disappearance of compound **2.1** and dA_{10}, when mixed in equimolar amounts. Furthermore, this gel shift assay proves that only one type of triplex (T•AT) is formed and not the A•AT which is too unstable under these salt conditions.[93]

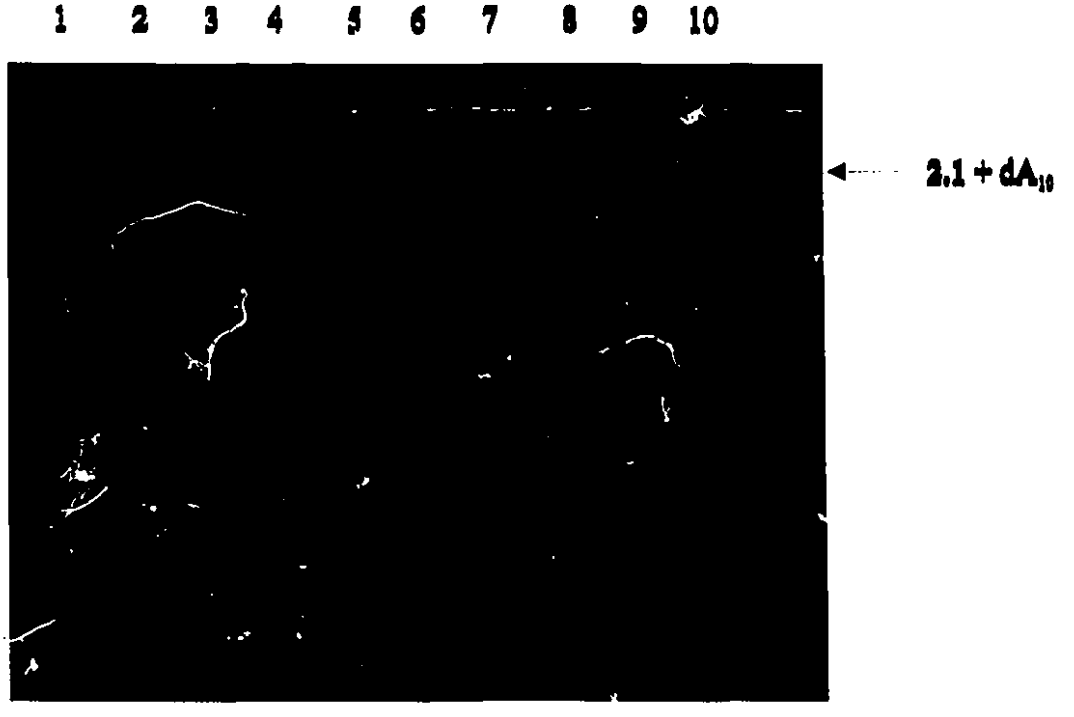

Figure 2.14 B. Photograph of an EtBr-stained native polyacrylamide gel (same gel as Figure 2.14A) containing single strands, duplex and triple helical complexes of branched and linear controls. DNA samples were loaded in 50mM $MgCl_2$, and 30% sucrose. Lanes 4-10 are dT_{10}, dT_{10}:dA_{10} (1:1),. dT_{10}:dA_{10} (2.5:1), dT_{10}:dA_{10}(4:1), dA_{10}, **2.1** + dA_{10}, and **2.1**, respectively. As can be noted the dT_{10}:dA_{10} triplex (lane 7) showed a slight retardation in the mobility relative to the corresponding duplex (lanes 5 and 6). The slowest mobility was observed in lane 9 for **2.1**:dA_{10}. Note that only the duplexes and triplexes showed ethidium bromide fluorescence (see Figure 2.14A).

Referring to Figure 2.142B, one notes that only duplexes and triplexes are stained with ethidium bromide, not single strands, consistent with what has been previously observed.[94] Interestingly, the **2.1**:dA_{10} complex has the lowest fluorescence intensity relative to the linear duplex and triplex controls. This may be attributed to less binding efficiency of the ethidium bromide to the antiparallel triplex. Thus, the decrease in fluorescence intensity is consistent with what was observed with the fluorescence studies (Section 2.4), proving unequivocally that the ethidium bromide's fluorescence intensity for antiparallel triplexes is less than for duplexes.

2.4 Detection of T•AT Triple-Helical DNA Using a Fibre Optic Biosensor.

2.4.1 Background on DNA Biosensors and Ethidium bromide Fluorescence.

Triple-helical oligonucleotides have been shown to be potentially used as: sequence specific artificial nucleases,[95] DNA-binding protein modulators/gene expression regulators,[96,97] genomic mapping,[98] and in screening methods to detect mutations within duplex DNA. Typically, a number of spectroscopic techniques[99] (CD, NMR, UV and fluorescence spectroscopy) in addition to gel mobility shift assays need to be implemented in order to study the formation of triple-helical nucleic acids. However, each of these methods have problems in terms of either the amount of material required for analysis (*e.g.* NMR and gel mobility assays), or are limited only to the investigation of certain triplex systems (i.e. only T•AT triplexes can be monitored by UV absorption spectroscopy at *ca.* 284nm). Various groups have developed methods for triplex detection.[100] The advantage provided by the optical sensor technology over standard fluorimetic investigations include the low detection limits provided by this methodology, reusability and reliability of the device, and the nondestructive nature of the assay (where samples may be collected and re-used). In addition this technique may easily be automated, thereby negating the requirement for skilled technicians to do the assay.

Piunno *et al.* had developed an effective and reliable biosensor for detection of duplex DNA.[62] This biosensor uses fluorescence as a method of transduction, and optical fibres as the waveguide of the fluorescence. Optical fibres were used for two reasons: firstly, the fibres could efficiently transmit light and an evanescent wave could be produced at the waveguide/solution interface. Secondly, the fibres transmit light via total internal reflection, and for every reflection point along the fibre there is an evanescent wave formed. Therefore, via total internal reflection the fluorophore can be excited and the emission of the fluorophore can then be detected with equipment to sense the light. The instrument setup of the biosensor developed by Krull and co-workers is illustrated in Figure 2.15.

Ethidium bromide, was the fluorescent dye chosen for the biosensor work since: (i) the maximum absorbance of ethidium upon binding to duplex DNA is 520nm - permitting an Argon ion laser with an output of 488nm to excite the dye, (ii) the bound dye's fluorescence increases over 100 fold relative to the free state, and (iii) upon intercalation the fluorescence maximum emission occurs at 590 nm enabling the emission/excitatory radiation to be separated by a dichroic mirror.[101]

Ethidium bromide binds to both duplexes and triplexes via an intercalation mode,[102] which has been studied extensively by fluorescence spectrophotometric methods. The fluorescence intensity of ethidium increases when it intercalates to duplexes[103] or triplexes, however, it has been shown that there is a marked difference between the fluorescence intensity between the two types of complexes.[104] LePecq and Paoletti were the first to observe that the fluorescence enhancement of ethidium during interaction with the duplex (poly rA)·(poly rU) was significantly greater than for binding to the triplex (poly rA)·(poly rU)$_2$.[105] More recent studies are in qualitative agreement, that the fluorescence of ethidium bromide is greater for duplexes than triplexes.[106] The results of molecular modelling studies suggest that reduced affinity of EtBr for triplexes (relative to duplexes) is due to the energetic cost of destacking base triplets as compared to successive base pairs.[107] Short homopolymeric T•AT triplexes have been the subject of

seminal fluorescence studies. Letsinger *et al.* have shown that for parallel T*AT triplexes, the fluorescence intensity decreases dramatically relative to the duplex.[108] Furthermore, independent confirmation of decreased fluorescence intensity for ethidium bound to parallel T*AT triplexes ($2xdT_{10}$:dA_{10}) relative to duplexes (T_{10}:dA_{10}) have appeared.[109]

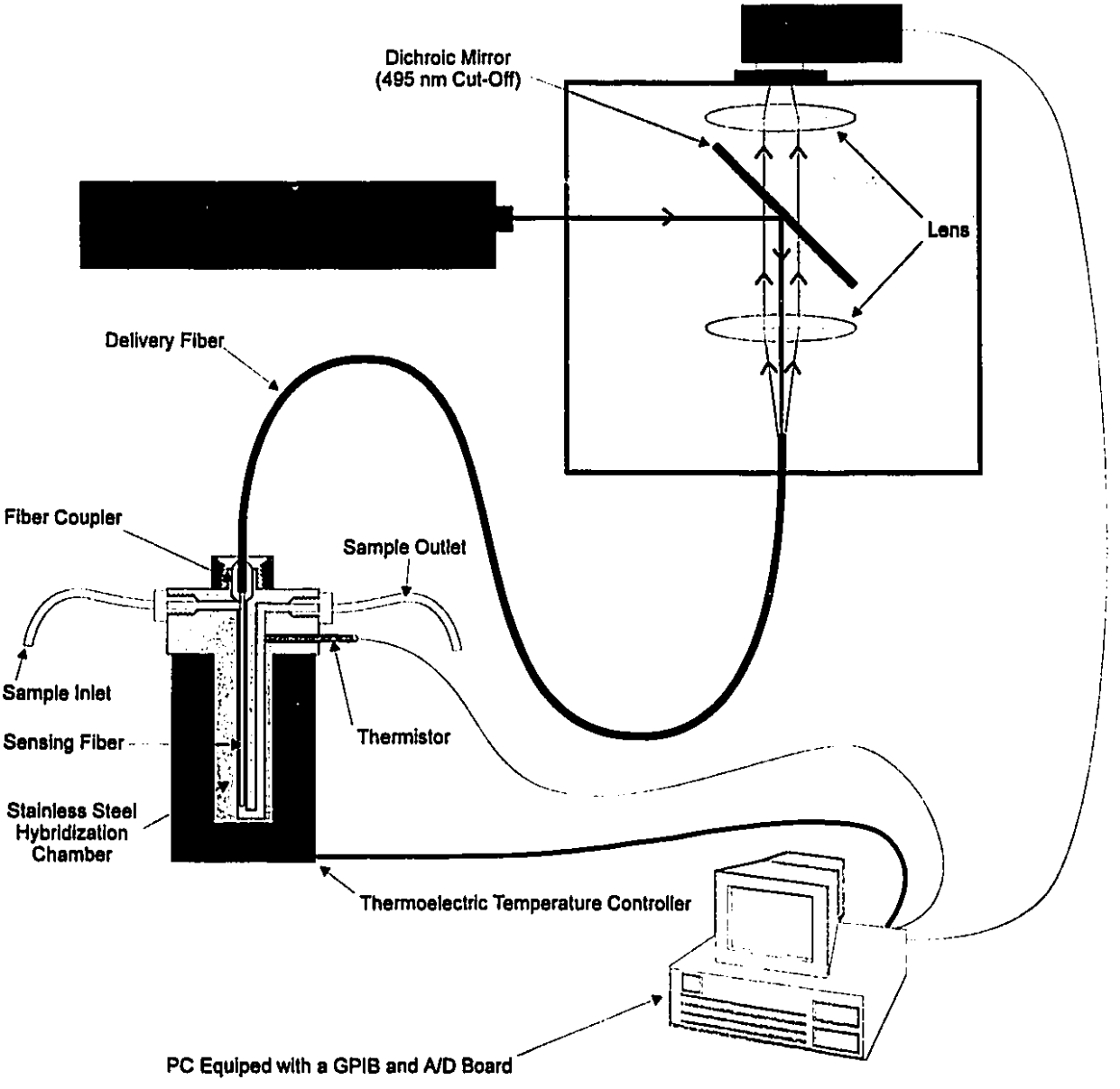

Figure 2.15. The optical fibre instrument setup, as developed by Piunno and Krull (Erindale College, University of Toronto). Unpublished results.

This biosensor technology was chosen to investigate whether it could be used to detect triple-helical DNA, in particular T*AT and T•AT triplexes. An assay for the rapid detection of triple-helical nucleic acids would provide a significant contribution to the biochemical community as a means to screen potential antigene candidates and determine their dose-dependent inhibitory properties.

2.4.2 Activation of Optical Fibres and subsequent Oligonucleotide Synthesis.

Prior to oligonucleotide assembly it was necessary to activate the surface of the optical fibres according to the procedure developed by Piunno *et al*,[101] illustrated in Figure 2.16. The first step involved cleaning the fibres to remove cladding, followed by activation with 3-glycidopropyltrimethylsilane (GOPS) and diisopropylethylamine (DIPEA) in dry xylene.[110] The addition of GOPS to the fibre accomplished two goals: (i) it formed a stable silyl ether bond with the surface and (ii) provided a handle for chain extension from the epoxide moiety. The next step involved nucleophilic ring opening of the epoxide, using monotritylated pentaethylene glycol (DMT-PEG) and a catalytic amount of sodium hydride in xylene. The loading of the DMT-PEG on to the fibres was followed by sampling portions of silica gel which were activated along with the fibres (Figure 2.17). The last step of activation involved capping of the free hydroxyl groups with chlorotrimethylsilane.

The resulting fibres (Figure 2.18) were further derivatized by growing dA_{10} via solid-phase phosphoramidite synthesis. The first set of fibres were derivatized with a conventional 3'-phosphoramidite, to give 5'-dA_{10}-3' on the fibres. A 5'-phosphoramidite (synthesis described below) was used to make the reverse 3'-dA_{10}-5' derivatized set of fibres. The decaadenylate was grown in both orientations since it was not possible to predict which direction would afford the best results. However, the "reverse" dA_{10} may allow for better binding with compound **2.1** since it had previously demonstrated that the branch point was sensitive to environmental changes.

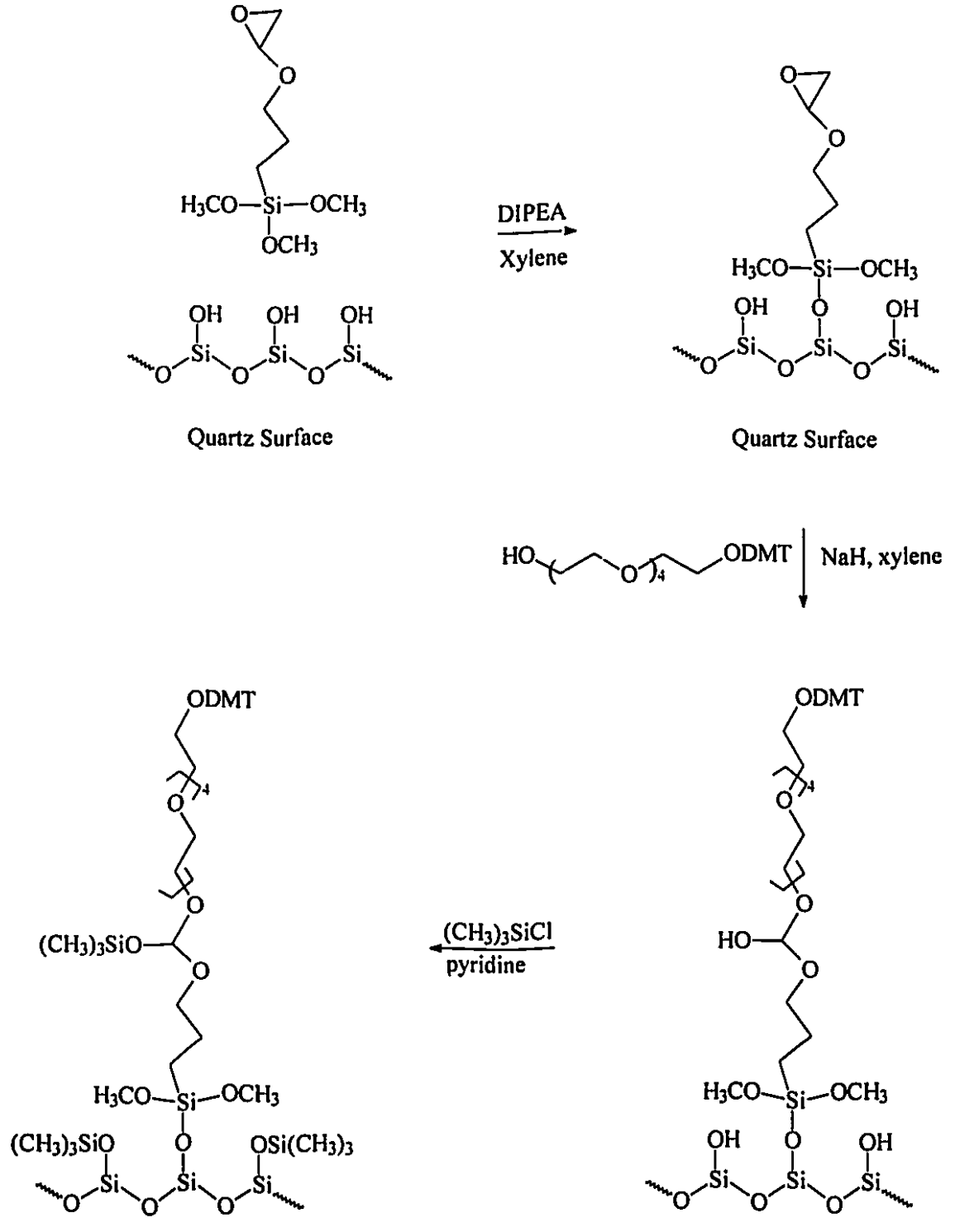

Figure 2.16. Derivatization of the Optical Fibre Surface according to the methodology developed by Dr. Krull and co-workers (University of Toronto), (unpublished results).

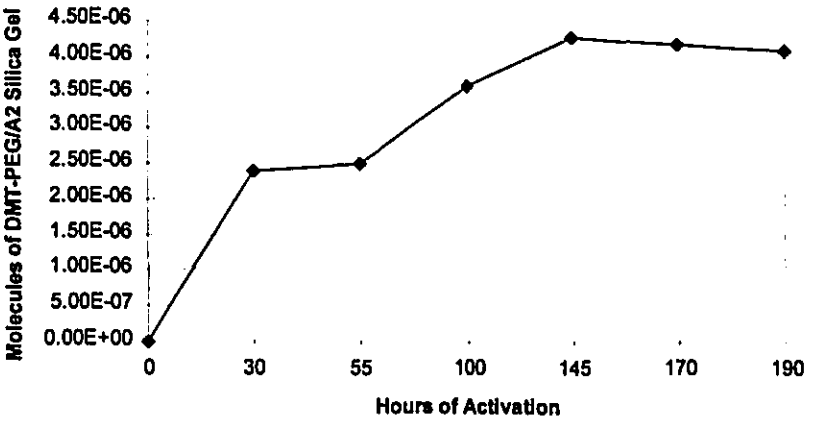

Figure 2.17. The Optical Fibre Activation Profile: loading of DMT-PEG as a measure of time. The loading of the DMT-PEG was followed by sampling portions of silica gel which were activated simultaneously with the optical fibres.

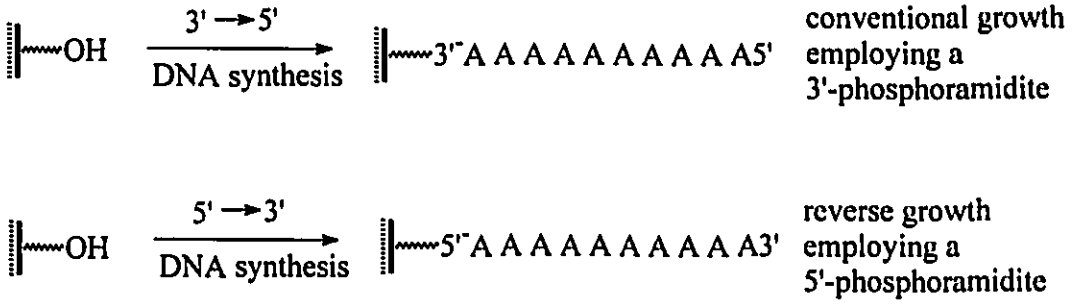

Figure 2.18. Orientation of dA_{10} on the Optical Fibres. Note: dA_{10} oriented in the conventional 5' to 3' direction is denoted as 5'-dA_{10}-3', and the reverse direction is denoted as 3'-dA_{10}-5'.

2.4.3 Synthesis of 5' Amidite Needed for Reverse dA_{10} Oligomer Growth.

Chemical synthesis of nucleic acids in the 5'- to 3'- direction rather than conventional 3'- to 5'- direction requires "reverse" 5'-phosphoramidite-3'-dimethoxytrityl nucleoside monomers. Referring to Figure 2.19, the first step of the synthesis involved taking commercially available 5'-O-dimethoxytrityl-N^6-benzoyldeoxyadenosine (**2.3**), and protecting the free 3' hydroxyl with the dimethoxytrityl ether using 4,4'-dimethoxytrityl chloride in anhydrous pyridine. A 4,4'-dimethoxytrityl ether was chosen as a protecting group as this would allow us to selectively remove the 5'-protecting group using zinc bromide, and it would permit us to monitor the coupling efficiency during DNA synthesis

upon release of the DMT^{+} cation (λ_{max}=504nm). This selective removal of the 5'-dimethoxytrityl group was done by reacting crude compound (**2.4**) with $ZnBr_2$ in anhydrous nitromethane at 0 °C for 24 minutes[111] to yield pure compound (**2.5**) in 73% yield (two steps) after flash chromatography. The N^6-benzoyl group was removed from compound (**2.5**) quantitatively using a 3:1 ratio of ammonia to ethanol to yield **2.6**. Protection of the exocyclic amine of crude (**2.6**) using phenoxyacetyl chloride afforded (**2.7**) in 42% yield (two steps) after column chromatography. A phenoxyacetyl protecting group was used instead of the benzoyl group since it is more labile and can be quickly removed under milder conditions (ammonia/ethanol 4:1, 2h., r.t.) and thus minimize loss of oligomers from the surface. Phosphitylation of pure (**2.7**) afforded the desired phosphoramidite (**2.8**) in quantitative yield.

2.4.4 Triplex Studies with 5'-dA_{10}-3' Derivatized Optical Fibres.

Characterization of the triple-helical complexes via thermal denaturation studies were made under the same conditions as used in this present study. Subsequently, fluorescent studies on the optical fibres were then conducted. As illustrated in Figure 2.18 (top), the dA_{10} was grown in the conventional direction. A solution of dT_{10} (or **2.1**) and ethidium bromide was heated in the hybridization chamber containing the decaadenylate optical fibres. Upon slow cooling, fluorescent measurements were taken at various temperatures. Figure 2.20, illustrates that as the dT_{10}:dA_{10} duplex was formed by lowering the temperature there was an increase in the fluorescence intensity, corresponding to ethidium bromide intercalation into this complex. After further lowering of the temperature a decrease in the fluorescence intensity was observed, indicative of triplex formation ($2xT_{10}$:dA_{10}), as illustrated in Figure 2.21. Interestingly, for the reverse-Hoogsteen forming **2.1** an increase in the fluorescence was observed (with comparable intensity as that of the background), as the temperature was lowered - indicative of no complex formation (data not shown). It is quite plausible that either the linker on the

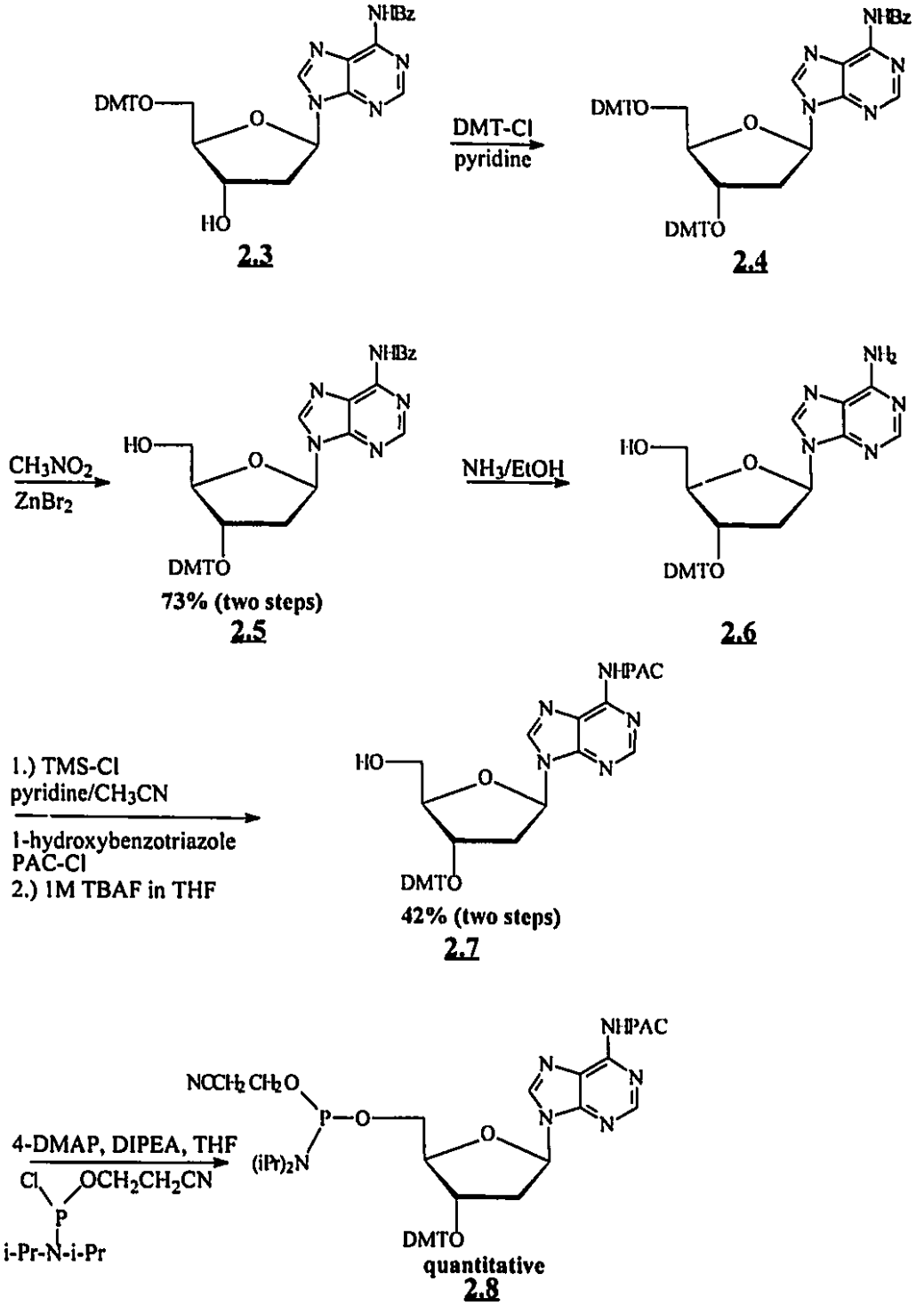

Figure 2.19. Synthesis of the deoxyadenosine 5'-phosphoramidite required for reverse dA_{10} oligomer growth.

surface or the packing density of oligomers prevented complex formation for these branched oligomers using this particular dA_{10}orientation. Previously it was shown that the branchpoint region was only modestly destabilized by mismatched targets. In addition, it was also demonstrated that a minimum of five base triplets were a requirement for antiparallel triple helix formation,[112] in agreement with recent studies of parallel triplexes.[113] In order to test whether steric interference surrounding the branch-point prevented triple-helical formation an oligomer was synthesized in the opposite direction (i.e. 5'→ 3').

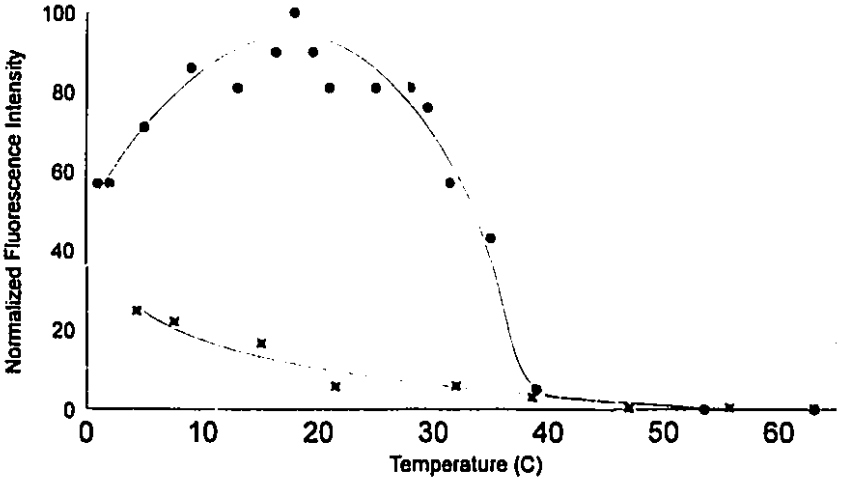

Figure 2.20. Fluorescent intensity as a function of temperature for dT_{10} using 5'-dA_{10}-3' derivatized fibres. Response (•) of the optical sensor with a 5'-end terminated recognition sequence to 1500ng/mL of linear dT_{10} in the presence of 2.5×10^{-8}M ethidium bromide. Response (**X**) of the optical sensor to 2.5×10^{-8} M ethidium bromide and no dT_{10}.

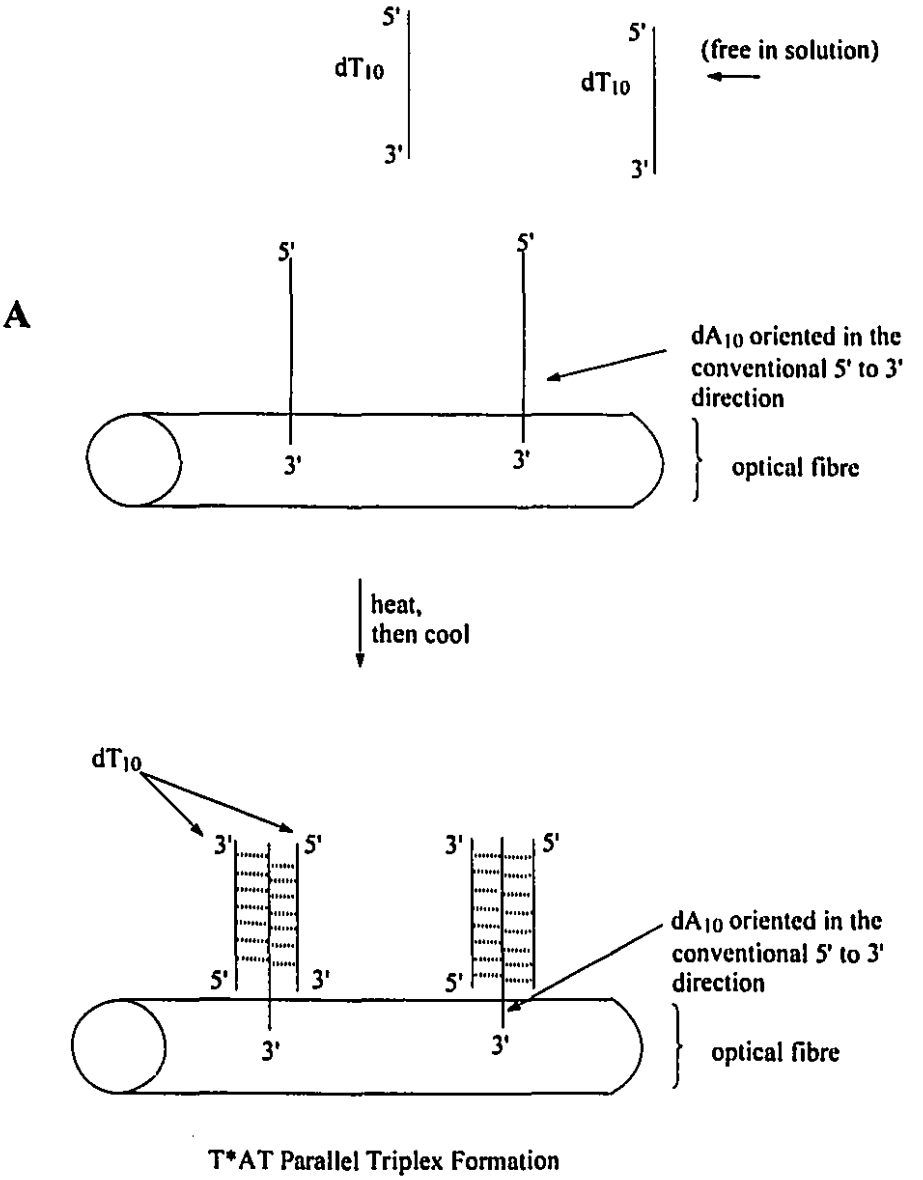

Figure 2.21. A Model of parallel (T*AT) triplex formation using dT_{10} and conventionally grown dA_{10}. After heating, the solution was cooled to form the dT_{10}:dA_{10} duplex first and then the triplex.

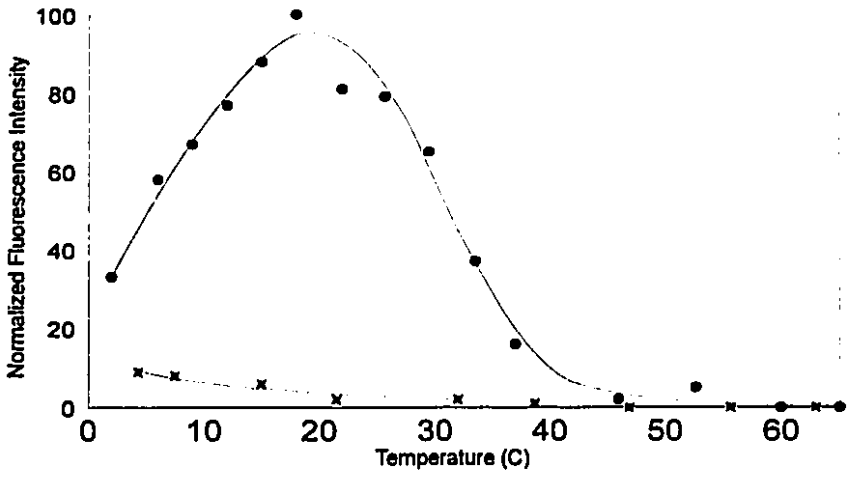

Figure 2.22. Fluorescent intensity as a function of temperature for dT_{10} using 5'-dA_{10}-3' derivatized fibres. Response (•) of the optical sensor with a 3'-end terminated recognition sequence to 1500ng/mL of linear dT_{10} in the presence of 2.5×10^{-8}M ethidium bromide. Response (**X**) of the optical sensor to 2.5×10^{-8} M ethidium bromide and no dT_{10}.

2.4.5 Triplex Studies with 3'-dA_{10}-5' Derivatized Optical Fibres.

The above findings indicated that these branched oligomers could not form a complex on the conventionally 5'-dA_{10}-3' derivatized surface. Thus, dA_{10} was grown on the fibres in a reverse orientation in order to optimize the binding conditions for these molecules, as illustrated in Figure 2.18 (bottom). From Figure 2.22, the fluorescent intensity versus temperature profile indicated that with dT_{10} there was an initial increase in fluorescence indicative of duplex formation, followed by a decrease in the intensity indicative of triplex formation. Testing the "V" compound **2.1** using the assay for triplex formation, showed that it did form a triple-helical structure as indicated by fluorescent results obtained in Figure 2.24. There was a decrease in fluorescence intensity for the reverse Hoogsteen complex **2.1**/3'-dA_{10}-5' below the melting temperature (35 °C) which is consistent with exclusion of some ethidium bromide from the triple-helical complex (Figure 2.23). In this regard, fluorescence studies involving ethidium bromide binding to triple-helices is in full agreement with several earlier findings.

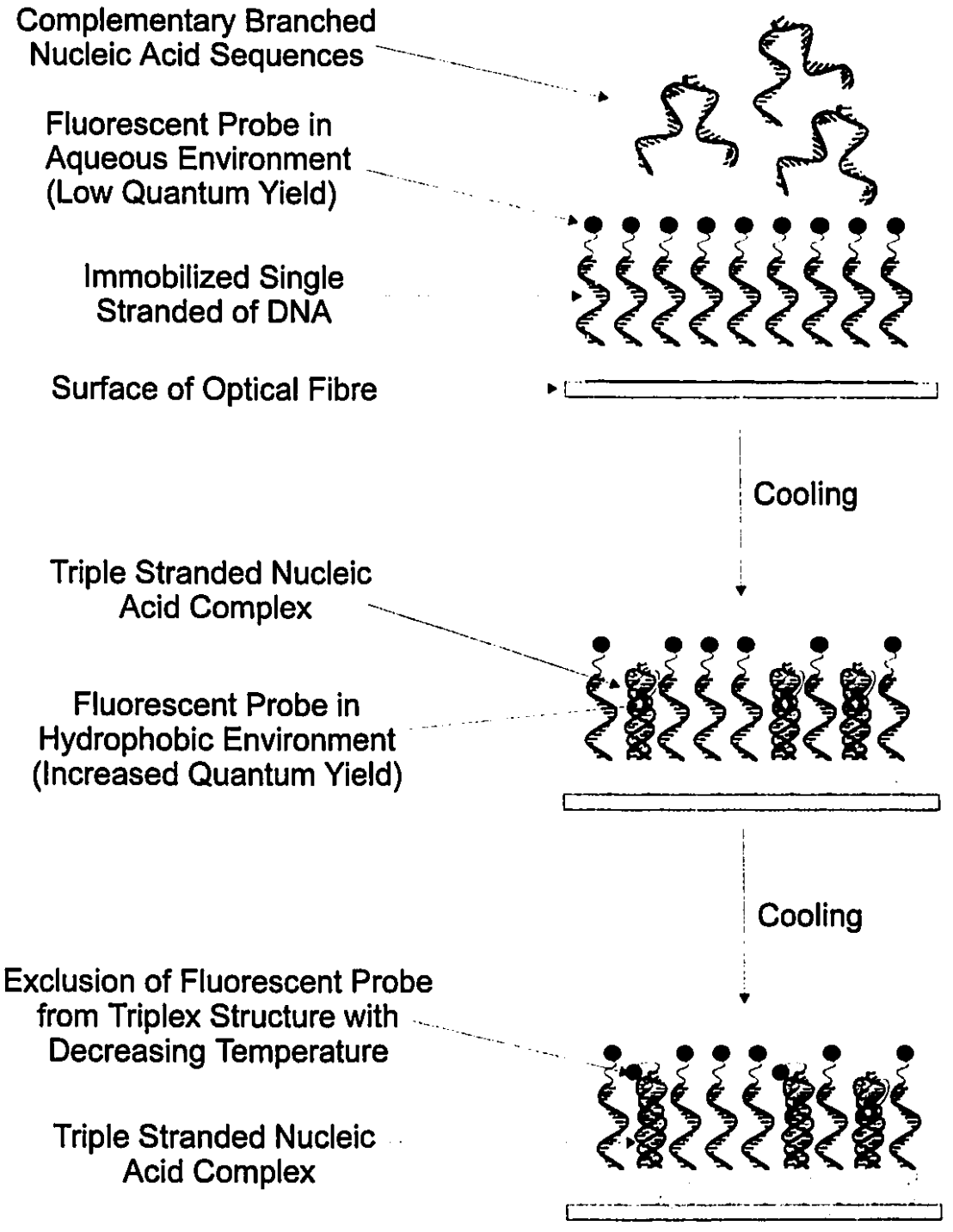

Figure. 2.23. The dA_{10} of the optical sensor capturing the branched "V" compound **2.1**. Note how the fluorescent probe is excluded from the triplex as the temperature is cooled. Also, in this illustration the fluorescent probe is attached to the optical sensing unit via a flexible linker, this particular modification was not employed in the fluorescent experiments that were done in this thesis.

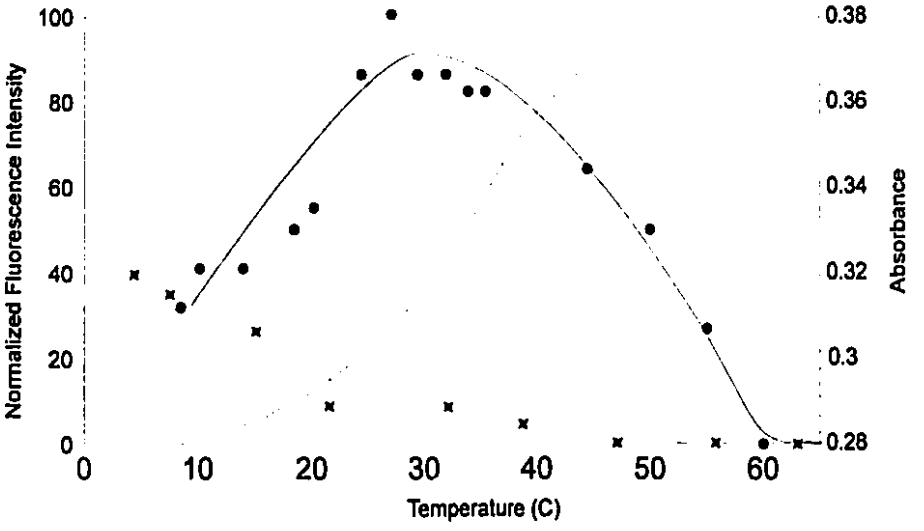

Figure 2.24. Fluorescent intensity as a function of temperature for **2.1** using 3'-dA_{10}-5' derivatized fibres. Response (•) of the optical sensor with a 3'-end terminated Recognition Sequence to 700ng/mL of **2.1** in the presence of 2.5 x 10^{-8}M ethidium bromide. Response (**X**) of the optical sensor to 2.5 x 10^{-8} M ethidium bromide with no **2.1**.

Based upon the fluorescent results that were obtained with compound **2.1**, there are different explanations to account for the increase and subsequent decrease in fluorescence as the temperature was lowered. One possibility is that once the triplex forms ethidium bromide is "pushed out" *ie.* the exclusion phenomena predominates since the triple-helical complex is more stable than the triplex with ethidium.

2.5 Conclusions.

For the first time, it was shown that branched poly(pyrimidine) oligonucleotides can promote the formation of antiparallel T•AT triple helices. Due to the rigid structural features of branched oligonucleotides, triple-helices that are not stable enough to form in an intermolecular complex may now be studied. These branched molecules will be particularly useful for studying complexes in which structural data is not yet available. It was also shown that branched "Y" molecules consisting of two binding motifs, can bind to a target single strand by both Watson Crick and reverse Hoogsteen modes. This "Y"

molecule demonstrates the potential usefulness of these branched oligonucleotides for targetting single stranded nucleic acids (*eg.* mRNA, DNA).

Furthermore, it was demonstrated that BePI selectively stabilized the antiparallel and parallel T•AT triplexes over duplex DNA. It was also shown that antiparallel triplexes are more sensitive to ligand binding than parallel triplexes. The minor groove binder Hoescht 33258 increased the duplex thermal stability more than either of the triplexes.

A rapid assay for specifically detecting TAT triple-helical DNA was developed. An assay for the rapid detection of triple-helical nucleic acids would provide a significant contribution to the biochemical community as a means to investigate biologically relevant three stranded structures. Also, given that the optical sensors created have been observed to maintain full activity even after autoclaving, this technology could be perhaps advanced to *in-vivo* investigations. Since there is a considerable amount of interest in antigene therapeutics as a new class of pharmaceuticals, a rapid method for screening potent drug candidates is required.[114] Fruitful studies involving this new triplex biosensor can be expected to follow.

Chapter 3- Novel Branched Oligonucleotides with an N^3 Functionalized Thymidine Linker: Synthesis and Hybridization Studies.

3.1 Introduction.

With recent advances in nucleic acid nanotechnology,[115] and with the progress made towards the synthesis of novel DNA macromolecules: "dendrimers",[58a] "circular",[9b,c, 116] and "cage"[117] oligomers, novel bNAs having a flexible linker may find use in biotechnology applications.[118] With the inability of DNA triplex structures to form under physiological conditions,[119] several strategies are being developed to enhance the ability of oligonucleotides to form more stable triple helices: the use of minor group binders,[120] the covalent attachments of intercalators,[121] and backbone and base modifications.[122]

A number of studies involving flexible linkers as non-nucleoside loop replacements have appeared in the literature, for enhancing the thermal stability of both duplexes[123] and triplexes.[9d,60a,69,71,117a] Linkers are useful since they can be used to reduce the number of nucleosides needed for bridging a duplex or a triple-helical complex. Furthermore, these aliphatic linkers would confer resistance to enzymatic degradation, which may find important uses for DNA-biosensors or other biological applications. "Comb"-like nucleic acids have been prepared by a combination of a linear synthesis and subsequent orthogonal synthesis involving branching off cytosine bases.[124] However, there has been no reported use of these compounds for triple helix formation.

A new synthetic methodology, for constructing bNAs whereby each "arm" of the compound having a different base sequence has been developed. That is, with the possibility of varying the base sequence by extension of the 5' end (after addition of the branching synthon), a "Y" branched molecule that has two binding domains was constructed. The "Y" compound synthesized in this study has one dT_{10} "arm" which is linked to the branched oligonucleotide. This linker served a two fold purpose: it enabled a branching synthesis with an independent sequence from the main oligonucleotide and it

served to join intramolecular triplex forming strand to the oligomer. This branched molecule will be able to recognize a single stranded target twice, once by the "guide" segment and again by the third triplex forming strand, as illustrated in Figure 3.1.

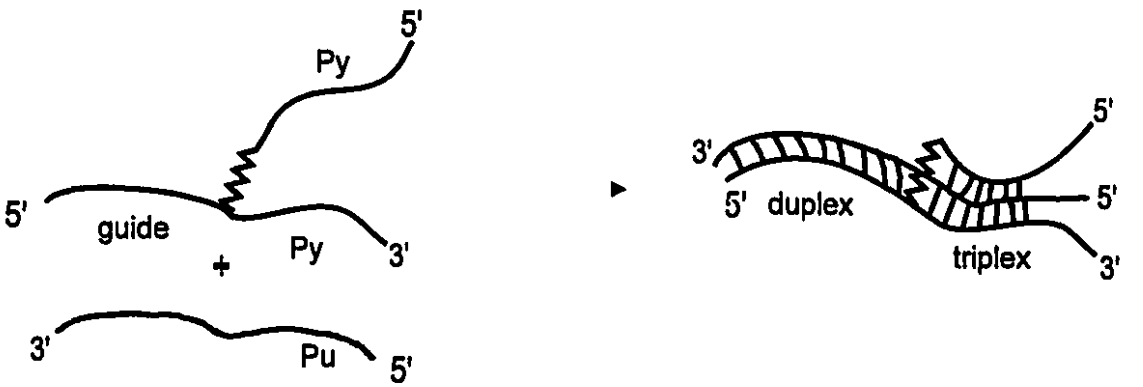

Figure 3.1. The branched strategy for capturing single stranded DNA or RNA. Note: Py and Pu represent pyrimidine and purine sequences, respectively.

Our studies on triplex forming branched oligonucleotides have been further motivated by the Damha laboratory's long-standing and continuing interest in the biological role of branched RNA. However, there has only been a very limited number of reports describing the solid phase synthesis for branched oligonucleotides of any base sequence and chain length.[125] Therefore, a novel synthetic methodology for constructing bNA's having a flexible linker was developed.

3.2 Results and Discussion.

3.2.1 Synthetic Methodology for "V" and "Y" bNA's containing a Flexible Linker.

In order to investigate the influence of the aliphatic linker length on triplex stability, **3.1** and **3.2** were prepared and fully characterized by Roman and Damha (Figure 3.2).[126] While the incorporation of non-nucleoside bridges as hairpin loops inside an oligonucleotide has been described, this new approach uses a N^3-funtionalized thymidine branched to an aliphatic chain. The main merit of this strategy is that this loop replacement provides a 5'-branching point for future substitutions or chain growth.

The incorporation of the branching synthon **3.1** and **3.2** into "V" type oligomers is illustrated in Figure 3.3A by the synthesis of oligomer **3.3** and **3.4**, respectively. Thus, dT_{10} (1.0 μmol) was assembled on an automated DNA synthesizer using standard phosphoramidite protocols and controlled-pore glass (23 μmol dT/g) as the solid support. The branching synthon (either **3.1** or **3.2**) was introduced as a 0.15 M solution with an 80% and 38% efficiency (unoptimized), respectively, based upon the yield of the dimethoxytrityl cation released after coupling. The terminal 5'-hydroxyl was then acetylated with capping solution. The levulinyl protecting groups were removed

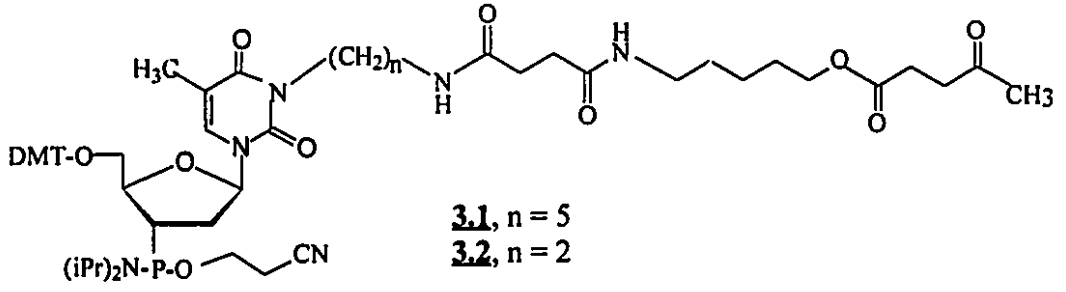

3.1, n = 5
3.2, n = 2

Figure 3.2. Structure of the Branching Synthon. A novel N^3-Functionalized Thymidine Linker. Linkers of two lengths (n=5 and n=2), correspond to compounds **3.1** and **3.2**, respectively, and were prepared by Roman & Damha.[126]

manually with a solution of hydrazine hydrate using conditions which did not cause the cleavage of the oligomer from the support.[127] After thorough washing with dry MeCN, the column was re-installed on the synthesizer, and chain assembly of another dT_{10} strand was continued in the normal fashion. Quantitation of trityl cations released, indicated that delevulination and subsequent coupling steps proceeded with *ca.* 98% yield. After deprotection with aqueous ammonia/ethanol (3:1, r.t., 24 h), the oligomer was purified by preparative polyacrylamide gel electrophoresis (PAGE) on denaturing gels (24%/7 M urea). Desalting by size exclusion chromatography (Sephadex G-25) afforded 22 A_{260} units (35%) of oligomer **3.3** and 2.1 A_{260} units (4.7%) of oligomer **3.4**.

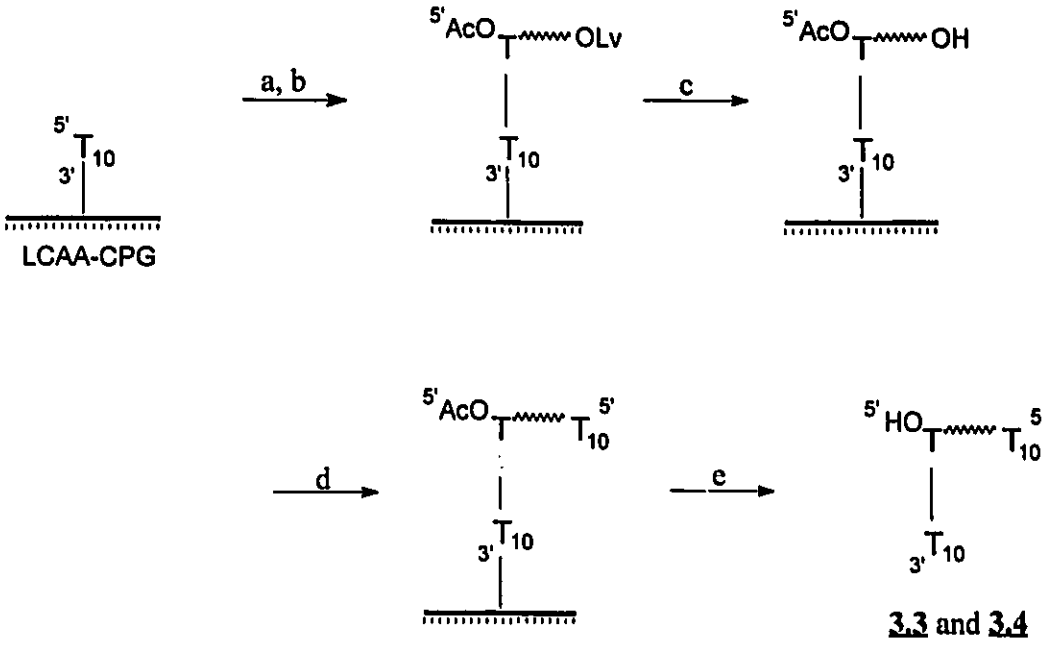

Figure 3.3 A. Synthesis of "V" Compounds **3.3** (n=5) and **3.4** (n=2). *Reagents and conditions*: a, coupling of **3.1** (n=5) or **3.2** (n=2), respectively (0.15M) dissolved in THF-MeCN, CH_2Cl_2 (2:2:1), tetrazole, 15 min.; b, Ac_2O/2,4,6-collidine/N-methylimidazole, 8 min.; c, 0.5M hydrazine hydrate in AcOH-pyridine, 5 min.; d, 3'→5' DNA synthesis; e, NH_3-EtOH (3:1), 24 h.

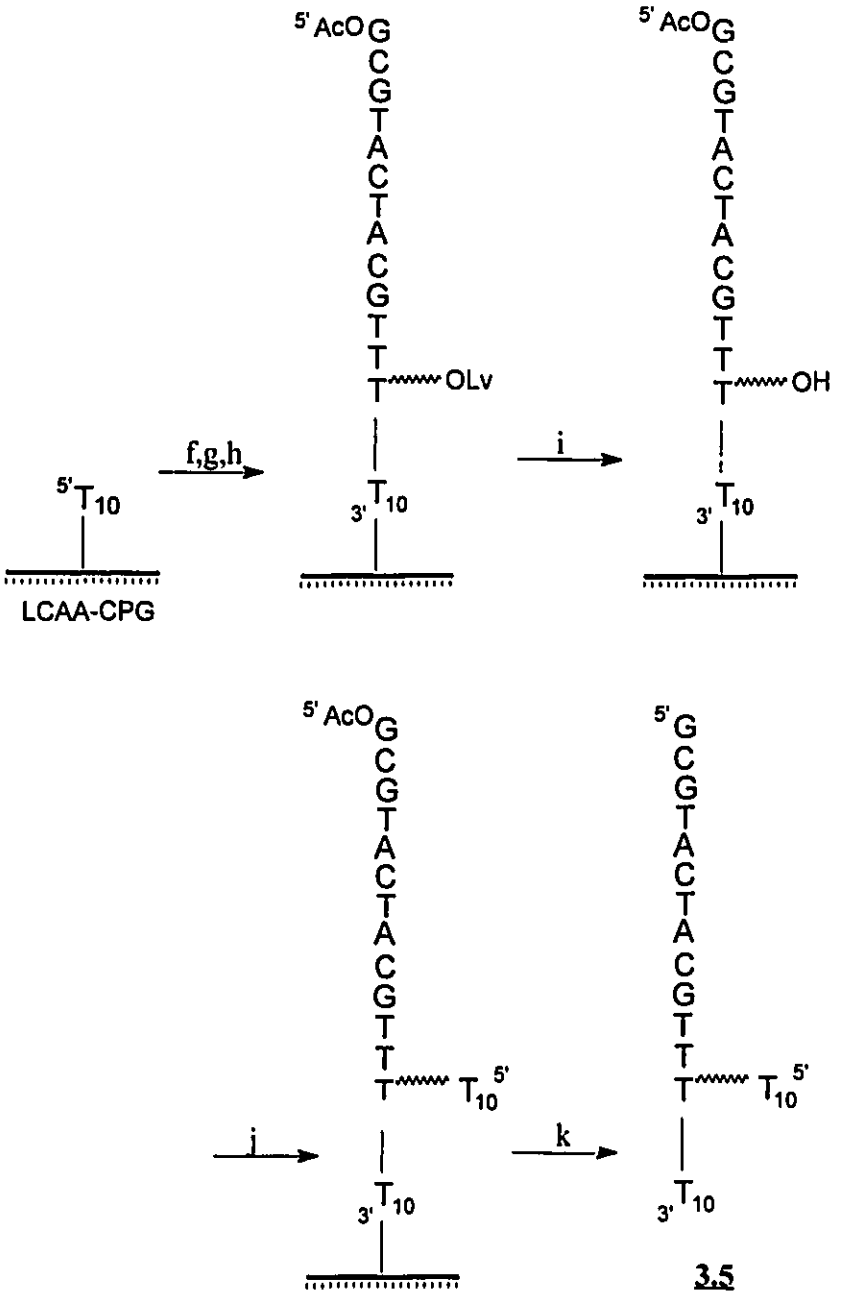

Figure 3.3 B. Synthesis of "Y" Compound **3.5** (n=2). *Reagents and conditions*: f, coupling of **3.2** (0.15M) dissolved in THF-MeCN, CH_2Cl_2 (2:2:1), tetrazole, 15 min.; g, 3'→5' DNA synthesis of mixed base composition; h, Ac_2O/2,4,6-collidine/N-methylimidazole, 8 min.; i, 0.5M hydrazine hydrate in AcOH-pyridine, 5 min.; j, 3'→5' DNA synthesis; k, NH_3-EtOH (3:1), 48 h. Note: all reactions were carried out at room temperature.

In designing the branched Y compound, a molecule which would bind to its target molecule first by Watson-Crick and then by Hoogsteen base pairs (in the 5' to 3' orientation) was chosen. Using hairpins with two binding motifs, Hélène and coworkers had shown that this orientation plays an important role for optimizing the complex stability. Therefore, the synthesis of the "Y" oligonucleotide with the linker (**3.2**) was conducted as illustrated in Figure 3.3B. First, dT_{10} (1.0 μmol) was assembled on an automated DNA synthesizer using standard phosphoramidite protocols and controlled-pore glass (23 μmol dT/g) as the solid support. The branching synthon (**3.2**) was introduced as a 0.15 M solution in THF/MeCN/CH_2Cl_2 (2:2:1) with a 38% efficiency (unoptimized) based upon the yield of the dimethoxytrityl cation released after coupling. The next step involved growing a mixed base sequence from the 5' hydroxyl. The terminal 5'-hydroxyl was then acetylated with Ac_2O/2,4,6-collidine/N-methylimidazole. The levulinyl protecting groups were removed manually with a solution of hydrazine hydrate using conditions which did not cause the cleavage of the oligomer from the support (0.5 M NH_2NH_2/H_2O in pyridine/acetic acid, r.t., 5 min). After thorough washing with dry MeCN, the column was re-installed on the synthesizer, and chain assembly of another dT_{10} strand was continued in the normal fashion. Based on the trityl cations released, the delevulination and subsequent coupling steps proceeded with quantitative yields. After purification by PAGE, compound **3.5** was obtained in 7.6% overall yield.

3.2.2 Characterization of "Y" and "Y" Molecules.

Analysis of compound **3.3** by analytical PAGE (Figure 3.4) and capillary electrophoresis (Figure 3.5) indicated that it was present as a single species, and its migration was comparable to that of unmodified sequences of similar chain lengths. The presence of the linker within the DNA sequence could be confirmed after hydrolysis with snake-venom phosphodiesterase and alkaline phosphatase, and analysis of the resulting mixture by HPLC (Figure 3.6). These enzymes hydrolyzed **3.3** to produce a mixture of dT and dT-

linker in the anticipated 20:1 ratio. Finally, the molecular weight determined for **3.3** by ion-spray MS was found to be in agreement with the calculated value.

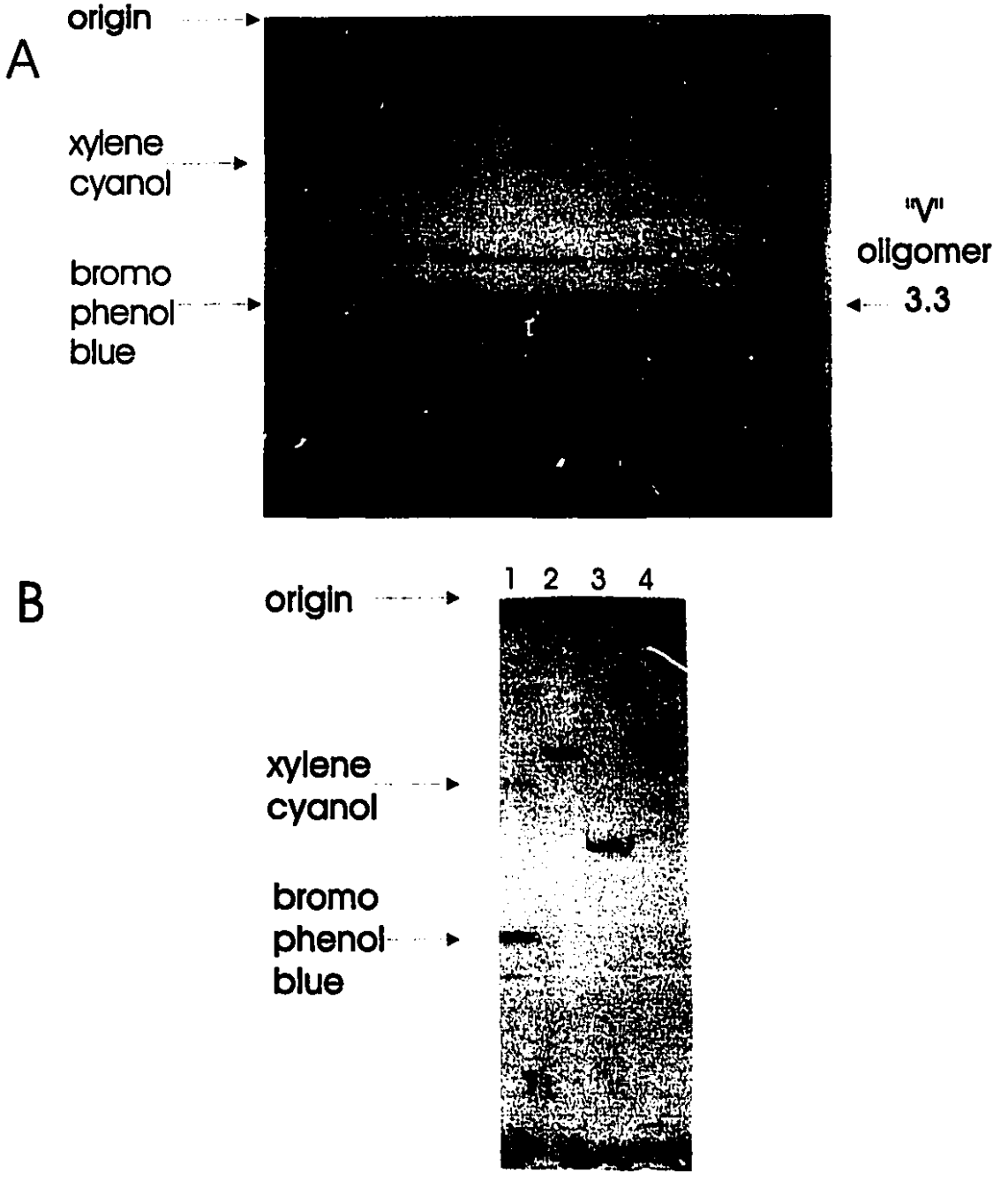

Figure 3.4. A. A 25% denaturing preparative PAGE showing the mobility of the crude product of compound **3.3**. This gel is a typical example of how a branched synthesis appears. B. A 25% denaturing PAGE gel showing relative mobilities of linear standards and the purified "V"-like oligomer (**3.3**). Lanes 1, 2, 3, and 4 contained: the dyes, oligomer (**3.3**), dT_{10} and a linear 33-mer marker, respectively.

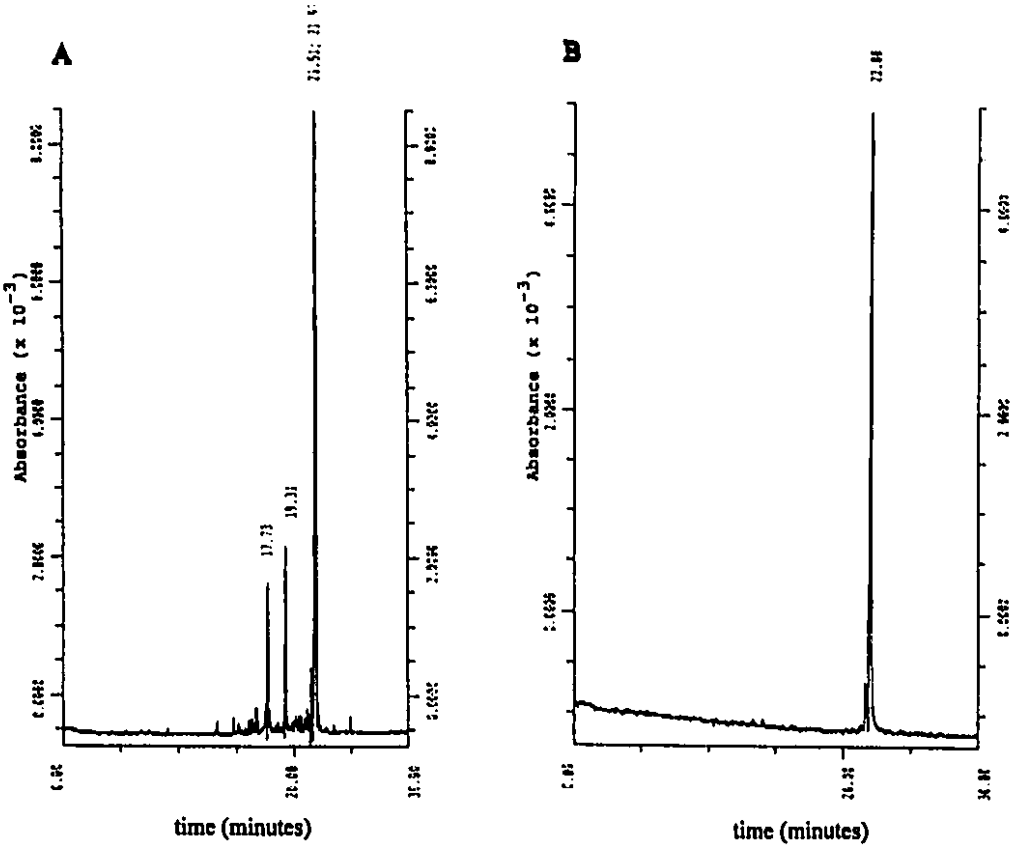

Figure 3.5. A. Capillary electrophoresis (CE) analysis of the crude product **3.3**. B. The CE analysis of pure **3.3**, with a retention time of 22.1 minutes. The CE system and method is described in the experimental section.

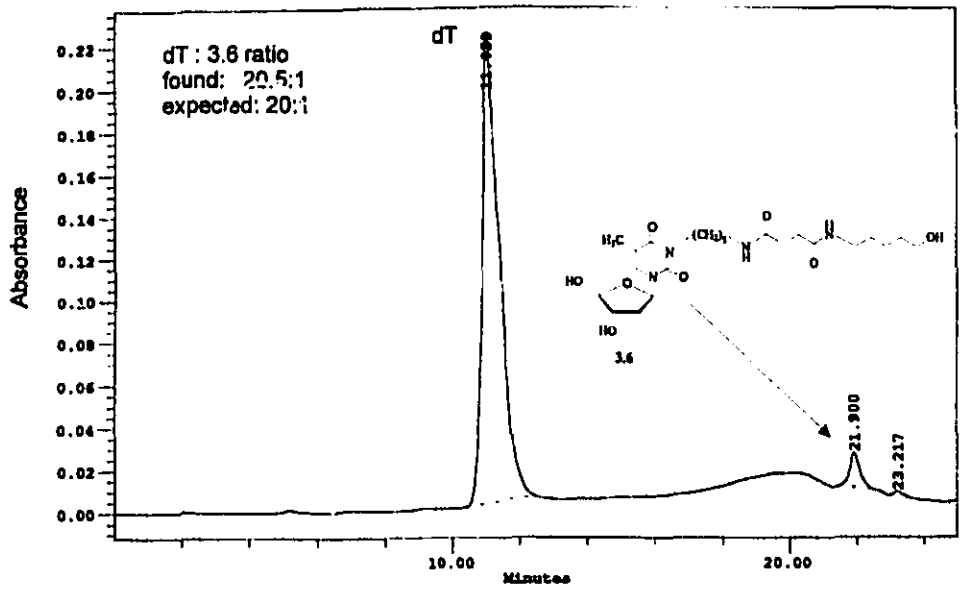

Figure 3.6. Nucleoside analysis of compound **3.3**, following snake venom phosphodiesterase/alkaline phosphatase enzymatic digestion. The identification of dT and compound **3.6** (**3.1** with no DMT, levulinyl, and phosphoramidite moieties) at (11 minutes and 21.9 minutes, respectively), was confirmed by co-injection of independently prepared standards. Refer to the HPLC experimental for preparation of **3.6**.

Sequences **3.4** and **3.5** also gave gave satisfactory capillary electrophoretic mobilities as illustrated in Figures 3.7A and B.

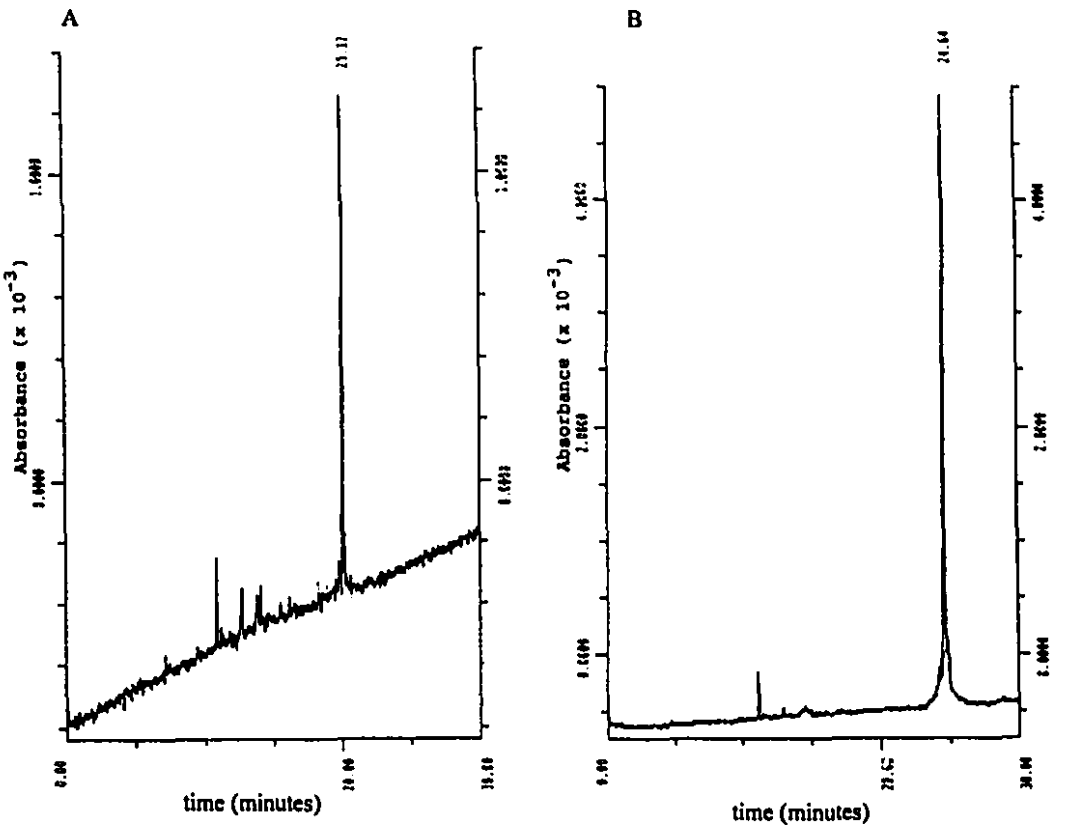

Figure 3.7. A. Capillary electrophoresis (CE) analysis of pure product **3.4** having a retention time of 20.1 minutes. **B.** The CE analysis of pure **3.5** having a retention time of 24.6 minutes. The CE system and method is described in the experimental.

3.2.3 Hybridization of "V" -Shaped Nucleic Acids.

The binding affinities of the "V" compound **3.3**, and the control sequence 5'-T_{10}-CCTC-T_{10}-3' for their single stranded target dA_{10} were measured by comparison of the melting temperatures of the complexes with 1 M NaCl, 10 mM Na_2HPO_4, pH 7.0 buffer, or 50 mM $MgCl_2$, 10 mM Tris pH 7.3 (Figure 3.8). In both buffers, the melting curves at 260 nm showed a single transition from bound to unbound species. That is, both compound **3.3** and the control sequence bind dA_{10} in a cooperative manner, whereby the Watson-Crick and Hoogsteen bonds would form/break in a one step process.

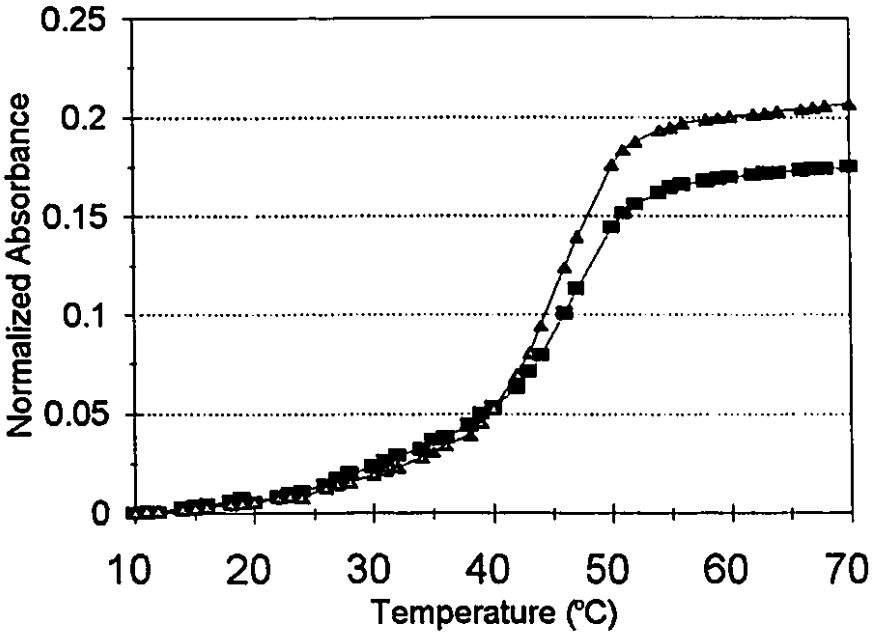

Figure 3.8. UV absorbance melting profile (monitored at 260nm) for one to one mixtures of **3.3** (-■-)and 5'-$T_{10}C_2TCT_{10}$-3' (-▲-) with dA_{10} complements. Solutions contained: 1M NaCl, 100mM Na_2HPO_4, pH 7.0, with a 2μM total strand concentration.

The same transition temperatures of both complexes (ca. 47 °C, in either Na^+ or Mg^{+2}) suggests that **3.3** and 5'-T_{10}-CCTC-T_{10}-3' bind to dA_{10} with the same affinity. The "V" oligomers **3.3** and **3.4** which had a length difference of 3 carbons, melted at the same melting temperature of 47 °C when complexed to dA_{10} in the Mg^{+2} buffer. By comparison, dT_{10} with its Watson-Crick complement dA_{10} forms a duplex which melts at 32.0 °C in Mg^{+2} buffer, demonstrating that **3.3**, **3.4**, and the control 5'-T_{10}-CCTC-T_{10}-3' bind to dA_{10} much more strongly. Evidently, this is achieved by forming Hoogsteen and Watson-Crick hydrogen bonds, i.e., T*AT base triplets, with the target dA_{10} strand (Figure 3.9).

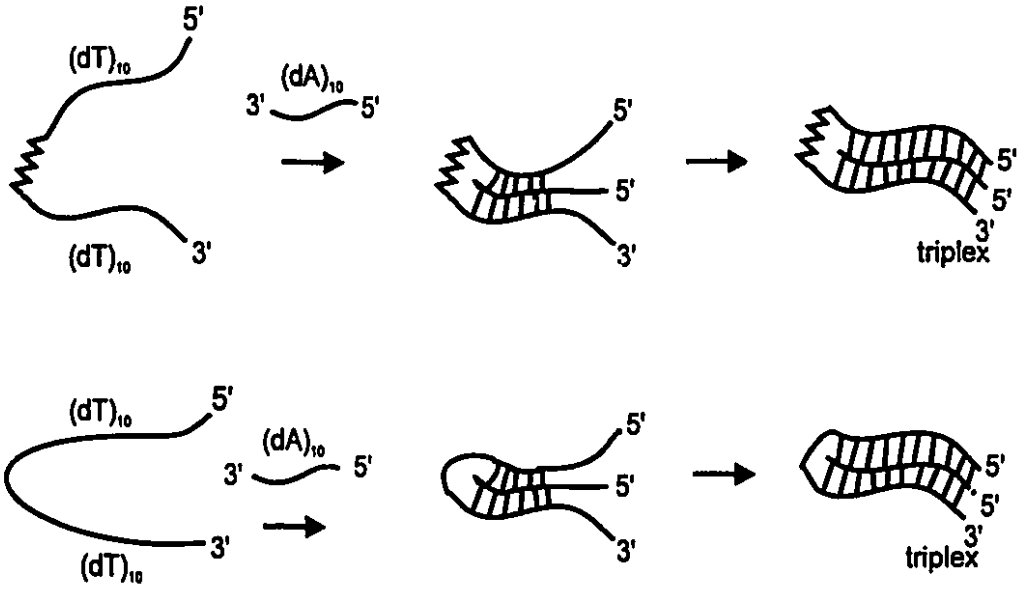

Figure 3.9. Triplex formation of oligomer **3.3** or **3.4** (top), and the control sequence 5'-T_{10}-CCTC-T_{10}-3' (bottom) with the complement dA_{10}.

Also supporting a triple helical structure are the observations that: (a) the melting transitions of the complexes of **3.3**, **3.4** and sequence 5'-T_{10}-CCTC-T_{10}-3' could be followed at 284 nm, a wavelength at which pyr*pur/pyr triplexes composed entirely of T*A/T base triads display significant changes in absorbance, but at which duplex A/T pairs do not;[9c, 9e, 66-70] (b) A single mismatch resulting from substitution of dT for dA in the target sequence, leads to a decrease in melting temperature of 13 degrees (T_m= 47 → 34 °C) whereas the corresponding decrease for the control duplex is more significant (T_m= 34 → 17 °C, or, ΔT_m= 17 °C); (c) circular dichroism spectra of **3.3**/dA_{10} and sequence 5'-T_{10}-CCTC-T_{10}-3'/dA_{10}, is similar to that of the known triplex dT_{10}*dA_{10}/dT_{10} (data not shown). Therefore, from these results one can conclude that the linkers chosen afford triple helices with comparable stability to one with a natural (CCTC) loop.

3.2.4 Thermal Stability of "Y"/dA_{10} versus "V"/dA_{10} complexes.

Since it was shown that "V" (3.3 and 3.4) compounds were effective for triplex formation, the next step was to compare the hybridization of the "Y" (3.5) branched molecule when complexed to dA_{10} (refer to Figure 3.10). In accord with what was observed with the "V" compounds, the "Y" molecule showed a monophasic transition at 260nm when bound to dA_{10}, with a melting temperature of 48.3 °C, comparable to 47 °C for the "V" complexes. By comparison, dT_{10} with its Watson-Crick complement dA_{10} forms a duplex which melts at 32.0 °C, demonstrating that both "V" and "Y" oligomers bind to dA_{10} more strongly. This high thermal stability is accounted for by forming both Hoogsteen and Watson/Crick hydrogen bonds, i.e., T*AT base triplets, with the target dA_{10}. Therefore, the complex of 3.5 with dA_{10} affords a triple helix with comparable thermal stability to "V"+dA_{10}. The significance of this finding is that DNA extension from the "V"s' 5' hydroxyl group does not interfere with binding to the triplex domain.

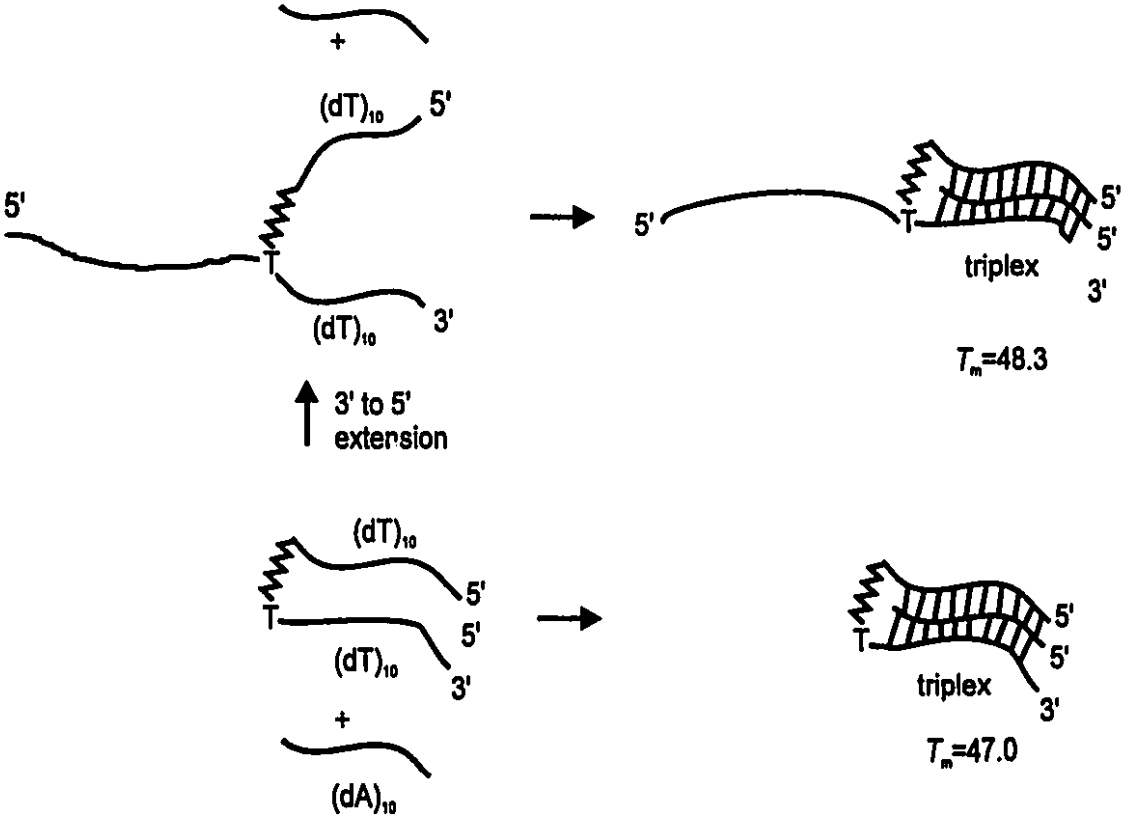

Figure 3.10. Model of "Y" (3.5) and "V" (3.3. and 3.4) Compounds binding to dA_{10}.

Structure	Compound	Designation
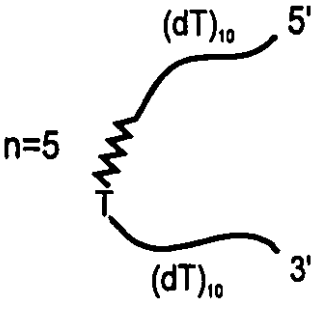	3.3	"V" (n=5)
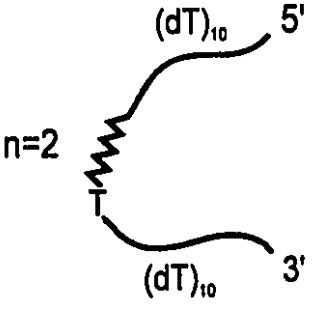	3.4	"V" (n=2)
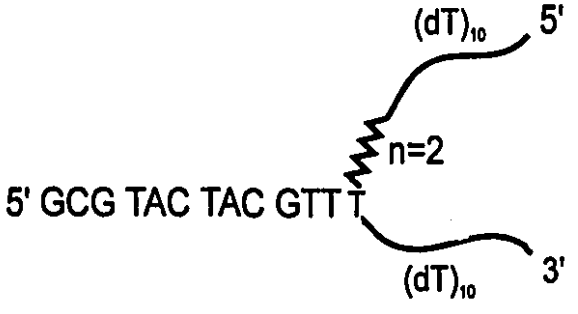	3.5	"Y" (n=2)
5' GCG TAC TAC GTT TT_{10} 3'	3.6	linear control
5' GCG TAC TAC $GTTTT_{10}G$ C C 3' $T_{10}C$	3.7	mixed hairpin

Figure 3.11. Structure of "V", "Y" and Linear Oligonucleotides.

3.2.5 Comparison of Thermal Stability for "Y" (3.5), linear control (3.6) and mixed hairpin (3.7).

The "Y" molecule (3.5) (shown in Figure 3.11) has two possible modes of binding to its target molecule, which are illustrated in Figure 3.12. The first one corresponds to only duplex formation (model I) which would imply that the third (triplex forming) arm was acting only as a "spectator". The second model implies that 3.5 would bind to its target molecule to give a combination of duplex/triplex regions (model II). In these studies, melting experiments have ruled out the possibility of model I.

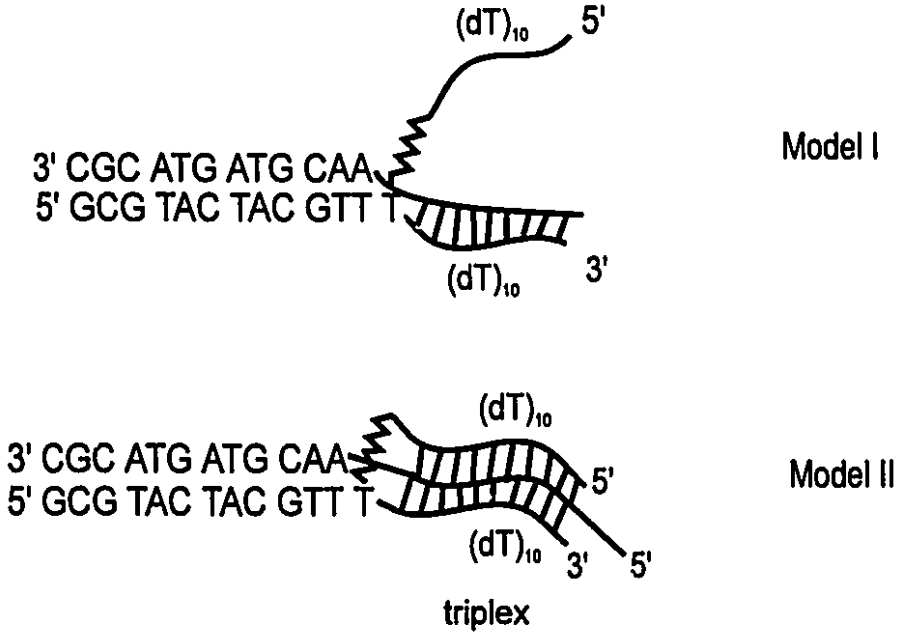

Figure 3.12. The two possible binding modes of the branched "Y" compound 3.5 with its linear target. The first model corresponds to only duplex formation, whereby the third (triplex forming) arm acts only as a "spectator". The second model implies that 3.5 would bind to its target molecule with a combination of duplex/triplex formation.

Table 3.1. Stability of Chimeric Hoogsteen/Watson-Crick forming complexes relative to Watson-Crick forming complexes.

Oligomer 1	Target Oligomer	T_m	%H
"Y" (3.5)	dA_{15}TAACGTAGTACGC	61.3	17.2
linear Control (3.6)	dA_{15}TAACGTAGTACGC	66.8	15.0
mixed hairpin (3.7)	dA_{15}TAACGTAGTACGC	63.3	18.9

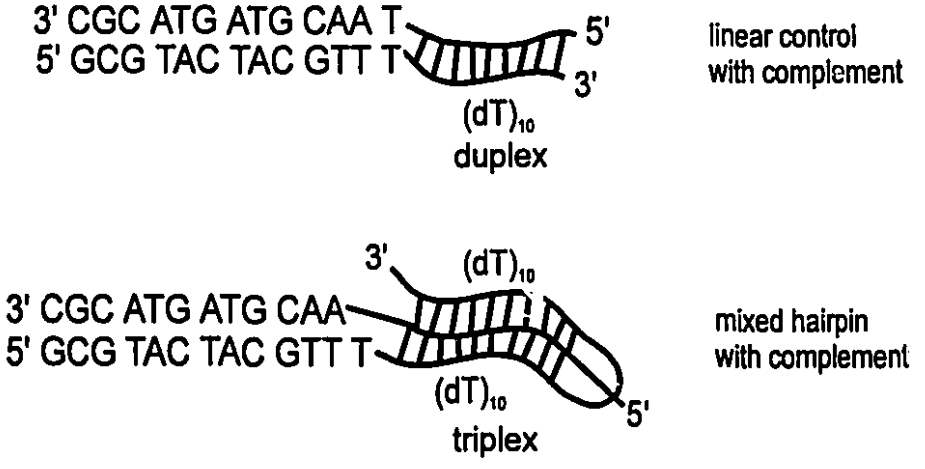

Figure 3.13. Binding modes for Linear Control (3.6) and Mixed Hairpin (3.7) with complement (dA_{15}TAACGTAGTACGC).

Both 3.5 and 3.7 capable of both duplex and triplex formation when targeted to dA_{15}TAACGTAGTACGC, showed a monophasic transition of comparable stability (T_m's of 61.3 °C and 63.3 °C, respectively). From these results, one can conclude that the triple helix region of these oligonucleotides was stabilized, relative to when 3.5 and 3.7 were complexed with dA_{10} (48.3 °C and 45.9 °C, respectively). Interestingly, 3.6 which is only capable of forming Watson-Crick hydrogen bonds with dA_{10} has a higher thermal stability than 3.5 and 3.7 which are capable of both Hoogsten and Watson-Crick hydrogen bonds. Thus, these experiments demonstrate that for this sequence a complete Watson-Crick double helix is more stable than a chimeric Watson-Crick/Hoogsteen complex. Alternatively, for the branched sequence a "bulge" surrounding the branchpoint may cause incomplete base pairing surrounding this region.

3.2.6 Mismatch Studies

Mismatch studies were conducted with the branched "Y" oligonucleotide, the linear control and the mixed hairpin, in order to determine the stringency for compound **3.5**. All triplex forming oligomers (**3.5**, **3.7** and $T_{10}C_4T_{10}$) had a higher T_m and hyperchromicity when complexed to the mismatch sequence $dA_2\underline{G}A_3\underline{G}A_3$, relative to the duplex forming linear control (**3.6**). Of the triplex forming oligomers (**3.5** and **3.7**), the mixed hairpin had the lowest melting temperature when complexed to $dA_2\underline{G}A_3\underline{G}A_3$. Referring to Table 3.2, since the "Y" (**3.5**)/ formed a more stable complex with the target oligomer than the mixed hairpin (**3.7**), one can conclude that this evidence for triplex formation aids in ruling out the "spectator" arm model.

Table 3.2. Mismatch results with Triplex, Duplex/Triplex and Duplex forming oligomers. The target oligomer binds only to the dT_{10} region.

Oligomer 1	Target Oligomer*	T_m (%H)	ΔT_m
"Y" (**3.5**)	dA_{10}	48.3 (14.7)	-
"Y" (**3.5**)	$dA_2\underline{G}A_3\underline{G}A_3$	17.2 (7.5)	31.1
linear control (**3.6**)	dA_{10}	35.1 (15.7)	-
linear control (**3.6**)	$dA_2\underline{G}A_3\underline{G}A_3$	9.9 (4.4)	25.2
mixed hairpin (**3.7**)	dA_{10}	45.9 (15.2)	-
mixed hairpin (**3.7**)	$dA_2\underline{G}A_3\underline{G}A_3$	16.3 (10.7)	29.6
$T_{10}C_4T_{10}$	dA_{10}	44.8 (18.0)	-
$T_{10}C_4T_{10}$	$dA_2\underline{G}A_3\underline{G}A_3$	17.7 (12.8)	27.1

* All nucleotides underlined indicate a mismatch base pair. Conditions: 10mM Tris, 50mM $MgCl_2$, pH7.3.

Table 3.3. Mismatch results with Full Length Target Oligomer.

Oligomer	Target Oligomer*	T_m (%H)	ΔT_m
"Y" (3.5)	dA_{15}TAACGTAGTACGC	61.3 (17.2)	-
"Y" (3.5)	$dA_2\underline{G}A_3\underline{G}A_3$TAACGTAGTACGC	50.9 (10.6)	10.4
linear "Y" (3.6)	dA_{15}TAACGTAGTACGC	66.8 (15.0)	-
linear "Y" (3.6)	$dA_2\underline{G}A_3\underline{G}A_3$TAACGTAGTACGC	60.9 (16.6)	5.9
mixed hairpin (3.7)	dA_{15}TAACGTAGTACGC	63.3 (18.9)	-
mixed hairpin (3.7)	$dA_2\underline{G}A_3\underline{G}A_3$TAACGTAGTACGC	54.7 (18.0)	8.6

*Nucleotides underlined indicate a mismatch basepair.

These mismatch studies are very interesting as they show the relative specificity of the compounds. The linear control (3.6) showed the least sensitivity to the mismatch, whereas both the mixed hairpin (3.5) and the "Y" compound (3.5) showed the greatest destabilization. From these results, one can conclude that the "Y" oligomer (3.5) is the most sensitive to correct base-pairing and we infer that the third branching arm must be involved in triple-helical formation. Had the third arm of the "Y" oligomer (3.5) acted as a "spectator" (Figure 3.12) *i.e.* it is not involved in hybridization, the T_m data would have reflected that of the linear control (3.6) complexed with the mismatch sequence. Therefore, this mismatch data provides further evidence for supporting the model II mode of binding.

3.2.7 Effect of BePI on Triple-Helical "Y" (3.5):dA_{10} and mixed base hairpin (3.7):dA_{10} complexes.

As discussed above, triplex stability under physiological conditions appear somewhat limited primarily because of electrostatic replusion between the duplex and third strand. Hélène and co-workers recently reported that a benzo[e]pyridoindole derivative (BePI, Figure 2.13) strongly stabilizes triple-helical DNA and showed preferential binding to triplex DNA over duplex DNA.

Table 3.4. Stabilization of Triple-Helical DNA by 3-methoxy-7H-8-methyl-11-[(3'-amino)propylamino]-benzo[e]pyrido[4,3-b]indole (BePI).

Oligomer	Target Oligomer	T_m (%H)	ΔT_m
"Y" (3,5)	A_{15}TAACGTAGTACGC	61.3 (17.2)	-
"Y" (3,5) + BePI*	A_{15}TAACGTAGTACGC	68.0 (13.3)	6.7
mixed hairpin (3,7)	A_{15}TAACGTAGTACGC	63.3 (18.9)	-
mixed hairpin (3,7) +BePI*	A_{15}TAACGTAGTACGC	65.6 (15.0)	2.3

* 10μM BePI in 10mM Tris, 50mM $MgCl_2$, pH7.3.

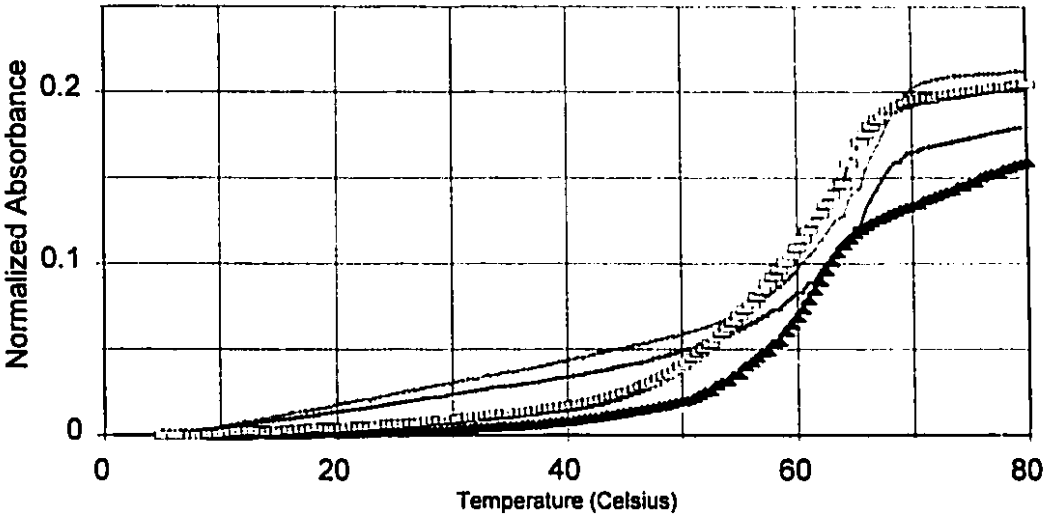

Figure 3.14. Melting temperature profiles of the "Y" oligomer (3,5) and the mixed base hairpin (3,7) hybridized to the target dA_{15}TAACGTAGTACGC obtained in the presence and absence of 10μM BePI. Strand concentration was 2.0μM. "Y" (3,5) without BePI [▲], "Y" (3,5) with BePI [+], mixed hairpin (3,7) without BePI [x], and mixed hairpin (3,7) with BePI [■].

In this study, BePI was used to stabilize oligonucleotides with two different binding domains, involving a mixed base duplex and a T*AT triplex forming region (Figure 3.12). Hélène *et al.*, have diligently characterized the ligand BePI, with regard to investigating its specific mode of binding to Hoogsteen*Watson-Crick T*AT triplexes.[85]

This is the first reported example involving the use of a triplex specific ligand employed to enhance the stability of a branched chimeric (duplex-triplex) complex.

A significant finding made in these studies is that the "Y" (3.5) with its complement in the presence of BePI showed a dramatic stabilization of its complex. Thus this enhanced stabilization for the "Y" complex provides further evidence in ruling out the "spectator" arm model. Furthermore, it shows the potential use of a triplex binding ligand such as BePI, being able to specifically enhance the thermal stability of a complex consisting of both Watson-Crick and Hoogsteen hydrogen bonds.

Conclusions.

In conclusion, it was demonstrated that a hairpin loop inside of an oligonucleotide can be replaced with linker nucleoside units 3.1 or 3.2 without significant changes in its hybridization properties. The main merit of this branched strategy is that this novel regioselective synthetic method allows for the creation of virtually any sequence at any "arm" using the branching synthons 3.1 and 3.2. Of significant importance is the ability of these branched molecules to have two different binding motifs. One arm has the role of a "guide" sequence to capture the target through specific Watson/Crick hydrogen bonding, while the role of the second pyrimidine strand is to "fold" over and form a triplex chimera.

Preliminary studies with a branched "Y" oligonucleotide show that it is possible to target a complementary DNA sequence with a high degree of selectivity. That is, these branched oligonucleotides are more sensitive to mismatches than the corresponding mixed hairpins or linear controls. Work is currently in progress in the Damha laboratory for developing branching synthons which will optimize the binding properties *ie.* by attaching flexible linkers through the 2'-hydroxyl of a nucleoside. Furthermore, by designing linkers of polyethylene glycol composition, these synthons should be more soluble in acetonitrile and thus increase the coupling efficiency. Such linkers may enhance resistance of

oligonucleotides to degradation in biological media, as well as its cellular uptake by increasing lipophilicity.[128]

Chapter 4 - Synthesis and Studies of 2',5'-Linked Oligoribonucleotides.

Section 4.1 Introduction.

4.1.1 The Significance of 2',5'-Phosphodiester Linkages.

One of scientific fields which has intrigued nucleic acid chemists is why nature favours 3',5' phosphodiester linkages over 2',5'-linkages along the sugar-phosphate backbone. 2',5' linkages are rarely found in nature, occurring only during intron splicing and in interferon treated cells. Switzer *et al.* using 2',5'-linked DNA containing guanine and cytosine have shown that these oligomers could associate, however, these duplexes were found to have approximately half of the thermal stability of the corresponding 3',5'-linked DNA.[129] For example, Breslow *et al.* and Switzer *et al.* independently showed that oligodeoxynucleotide complexes containing 2',5'-linkages, had weaker associations and were seen only at higher salt concentrations.[130] Breslauer went on to demonstrate that 2',5'-linked triple helices exhibited greater thermal stability than the corresponding 3',5' triplexes.[131] Turner *et al.*, and the Damha laboratory, independently demonstrated that 2',5'/2',5'-oligoribonucleotides duplex structures are less stable than 3',5'-RNA/3',5'-RNA complexes.[132] This finding was also confirmed by thermal studies involving both 2',5' and 3',5' linked rU_7 and rA_9 hybrids.[133] The preference of 3',5'-linkages in nature over 2',5' linkages may be partially attributed to the higher thermal stability of the former complexes.

4.1.2 Antisense Oligonucleotides containing 2',5'-Linkages.

One of the prequisites in the design of antisense therapeutics are that the oligonucleotides are resistant to nucleases and form stable and selective complexes with DNA or RNA. Giannaris and Damha were the first to propose the use of 2',5'-linked oligonucleotides as antisense agents.[134] These studies involved both homopolymers and partially mixed 2',5'- linkages, and showed that these compounds were resistant to enzyme degradation

and, amazingly, bound to RNA more selectively than single-stranded DNA sequences. In addition, the Damha group showed that 2',5'-r(Ap)$_9$A was capable of forming a triple-helix with poly rU having a 1A to 2U stoichiometry. Matteucci *et al.* from Gilead Sciences, Inc. went on to publish and patent 3'-deoxynucleotides containing 2',5' formacetal and thioformacetal linkages, based upon the results by Damha *et al.* that 2',5'-linked compounds had an exceptional selectivity for RNA.[135] More recently, Matteucci has investigated the hybridization of a 2',5' formacetal linked oligomers containing conformationally restricted ribose moieties. The 5,5 bicyclic ring system used in this study was shown to have worse binding properties than the control 2',5'-linked formacetal oligomers,[136] which is attributed to the ribose distortion of the sugar pucker.

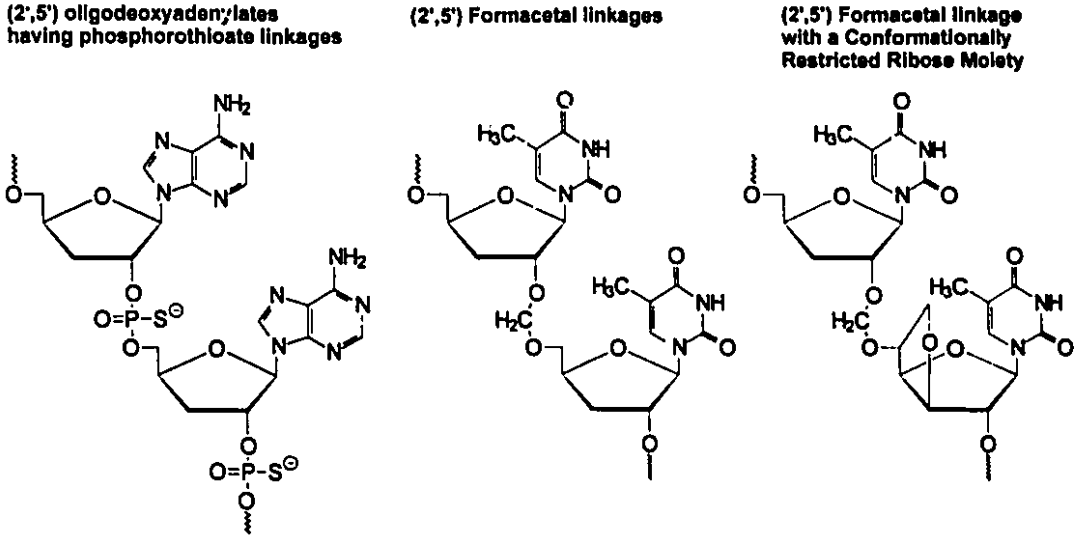

Figure 4.1. Structural Modifications of 2',5'-Linked Oligonucleotides.

Another study showed that a 2',5'-linked octadeoxyadenylate containing either natural phosphodiesters or phosphorothioates bound selectively to RNA with no binding to DNA, and had an increased enzymatic stability. It should be noted that all the latter studies described in this section were done on oligomers containing a single base. From these studies, selective binding to RNA and increased nuclease resistance appears to be a generalization for both DNA and RNA oligomers containing 2',5' linkages. Both the Damha and Breslauer laboratories demonstrated that the 2',5' linked oligomers exhibited differential properties relative to their corresponding natural 3',5' linked compounds,

with these differences depending, in part, on the number of modified phosphodiester linkages and the ionic strength of the media used.

4.2 Hybridization Properties of 2',5'-Linked Oligomers containing the Four Natural Bases.

4.2.1 Binding Studies of 2',5'-Linked Antisense Oligomers Complementary to the 5'-Long Terminal Repeat (LTR) of HIV-1.

First, the binding properties of a 2',5'-linked RNA oligomer containing all four bases was investigated. Two RNA sequences 18 nucleotides in length were synthesized, both complementary to the 5'- long terminal repeat (LTR) of HIV-1 genomic RNA (strain 3B). These completely 3',5' linked or 2',5' linked RNA 18 mer sequences being complementary to the HIV genome, would thus act as potential antisense agents for HIV reverse transcriptase (see section 4.5).

In order to compare the relative affinities of the 3',5'- versus 2',5'-linked antisense compounds bound to the viral RNA, two model systems were used. Two 18 mer oligonucleotides (sense strands) composed of either RNA or DNA and which had the same sequence as the 5'-LTR of the HIV-1 genome. The melting temperatures (T_m's) of the 3',5' and 2',5'-linked RNA antisense oligomers hybridized to their complementary unmodified ssDNA and RNA sense strands were measured (Table 4.1). The following conclusions can be made: as had been previously reported for homopolymers containing 2',5'-linkages, 2',5'-linked RNA of mixed base composition binds much more tightly to RNA than with DNA. Although this selectively is also observed with the 3',5' linked antisense RNA strand, it is more pronounced for the 2',5'-linked RNA antisense oligomer. Furthermore, the T_m of the 2',5'-RNA/3',5'-RNA complex was 71 °C compared with 87 °C for the 3',5'-RNA/3',5'-RNA complex, suggesting that annealing of 2',5'-RNA to 3',5'-RNA is thermodynamically less favourable than annealing of 3',5'-RNA to 3',5'-RNA. Thus, from this and previous studies, the selective RNA binding

properties of an all 2',5'-linked antisense oligomer make it better suited as an antisense agent compared to a 3',5'-linked oligomer.

Table 4.1. Thermal Melt Data for 2',5' and 3',5'-Linked Oligomers Complementary to a section of R region from the HIV LTR.

Antisense Oligomer	ssDNA T_m (%H)	ssRNA T_m (%H)	ΔT_m RNA-DNA
2',5'-Linked rAGCUCCCAGGCUCAGAUC	37.2 (4.7)	70.9 (11.3)	33.7
3',5'-Linked rAGCUCCCAGGCUCAGAUC	68.8 (5.8)	86.6 (13.2)	17.8

T_m buffer = 140mM KCl, 5mM Na_2HPO4, 1mM Mg_2Cl pH7.2. These salt conditions were chosen to approximate the intracellular cationic environment. Antisense oligomers were melted with the complementary 18mer RNA and DNA targets.

Besides having RNA-specific hybridization 2',5' linked oligonucleotides have several properties which may them excellent candidates as potential antisense agents: they are stable to enzymatic degradation, they are water soluble, relative to natural 3',5' linked oligomers they are only slightly destabilized when binding to RNA, and they can be prepared via standard solid phase phosphoramidite chemistry.

4.2.2 Triplex Studies Involving Unmodified 2',5'-Linked Oligomers.

Previous studies have demonstrated that under certain conditions, 2',5'-linked oligomers associate to form stable triple helices. Given the ability of 2',5'-linked RNA and DNA to form stable duplexes with RNA, it was of interest to determine if these compounds would be capable of forming triple-helices with a natural DNA or a DNA/RNA duplex. Typically, triplex dissociation occurs through a two-step process *i.e.* dissociation of the triplex to a duplex and single strand, followed by dissociation of the duplex to single strands. In order to separate these transitions, the self complementary hairpin $dA_{10}dC_4T_{10}$ having a T_m of 67.2 °C was constructed. Binding studies conducted in 50mM $MgCl_2$, 10mM Tris buffer (pH 7.3) showed that both 3',5' linked rU_{10} and dT_{10} bind to

$dA_{10}dC_4T_{10}$. The hybridization profile of $dA_{10}dC_4T_{10}$ in the presence of either dT_{10} and 3',5'-linked rU_{10} had a biphasic melt profile, indicating two separate cooperative dissociation events *ie.* triplex → duplex + single strand→ single strands melting transitions. A biphasic transition was not observed for either the hairpin alone or for a 1:1 mixture of the hairpin and 2',5'-linked rU_{10}, indicative of no triplex formation. From these initial studies, 2',5'-linked rU_{10} proved to be incapable of triplex formation, as it showed no binding to the hairpin.

Table 4.2. Thermal Melt Data for all DNA and Chimeric DNA/RNA Hairpins with dT_{10} and rU_{10} Complexes.

Hairpin	Complement	T_m (°C)[a]	%H[b]	Curve Shape
$dA_{10}dC_4T_{10}$	-	67.2	13.2	monophasic
$dA_{10}dC_4T_{10}$	dT_{10}	13.2, 66.1	4.5, 13.7	biphasic
$dA_{10}dC_4T_{10}$	3',5'-rU_{10}	11.5, 64.5	3.1, 13.8	biphasic
$dA_{10}dC_4T_{10}$	2',5'-rU_{10}	66.9	13.3	monophasic

[a] T_m's were determined from the first derivative plots of absorbance versus temperature and were run in 50mM MgCl2, 10mM Tris, pH 7.3, adjusted with HCl. [b] %H was calculated via $\%H=(A_f-A_o)/A_f$.

Preliminary results involving the investigation of whether 2',5'-linked oligonucleotides could form triple helical complexes proved discouraging. However, work to determine if a 2',5'-linked mixed pyrimidine sequence can form a Hoogsteen triple helix is currently in progress in the Damha laboratory. As well, the possibility that branched "V" compounds of the composition $rA^{U10}{}_{U10}$ (where the rU_{10} is either all 2',5' linked or 3',5' linked) are capable of forming reverse Hoogsteen triplexes is also being investigated.

4.3 Synthesis and Hybridization of an Oligonucleotide containing 3'-O-Methyl Adenosine.

4.3.1 Importance of Synthesizing 3'-O-Methyl Monomers.

2'-O-Methyloligoribonucleotides have been widely explored as potential antisense/antigene inhibitors of gene expression,[137] and as molecular biology probes[138] (*eg.* site specific elicitation of RNase H with chimeric DNA splints). They are well suited for this purpose due to their high biochemical stability. A major consequence of the presence of a methyl group at the ribose 2'-hydroxyl is that the polymer becomes resistant to cleavage by both alkali and by a wide range of DNA and RNA specific nucleases.[139]

It would be of interest to synthesizing 2',5'-linked oligonucleotides containing 3'-O-methyl ribose monomers (Figure 4.2) for several reasons: (i) both 2'-O-methyl RNA[140] and 2',5'-linked RNA bind very selectively to RNA, (ii) both 2',5'-linked RNA and 2'-O-methyl oligomers are more stable to nucleases than natural 3',5'-linked RNA, (iii) 2'-O-methyl oligonucleotides can form stable complexes with either RNA and DNA, and (iv) chimeric deoxy/2'-O-methyl oligonucleotides elicit site specific RNase H activity when bound to RNA. Thus, the next rational step was to synthesize 3'-O-methyl oligomers containing 2',5' phosphodiester linkages in order to determine what affect these modifications would have on their binding properties.

4.3.2 Synthesis of 3'-O-Methyl Monomers.

Synthesis of 2'-O-methyl ribonucleotides, starting from protected or unprotected ribonucleosides has been extensively described in the literature. As illustrated in Figure 4.3, Ts'o and co-workers[141] directly methylated adenosine using sodium hydride and methyl iodide yielding only 7% of the desired 3'-O-methyl isomer with a mixture of dimethylated and 2'-O-methylated products. Based upon Ts'o's results, the tert-butyldimethyl silyl group was used for the synthesis of the 3'-O-methyl monomer. Methylation of 5'-O-

dimethoxytrityl-2'-O-*t*-butyldimethylsilyl- N^6-benzoyl-adenosine (**4.1**) (Figure 4.4), with sodium hydride/methyl iodide (DMF, 0 °C.), yielded a mixture of isomers **4.2a** and **4.2b** (4:1 ratio, respectively) in 65% yield. Of interest was that if the 3'-O-silyl regioisomer was used, the same ratio of methylated products was obtained. These results show that equilibration of silyl isomers (2' + 3') occurred at a faster rate relative to methylation. The ratio obtained in favour of the desired 2'Si, 3'Me isomer most likely reflects the relative

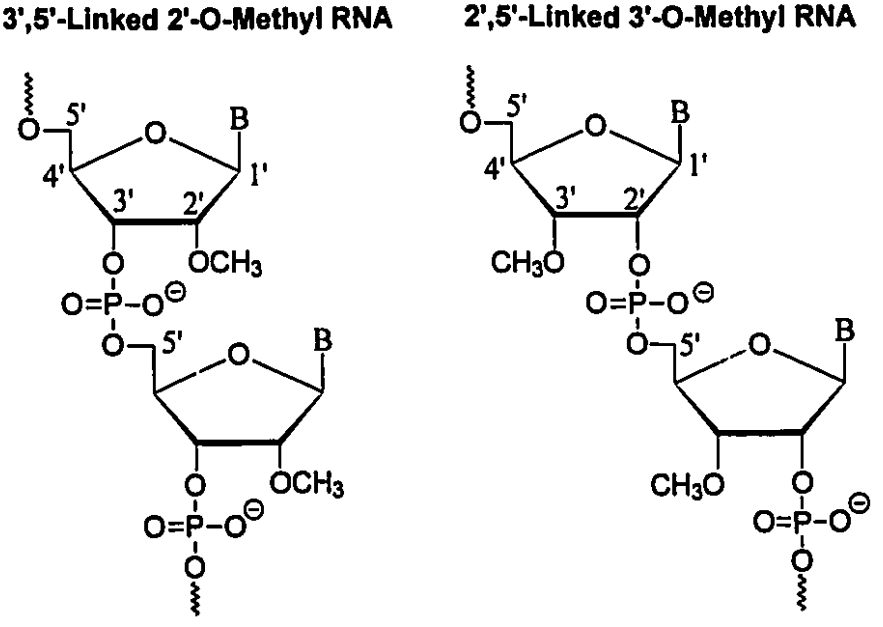

Figure 4.2. Structure of methylated 2',5' and 3',5'-linked RNA, where B denotes any base.

stability of 2'Si, 3'OH vs. 3'-OSi, 2'-OH. The latter being less stable due to steric compression (5'-DMT ↔ 3'-Si). Reaction with 1M TBAF in THF went cleanly, however, separation of the 3'-O-methyl derivative, compound **4.3a**, from the 2'-O-methyl isomer **4.3b** proved very difficult, affording **4.3a** in only 20% yield. Phosphitylation of **4.3a** with N,N-diisopropyl(2-cyanoethyl)phosphonamidic chloride gave compound **4.4** nearly in quantitative yield.

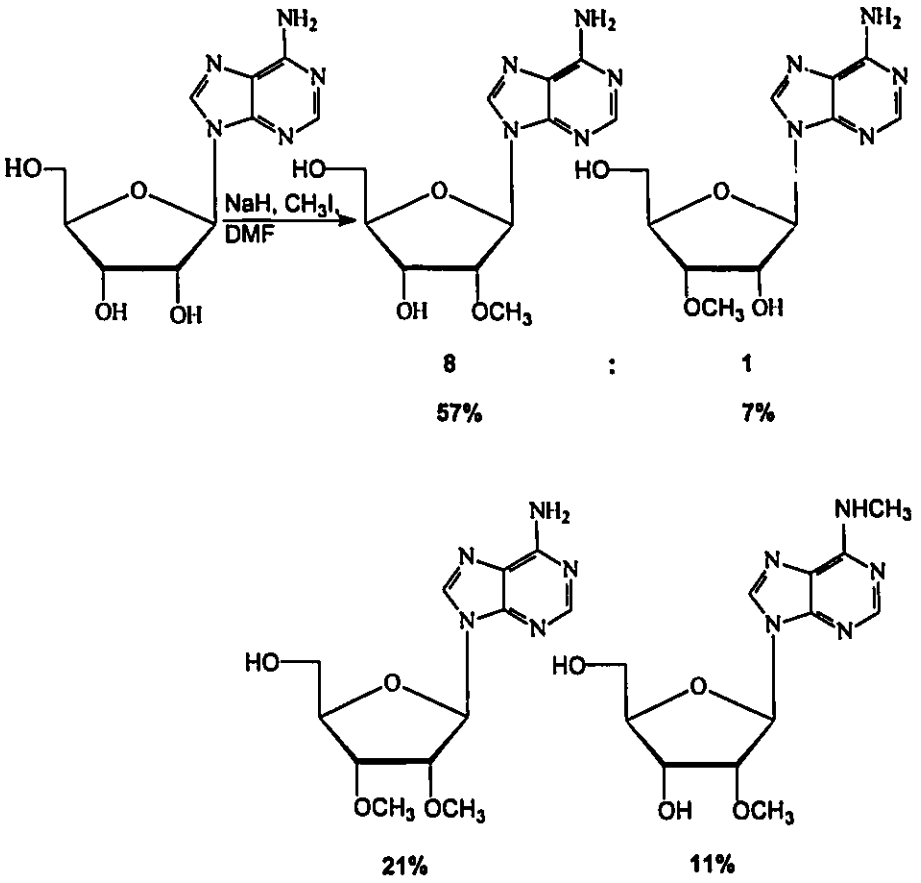

Figure 4.3. Direct Methylation of Adenosine and the subsequent products.

Due to the problems of silyl migration, the more stable (2-trimethylsilylethoxylmethyl chloride) protecting group was chosen.[12] Furusawa's laboratory was the first to employ the SEM group as a replacement for the *t*-butyldimethylsilyl group during oligonucleotide synthesis,.[13] SEM had also been previously used to protect the N^3 position of uridine.[14] Referring to Figure 4.5, SEM-Cl reacted with DMT-U (**4.5**), protecting the N^3 position of the base and the sugar in one step. The 2' and 3' isomers (compounds **4.6a** and **4.6b**) were then separated in 38% and 36% yields, respectively. Subsequent methylation of compound **4.6a** was carried out in high yield using iodomethane and silver oxide, to produce the 3'-O-methyl derivative **4.7**. (98% yield) Unfortunately, removal of the SEM protecting groups proved difficult. For example, treatment of **4.7** with a number of fluoride reagents eg. 3M TBAF in THF,[25] TEA 3HF, and tetrafluorosilane in acetonitrile[142] failed to produce the

desired compound 4.8. Several products of similar polarity were observed on TLC, making their separation very difficult. At this point, it was decided to prepare the desired 3'-O-methyl ribonucleosides via the silyl protection method (Figure 4.4) and although this route necessitated tedious chromatograpic separations, it provided sufficient quantity of material for further studies.

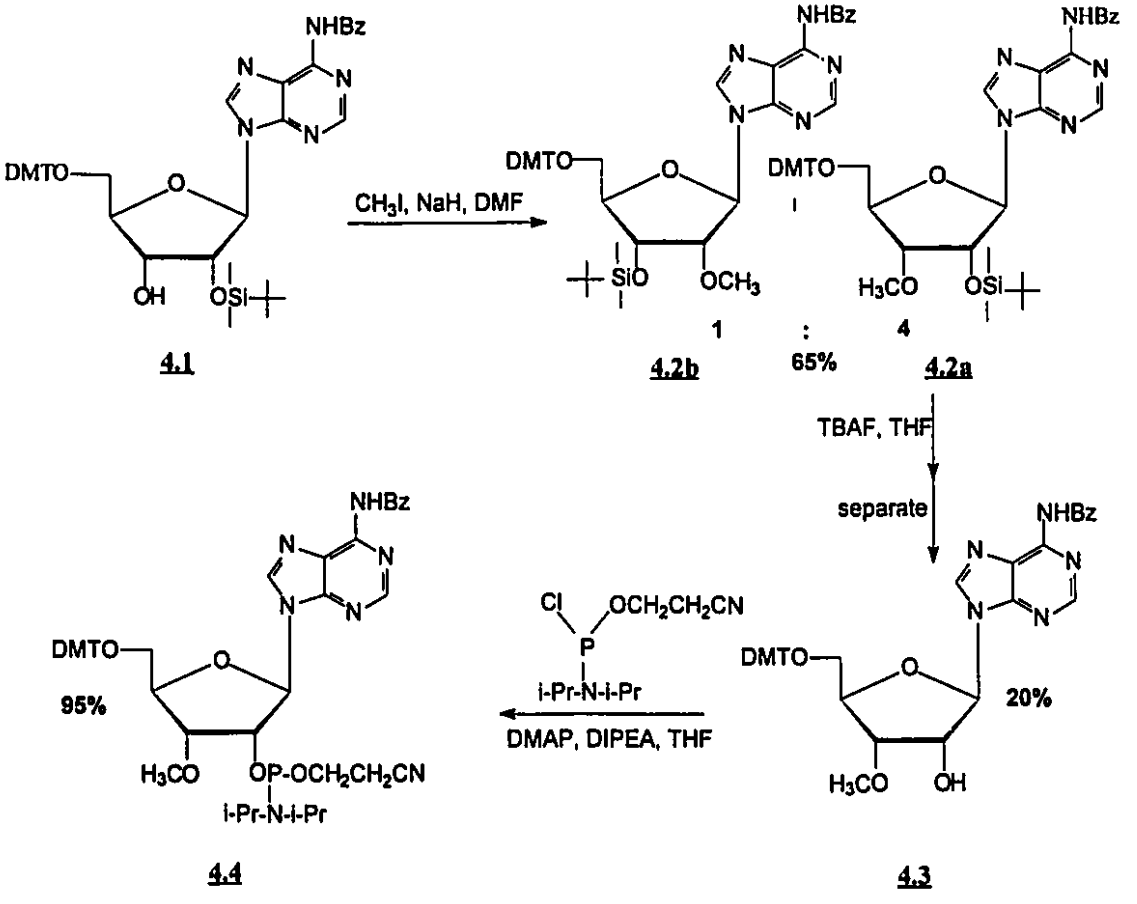

4.1 4.2b 4.2a 4.4 4.3

Figure 4.4. The synthetic route to synthesizing the 3'-O-methyl adenosine synthon, via tBMDS protection.

With desired amidite 4.4 in hand, an oligonucleotide sequence was readily assembled by using standard 2'-deoxynucleoside phosphoramidite monomers and the control pore glass as the solid support (Table 4.3). Overall coupling yields as determined by the trityl assay method were 98.5% and 80% for the DNA and 3'-O-methyl adenosine amidite monomers, respectively. The yield of the OPC purified oligonucleotide carrying four 3'-O-methyl-

adenosines was 1.5 A_{260} units. It should be noted that this synthesis has not been optimized. For future work involving this monomer **4.4**, it would be well to use a higher concentration of amidite (0.2M - 0.3M instead of 0.15M) and use 2-ethylthiotetrazole as a replacement for the acid activator tetrazole.

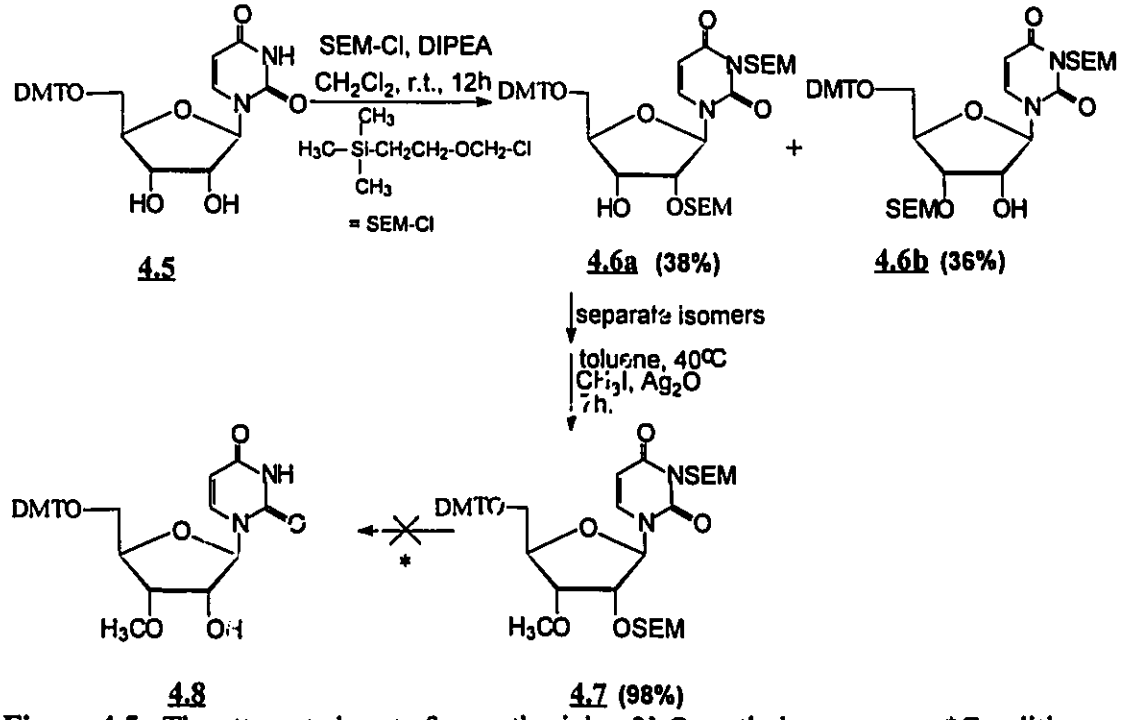

Figure 4.5. The attempted route for synthesizing 3'-O-methyl monomers. *Conditions used were: 1.) 1M TBAF/THF, 40 °C, 7days, no reaction; 2.) TEA•3HF, 40 °C, 7 days, no reaction; 3.) 3M TBAF/THF, 40 °C, 12h, mixture; 4.) SiF_4/CH_3CN, 1h, r.t., mixture and detritylation.

4.3.3 Binding Properties of Oligonucleotide containing 3'-O-Methyl Adenosine.

In order to evaluate the effect of the 3'-O-methyl adenosine residues on complexation with natural nucleic acids and the selectivity for RNA, we studied the association of sequence **4.10** and the unmodified sequence **4.9** with their complementary ssDNA and RNA (Table 4.3). In "physiological" buffer (see Table 4.3), **4.9** formed a duplex with its ssDNA and RNA complement which melted at similar temperatures (66 and 69 °C, respectively). In

contrast, the 3'-O-methyl modified oligomer **4.10** forms a more stable duplex with target RNA (T_m = 58 °C) than with DNA (47 °C), indicating that substiution with 3'-O-methyl 2',5'-linked adenosines destabilizes binding to RNA less than to ssDNA. Of note, the T_m's of the C/T mismatch duplexes are the same whether the target oligomer is ssRNA or ssDNA (i.e. sequence **4.11**, Table 4.3). Comparison of the drop in T_m recorded with the single C/T mispair containing **4.11**/ssRNA indicates that each 3'-OMe-rA/U base pair has a destabilizing effect that is one-third (1/3) of that introduced by the mispair. These results indicate that a DNA/RNA hybrid can accomodate a 3'-O-Me-rA/U base pair with only a moderate loss of stability (*ca.* 3.6 °C/3'-OMe-rA/U pair). Thus, the marked selectivity of oligomer **4.10** for RNA over ssDNA is also characteristic of other oligonucleotides containing 2',5'-linkages (Section 4.2.1).[134]

Table 4.3. Thermal Melt Data of DNA and 3'-O-methyl 2',5'-linked oligonucleotides with RNA and DNA complement.

Antisense Oligomer	ssDNA T_m (%H)	ssRNA T_m (%H)	ΔT_m RNA-DNA
dAGCTCCCAGGCTCAGATC (**4.9**)	66 (11.6)	69 (12.6)	3
dA$^{\bullet}$GCTCCCA$^{\bullet}$GGCTCA$^{\bullet}$G$^{\bullet}$ATC (**4.10**)	47 (6.8)	58, (6.7)	11
dAGCTCCCCGGCTCAGATC (**4.11**)	58.5 (12.8)	58.5 (8.0)	0

T_m's were measured in °C and in the buffer = 140mM KCl, 5mM Na_2HPO4, 1mM Mg_2Cl pH7.2 These salt conditions were chosen to approximate the intracellular cationic environment. %H was calculated via $\%H=(A_f-A_o)/A_f$. All bases are deoxynucleotides except for A$^{\bullet}$ which indicates a 3'-O-methyl adenosine insert. The underline indicates a mismatched base. Antisense oligomers were melted with the complementary 18mer RNA and DNA targets.

4.3.4 Structural Basis of the RNA Selectivity of 2',5'-Linked RNA: "Fine Tuning" of Sugar Puckering.

As described in section 1.2, the pentofuranosyl moiety of nucleosides/nucleotides in solution is involved in a two-state conformational equilibrium between North [N C3'-endo] and South type [S (C2' endo)] which can be monitored through the analysis of vicinal

proton-proton coupling constants ($^3J_{HH}$). In natural nucleosides, the C3'-C2' endo equilibrium of the furanose moiety is dominated by the gauche effects of the sugar and the anomeric effect of the base. The gauche effect of 3'-OH [O4'-C4'-C3'-O3'] drives the sugar equilibrium toward C2' endo, however, the 2'-OH [O4'-C1'-C2'-O2'] drives the equilibrium toward C3' endo (A type RNA). Coupling constants $J_{H1'-H2'}$ of nucleosides which have their furanose sugars "frozen" in the N and S conformation are typically ~ 0 and 8 Hz, respectively.[143] Although compound **4.3a** is not the ideal model to study since it lacks the 2'-phosphodiester, the coupling constants ($J_{H1'-H2'}$= 4.39, $J_{H3'-H4'}$=6.84) of this nucleoside indicates that a greater proportion of its sugars are found in the N conformation. In the presence of a charged 2'-phosphate the sugar can undergo "N tuning" depending on its interactions with the local environment, [144] since it has been shown that electronegative C2' substituents drive the N to S equilibria toward adoption of an N (C3' endo) conformation.[145] The RNA selectivity of 2',5'-oligoribonucleotides may be attributed to the tendency to adopt a C3'-endo pucker, a conformation that is inconsistent with the B form structure of helical DNA. Circular dichroism and n.m.r. structural studies of 2',5'-linked oligomers are currently in progress in the Damha laboratory to test this hypothesis. 2',5'- RNA containing 3'-O-alkyl groups remains a dimension of nucleic acid chemistry awaiting exploration.

4.4 Synthesis and Hybridization Properties of Enantiomeric L-2',5'-Linked RNA.

4.4.1 Background on L-Oligonulcleotides.

In order to understand why the binding properties of L-2',5' linked RNA were studied, a brief overview of L-oligomers is given here. Fujimori, Shudo and Hashimoto showed that L-dA_6 hybridized preferentially to poly (rU) over poly (dT), and although the L-dA_6/polyrU complex was substantially less stable than the D-dA_6/poly rU complex, it was suggested that L oligomers could potentially act as RNA-specific antisense agents.[146] L-$d(Ap)_4$ covalently attached to acridine at the 3' terminus via a pentamethylene linker, formed complexes with both poly (rU) and poly (dT). The 3'-acridine derivatives of L-

$(dUp)_8$ and L-$(dTp)_8$,[147] like their nonsubstituted derivatives,[148] did not interact with either poly (rA) or poly (dA). Ashley demonstrated that L-rU_{12} could bind to poly (rA) but not poly (dA), however, L-dU_{12} mixed with natural poly (dA) or poly (rA) formed no detectable complexes.[149] It should be noted that Ts'o *et al.*[150] showed that L-2',5' rApA dimers were both extremely resistant to nuclease degradation and could form triplexes of comparable stability as D-3',5'-rApA when bound to poly (rU). Garbesi *et al.* were unable to detect via UV spectroscopy, CD, or PAGE mobility retardation assay, any association between L-deoxyoligonucleotides containing all four bases and complementary DNA or RNA.[151] These latter studies showed that oligomers constructed from all four L-deoxynucleosides cannot form the basis of an effective antisense strategy. However, the Damha laboratory has shown that oligodeoxynucleotide "L/D" chimeras were not only more stable to nucleases than natural D-oligomers, but also were capable of forming stable hybrids with either DNA or RNA, and could elicit site specific RNase H activity.[152] Given their favourable physical and biological properties, L/D-chimeric oligomers could act as potential antisense agents.

4.4.2 Association of an L-2',5'-Oligoadenylate with poly (rU) and (dT).

Further investigating 2',5' linked oligonucleotides, whether L-2',5'-RNA binds to natural RNA and DNA sequences and whether L-2',5'-RNA exhibits RNA binding selectivity, as seen for its enantiomeric D-2',5'-RNA counterpart. A 2',5' linked L-rA_9dT oligomer was synthesized and its hybridization with poly (rU) and poly (dT) was studied. Consistent with the purines of the D-2'-phosphoramidites, a coupling efficiency of ~95% was achieved (unoptimized) with L-5'-O-dimethoxytrityl-3'-O-t-butyldimethylsilyl-N^6-benzoyl-adenosine-2'-O-N,N-diisopropylamino-2-cyanoethylphosphoramidite **4.12**. However, enough of the oligomer was obtained to conduct preliminary melting temperature studies.

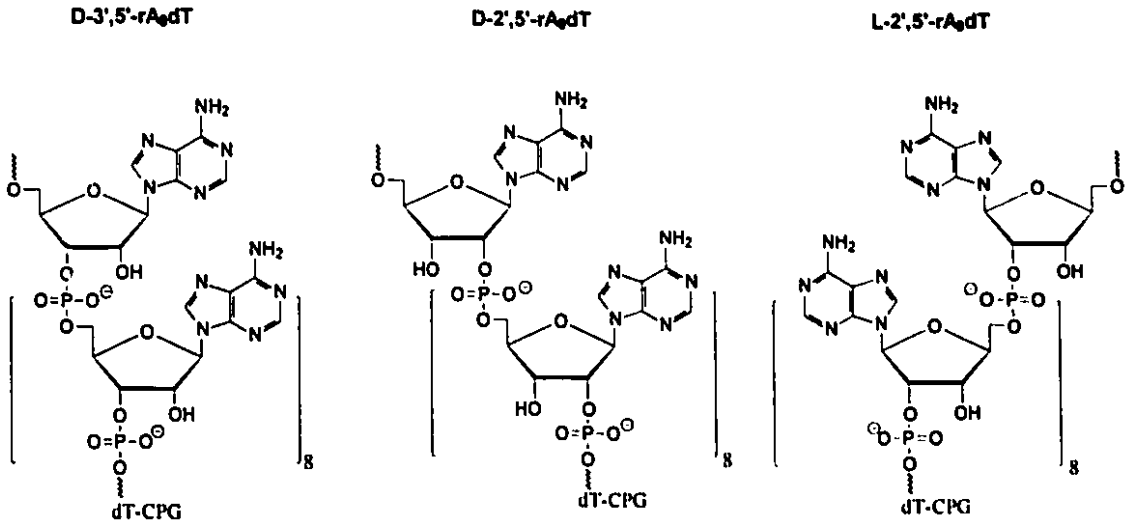

Figure 4.6. The structure of D-3',5' and 2',5'-linked RNA and L-2',5'-linked RNA.

Thermal profiles of 1:1 D-3',5'-(rA_9)dT:poly rU and D-3',5'-(rA_9)dT:poly dT mixtures (Figure 4.6) gave helix-coil transitions (T_m's) of 52 and 33 °C, respectively. The poly dT oligomer had a weaker interaction than poly rU with the oligoadenylate as evidenced by reduced T_m and base stacking (hyperchromicity) in the helical state. This is consistent with previous studies that have shown that RNA/RNA duplexes are generally more stable than RNA/DNA duplexes. In agreement with the studies described in Section 4.2.1, the D-2',5'-(rA_9)dT oligomer exhibited selective RNA binding to poly rU and not poly dT (Figure 4.7, Table 4.4). Thermal profiles of 1:1 mixtures of the polynucleotide strand with L-(rA_9)-D-dT showed strikingly different results (Figure 4.7, Table 4.4). A mixture of 1 equivalent of L-(rA_9)-D-dT with 1 equivalent of poly dT had a T_m (62.2 °C) that was greater than any of the other complexes, but which was approximately equivalent to that of the L-(rA_9)-D-dT /poly rU complex.

Thus, unlike its D isomer, the L-2',5' oligoadenylate bound to both the RNA and DNA targets showing no selectivity for RNA or DNA. Furthermore, the unusually high hyperchromicity for the L-(rA_9)-D-dT complexes compared to those formed by the (2',5' or 3',5') D isomers, indicates a larger degree of base stacking and/or hydrogen bonding

Table 4.4. Binding of D and L-2',5'-(rA_9)-D-dT[a], and D-3',5'-r$(Ap)_9$dT with poly rU and poly dT.

Oligomer	Complement Strand	T_m	%H
3',5' D-(rA_9)dT	poly rU	57.2	20.2
3',5' D-(rA_9)dT	poly dT	32.8	14.9
2',5' D-(rA_9)dT	poly rU	40.9	19.4
2',5' D-(rA_9)dT	poly dT	nto[a]	nto
2',5' L-(rA_9)-D-dT	poly rU	21.3, 62.8	11.2, 24.2
2',5' L-(rA_9)-D-dT	poly dT	62.2	19.4

[a]dT is of the D configuration. All mixtures contained 1:1 adenylate/target strands and these runs were done in 1M NaCl, 10mM NaH_2PO_4, pH 7.0 adjusted with HCl. No hyperchromic transition = nto

interactions in the former complexes. Also, when dissociated from the poly (rU), the 2',5' L-(rA_9)-D-dT oligomer showed a biphasic transition, the first one at *ca.* 21 °C indicative of triple strand (triplex) dissociation and the second at 63 °C characteristic for duplex dissociation. Interestingly, the 2',5' L-rA_9dT melting profiles are very similar in shape to what Shudo observed when 3',5'-D-dA_6 and 3',5'-L-dA_6 were complexed to poly rU with a 1:2 stoichiometry. More importantly, of the three molecules, *i.e.*, L-2',5'-adenylate, D-2',5'-adenylate, and D-3',5'-adenylate, the former has the highest affinity for single stranded DNA and RNA. Based upon these exciting findings, further work involving the synthesis of 2',5' oligonucleotides containing all L-nucleotides is ongoing in the Damha research group.

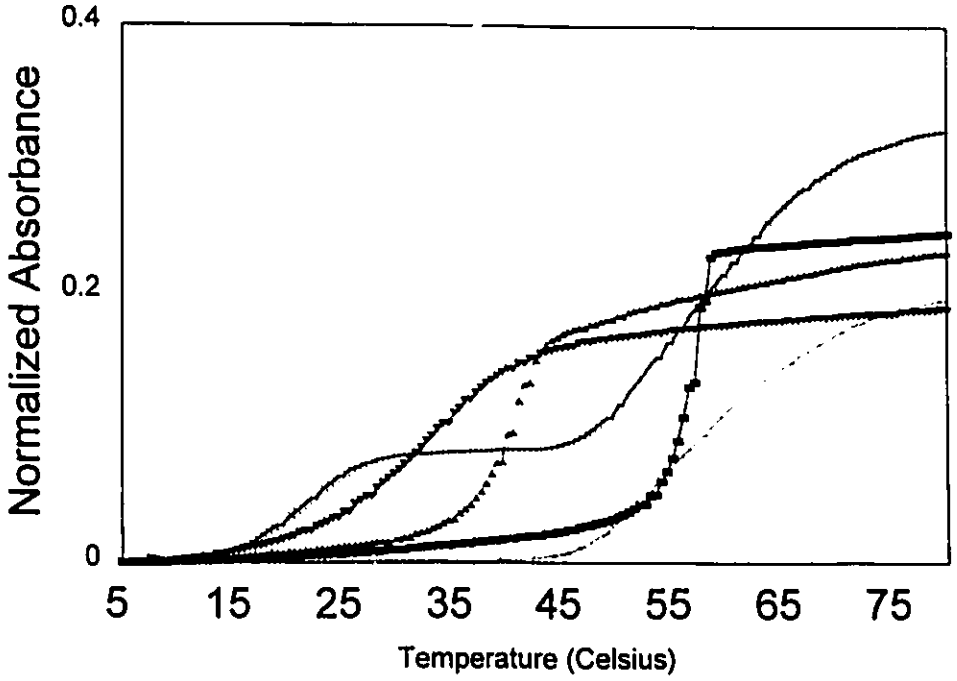

Figure 4.7. Thermal Denaturation Profiles for 3',5'-linked D-(rA_9)dT:poly (rU) [■], 3',5'-linked D- (rA_9)dT:poly (dT) [▼], 2',5'-linked D-(rA_9)dT dT:poly (rU) [▲], 2',5'-linked L-(rA_9)-D-dT:poly (rU) [+], 2',5'-linked L-(rA_9)-D-dT:poly (dT) [x]. All oligomers were measured with a 1:1 stoichiometry.

4.5 Inhibitory Potency of Antisense Oligonucleotides Against *in vitro* DNA Polymerization / Inhibition of HIV-1 Infected Cells using Antisense Oligonucleotides.

4.5.1 Background on HIV-1 Reverse Transcriptase.

An early, critical step in the human immunodeficiency virus type 1 (HIV-1) life cycle is reverse transcription of viral RNA into proviral DNA. As illustrated in Figure 4.8, this process is carried out by the multifunctional viral enzyme, reverse transcriptase (RT) and requires a primer annealed to the genomic viral RNA to initiate DNA synthesis. Shortly

after retrovirus infection of a cell, the plus strand viral RNA is transcribed into the minus DNA strand by the RNA-dependent DNA polymerase function of the RT. Then the RNA is hydrolyzed by the ribonuclease H activity of the enzyme and finally, the minus strand DNA serves as a template for the synthesis of the second DNA strand, a reaction catalysed by the DNA-dependent DNA polymerase function of RT. Parniak/Wainberg and coworkers of the McGill AIDs Centre, have developed an *in-vitro* reverse transciption assay[153] to study the properties of priming, RNA-dependent DNA polymerization, and template switching by HIV-1 RT, *i.e.*, the same reactions that occur in infected cells.

In order to evaluate antisense as a potential strategy to inhibit HIV replication, 18 unit long oligonucleotides were used (5'-AGC TCC CAG GCT CAG ATC-3', see Figure 4.8) that are complementary to a sequence near the 5' end of the viral HIV-1 genomic RNA (the R-region, see Figure). These end LTR sequences are highly conserved in all HIV genomes and are therefore attractive targets for selective antisense oligonucleotide binding.[154] Three AON were prepared: a 2',5'-linked RNA, a 3',5'-linked RNA and a natural DNA oligomer all of which contained the sugar with a D-configuration.

The hybridization properties of these oligomers were described in Sections 4.2.1 and 4.3.3. In principle, AONs complementary to the viral mRNA can prevent reverse transcription via different modes of action: competition with the tRNA primer for binding to the PBS region (Figure 4.8), interaction with reverse transcriptase, extension of the antisense oligomer via priming of the AON, and termination of cDNA polymerizations via steric blockage of DNA synthesis. In this section, an *in vitro* experiment shows that 2',5' and 3',5' linked RNA and natural DNA strands targeted to a sequence in the R-region near the end of the 5'-LTR of HIV-1 genomic RNA, inhibits the synthesis of viral DNA synthesis [(-) strong stop DNA]. These *in vitro* inhibition studies were done in the presence and absence of HIV recombinant nucleocapsid protein (NCp7). Nucleocapsid protein (NCp7) which is found in the viral core, is an important component of the assay as it facilitates tRNA annealing to the viral genomic RNA, and enhances the rate of DNA

strand transfers catalyzed by HIV RT.[155] Also, it was shown that 2',5'-linked RNA is a more useful antisense probe than natural DNA for viral inhibition of HIV-1 in infected MT-2 cells.

4.5.2 Inhibition of (-) strong stop DNA synthesis by AON.

The (-) strong stop DNA encoded by reverse transciption from the PBS oligonucleotide annealed to the pHIV-PBS RNA template in the absence of AON is 192 nucleotides (nt) in length (Figure 4.9). Nonetheless, in these *in vitro* assays, shorter DNA polymerization products are also observed (Figure 4.10-A, lane 1) due to "pausing" of RT during reverse transcription. The antisense oligonucleotide prevents full length polymerization of (-) strong stop DNA (Figure 4.9), producing a 162 nucleotide oligomer which is not noted in the absence of antisense inhibitors (Figure 4.10-A, lane 1). Therefore, observation of DNA products larger than 162 nt provides an estimate of the "break-through" and thus efficacy of AON in inhibiting HIV-1 (-) strong stop DNA synthesis in this *in vitro* system.

In the absence of AONs, high molecular weight (-) strong stop DNA products accounted for over 90% of the total RT DNA synthesis. Each of the three AONs inhibited RT-catalyzed synthesis of full-length (-) strong stop DNA, as evidenced by the appearance of significant amounts of the predicted 162 nt polymerization product (Figure 4.9). Based upon these results, one can conclude that RT is not capable of displacing the AON, otherwise a 192 nt product would have been observed for the lanes containing AON. In addition, in the presence of nucleocapsid protein the order of efficiency for prevention of DNA polymerization is: 3',5'- linked RNA>DNA>2',5'-linked RNA. Of the three oligomers only DNA is known to elicit RNase H activity, thus it can also be concluded that RNA cleavage by RT-associated RNase H activity was not a prequisite to observe the antisense effect. Our preliminary studies *in vitro* clearly demonstrated inhibition of (-) ss DNA by these 18 nt long oligomers even at ratios of AON to template of 1:1. Since a DNA oligo may serve as a primer for RT, one might expect that elongation of this antisense oligomer would strengthen its association with the HIV RNA target.

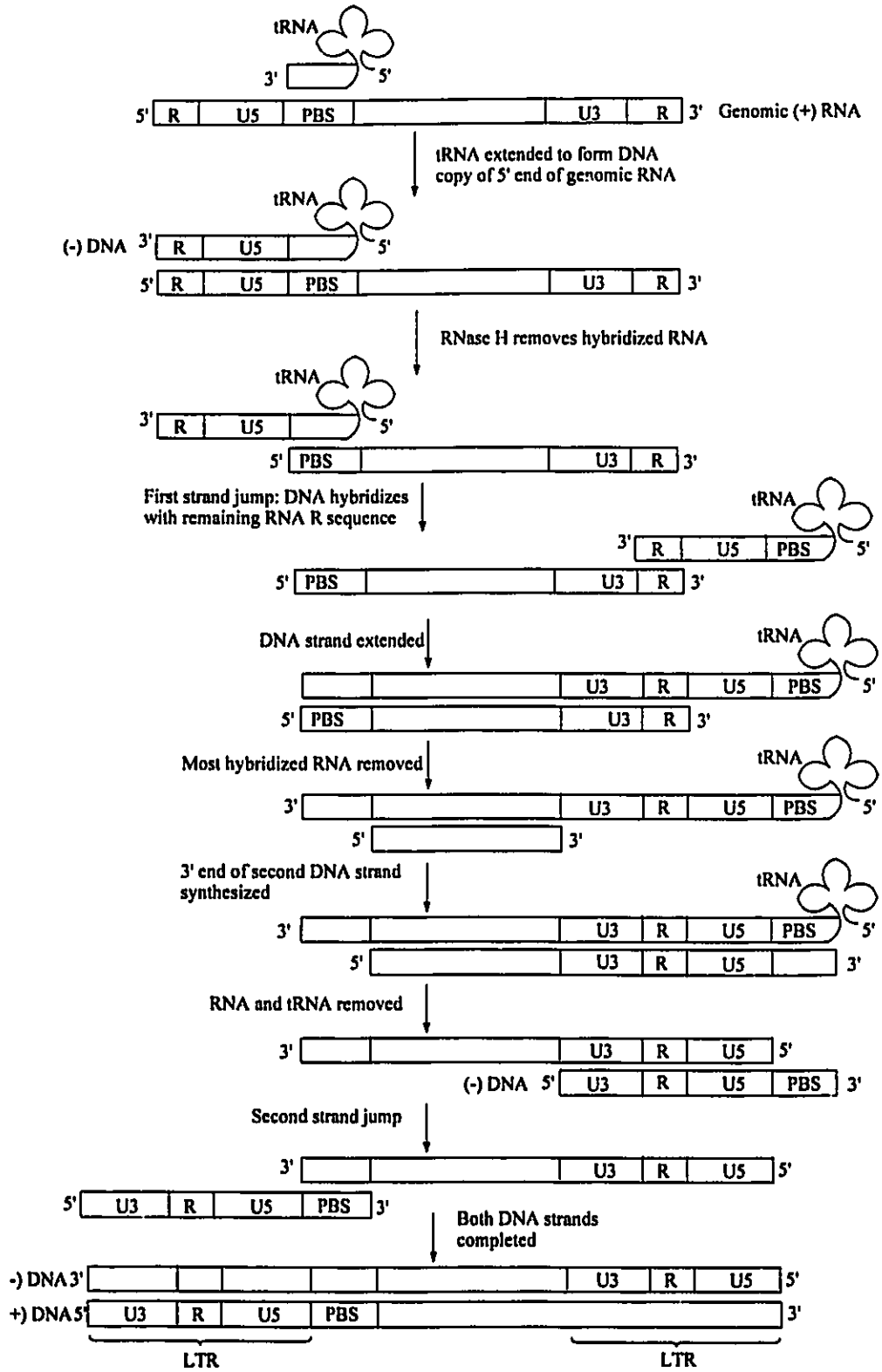

Figure 4.8. The mechanism of reverse transcription - conversion of HIV genomic viral RNA into double stranded DNA. Adapted from Stryer.[156]

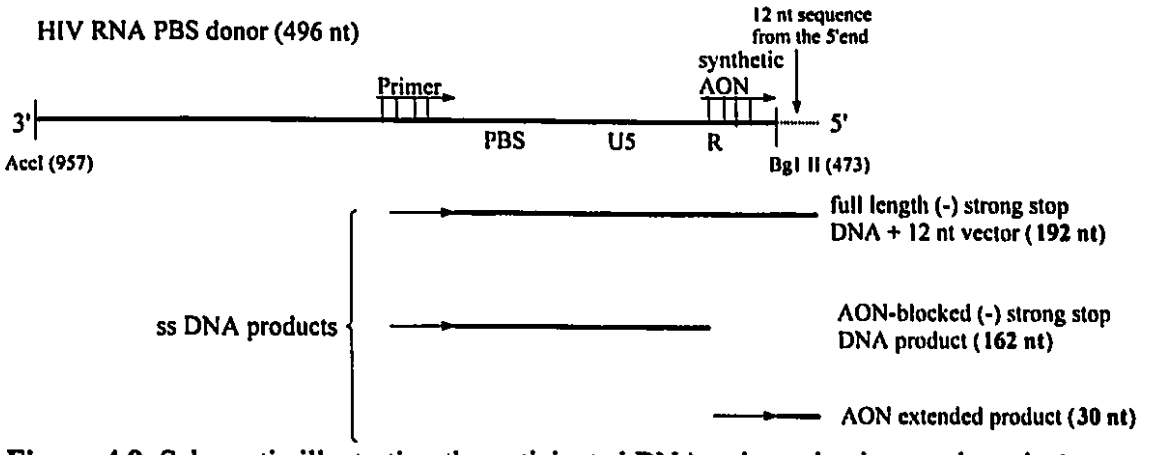

Figure 4.9. Schematic illustrating the anticipated DNA polymerization products in *in vitro* DNA polymerization reactions. Polymerization products expected in experiments testing the effect of AONs on (-) strong stop DNA synthesis, using pHIV-PBS RNA containing an additional 12 nt of vector-derived sequences. DNA primers were used instead of the natural tRNA primer.[153]

Indeed, significant amounts of a 30 nt DNA product (Figure 4.9) were noted in reactions containing the antisense DNA (Figure 4.10A - lanes 10-13, and B - lanes 10, 9, and 12). This product is due to RT-catalyzed 12 nt extension from the 3'-end of the AON. These 30 nt DNA products were not observed when reactions were carried out in the presense of 2',5'-linked RNA and 3',5' linked RNA. Although primer extension will certainly stabilize the antisense binding (especially since the extended 30nt portion has *ca.* 50% GC base pairs), our preliminary studies *in vitro* clearly demonstrated similar inhibition of (-) ss DNA by the 3 oligonucleotides, even if only the DNA strand served as a primer. Also, of significance was that the presence of nucleocapsid (NCp7) had no effect on the AON inhibition.

4.5.3 Inhibition of HIV-1 replication in infected MT-2 cells.

In order to evaluate the inhibition of HIV expression with infected MT-2 cells using AON, the DNA antisense oligomer was compared to the RNA antisense oligomer containing only 2',5' linkages. p24 is a marker that is used to measure the amount of HIV viral expression

in infected cells. As illustrated in Figure 4.11, with respect to viral antigen p24 expression, the 2',5'-linked RNA antisense inhibition was concentration dependent. From the cellular viral inhibition studies, it is evident that the *in vitro* DNA polymerization inhibition assay is not always a good predictor of antisense potency. In the DNA polymerization inhibition assay, it was shown that the DNA antisense agent was a better inhibitor of DNA polymerization relative to the 2',5'-linked RNA antisense oligomer.

However, in a cellular assay, the DNA AON was a poor inhibitor of viral replication relative to the 2',5'-linked RNA antisense oligomer. One reason, for the poor inhibition by the DNA antisense oligonucleotide may be attributed to its degradation by exonucleases present either in the cells or outside of the cells *ie.* the tissue culture media may have had nucleases. Previously the Damha laboratory had demonstrated that 2',5'-linked RNA were resistant to nuclease attack. Another possibility was that the DNA oligonucleotides may have had a worse cellular uptake than 2',5'-linked RNA. Also the poor inhibition by the DNA AON may be attributed to cellular dissociation factors, which recognize DNA/RNA duplexes. For example, cellular factors can destabilize RNA secondary structure, which may be capable of dissociating the DNA AON from the viral RNA. Also, an RNA helicase was found to unwind DNA/RNA hybrids *in vitro*.[157] Moreover, the Damha laboratory has established that 2',5'-linked RNA binds selectively to RNA relative to DNA. Thus, it is quite possible that the 2',5'-RNA antisense oligomer may associate to a greater extent with HIV RNA rather than with other cellular factors. Also, it was questionable of whether the antisense oligomers were binding to regions of viral RNA free of both secondary and tertiary structure. This preliminary study essentially showed that 2',5'-linked RNA is a potential HIV-1 inhibitor in cellular assays.

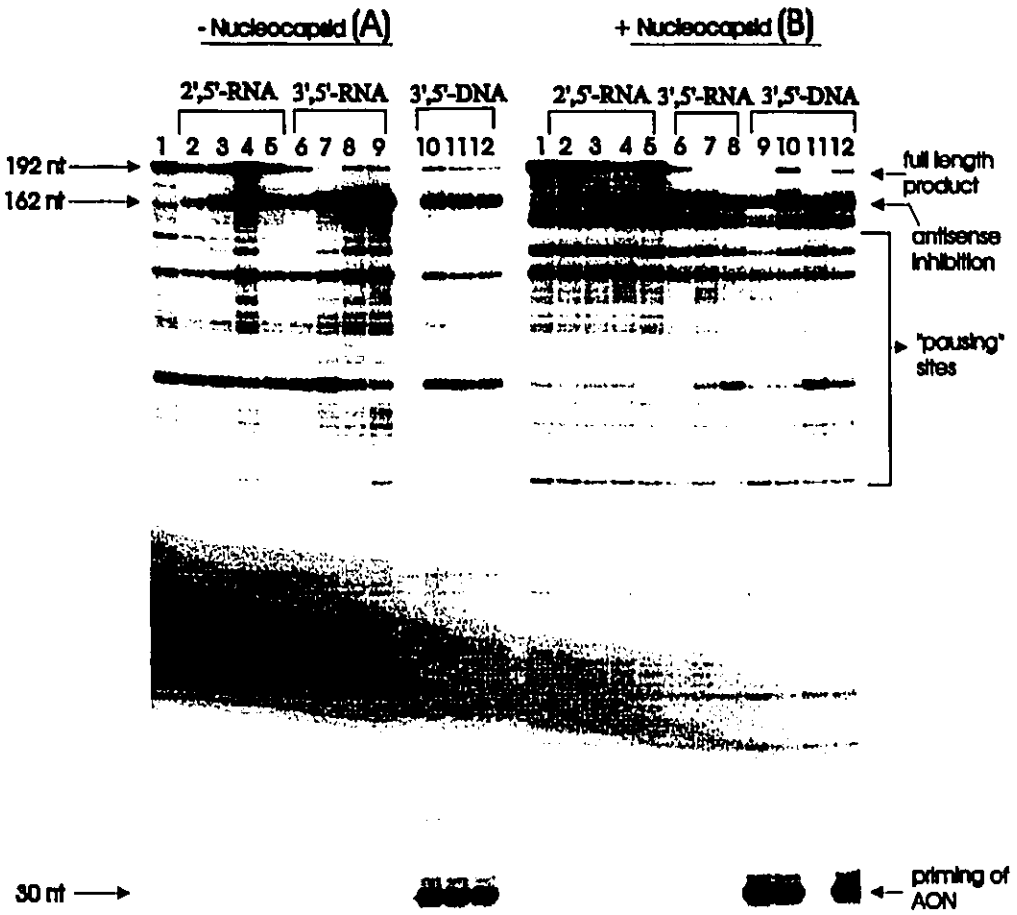

Figure 4.10. DNA polymerization product profiles in the absence or the presence of antisense oligonucleotides (AONs). Effect of antisense inhibition without (A) and with (B) nucleocapsid protein (1.5 μg). (A) Lane 1 corresponds to 2:1 primer: template in the absence of antisense oligonucleotide (AON). Lanes 2-5 correspond to 1:1, 5:1, 10:1, 20:1 D-2',5'-linked RNA :HIV RNA template, respectively. Lanes 6-9 correspond to 1:1, 5:1, 10:1, 20:1 D-3',5'-linked RNA:HIV RNA template, respectively. Lanes 10-12 correspond to 1:1, 5:1, 10:1, 20:1 DNA:HIV RNA template, respectively. (B) Lane 1 corresponds to 2:1 primer: template in the absence of antisense oligonucleotide (AON). Lanes 2-5 correspond to 1:1, 5:1, 10:1, 20:1 D-2',5'-linked RNA:HIV RNA template, respectively. Lanes 6-8 and 11 correspond to 1:1, 5:1, 10:1, 20:1 D-3',5'-linked RNA:HIV RNA template, respectively. Lanes 9, 10, and 12 correspond to 1:1, 5:1, 10:1 DNA:HIV RNA template, respectively.

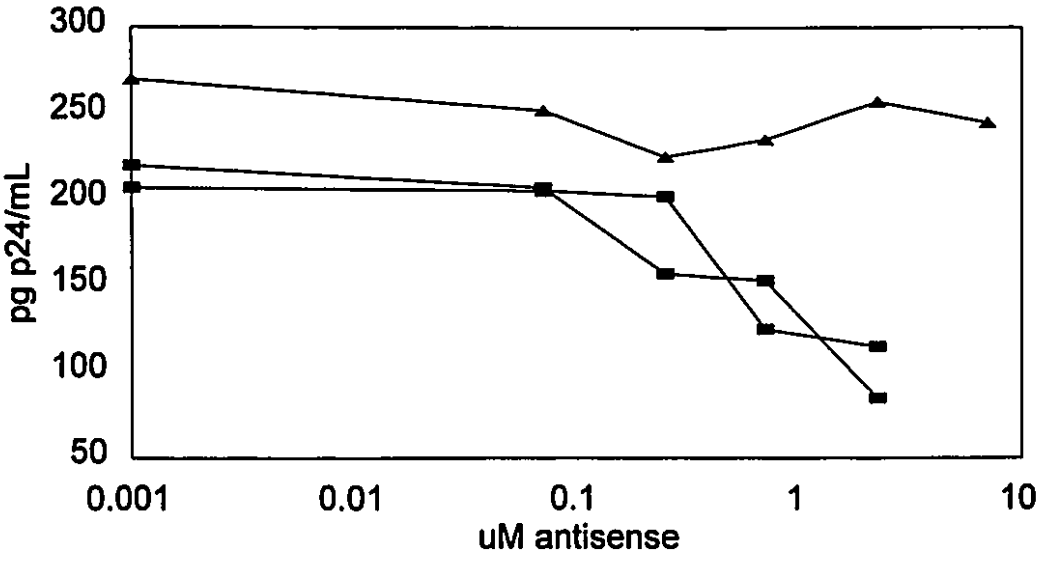

Figure 4.11. Inhibition of HIV-1B replication in MT-2 cells using antisense oligonucleotides. The p24 assay, which is a marker for HIV-1B was used to measure the relative amount of HIV-1 virus. Inhibition via the unmodified 2',5'-linked RNA (■) and natural DNA (▲), both sequences were complementary to the R region of the LTR HIV genomic RNA. Note two separate experiments were done with the 2',5'-linked RNA, thus accounting for the two series of data.

4.6 Conclusions.

In summary, D-2',5'-linked oligonucleotides having an unmodified 3' hydroxyl or a 3'-O-methyl showed binding selectivity for RNA, consistent with what has previously observed for 2',5'-linked oligomers. An all 2',5'-D-oligonucleotide consisting of all four bases was synthesized for the first time, and its hybridization with complement showed selective discrimination for binding to RNA. Preliminary results with L-2',5' linked RNA showed an increase in thermal stability of complexes relative to 3',5'-rA_9T, without any selective binding to either RNA or DNA. In light of these promising results with the L-2',5'-rA_9T, the Damha research group is currently synthesizing all four L nucleosides and 3'-O-methyl nucleosides for incorporation into a 2',5' linked oligonucleotide. In collaboration with the

McGill AIDs Centre, work is ongoing to investigate the use of antisense agents with nucleoside and non-nucleoside reverse transcriptase inhibitors in a combination therapy. Furthermore, work at the AIDS Centre will investigate targeting regions of the genome which have minimum secondary and tertiary structure, in order to optimize both AON binding and RNase H activity.

Chapter 5. Contributions to Knowledge

"...any discovery we make, however small, will remain acquired knowledge."
- Pierre Curie

The T•AT antiparallel triplex was stabilized by employing the branched molecule $A^{T10}{}_{T10}$. By employing a rigid branch point, it served to pre-organize poly dT tails and stabilize this unstable triplex. This triple helix was studied using thermal denaturation analysis, and circular dichroism spectroscopy. The melting curves at 260 and 284 nm showed a single transition from bound to unbound species, indicative of cooperative melting. A linear oligonucleotide with a loop made of four dC residues between two dT_{10} strands, and with a 5'-5'phosphodiester linkage at one of the C/T_{10} junctions did not form a similar triple helical structure. This result showed that the conformational rigidity imparted to the pyrimidine strands, by the branch point in **2.1**, serves to pre-organize and stabilize the complex. In a potassium buffer it was shown via a thermal melt profile at 260 and 284 nm, and by CD analysis that this cation inhibited triplex helix formation. In accord with what has been demonstrated previously for "parallel" Py*PuPy (Hoogsteen*Watson/Crick) triplexes, it was shown that short oligoadenylates (i.e., dA_4 and dA_5) can bind cooperatively to the branched oligomer. Furthering studies of this triple-helical complex, the "Y" branched molecule was constructed, 5'-dGCGTACTACGTT-rA $^{2',5'\text{-}dT10}{}_{3',5'dT10}$ and via melting with its target molecule the antiparallel triplex melting transition was observed. In addition, three DNA-binding ligands (ethidium bromide, BePI, and Hoescht 33258) were investigated for their ability to stabilize TAT antiparallel and parallel triplexes and an AT duplex. It was evident that the intercalators ethidium bromide and BePI were able to stabilize the antiparallel triplex to a greater extent than the parallel triplex or duplex. However, the minor groove binding Hoescht stabilized the duplex to a greater extent than either of the triplexes. A native PAGE retardation assay was run with "V" + dA_{10} and T_{10} +dA_{10}, in order to delineate two important properties of T•AT antiparallel triplexes. First, employing native gel electrophoresis it was demonstrated that these complexes could form in 50mM $MgCl_2$, the

same concentration of magnesium used in the T_m experiments. Second, it was shown that ethidium bromide bound and showed fluorescence with only the duplexes and triplexes, and not the single stranded species. In collaboration with Piunno, Krull and Hudson, a novel triplex assay for detecting TAT triple helical formation was developed by adapting the DNA duplex detecting biosensor. Two sets of optical fibres were created in which the orientations of the immobilized dA_{10} oligonucleotides were 3' to 5' and 5' to 3' from the surface, respectively. Fluorescent studies showed that not only could TAT triplexes be detected, but that the antiparallel complex could form a triple-helix only if the dA_{10} was attached to the optical fibre in the reverse direction. This essentially showed that binding of the branched oligomer may have been sterically inhibited by the surfaceand thus prevented the "V" molecule from forming an antiparallel triplex. This biosensor may have a number of applications, including screening of potential antigene candidates, investigation of point mutations, detection of oncogenes, and/or for studying cellular functions such as transcription and cell replication.

A novel and efficient synthetic strategy for constructing "V" and "Y" branched oligonucleotides having a flexible linker was also developed. The flexible "V" oligomers could be used as an effective nucleotide loop replacement for compounds forming triple helices. The branching aliphatic arm should not only confer further nuclease resistance but also should facilitate the cellular uptake due to the increased lipophilicity of these nucleic acids. The flexible "Y" molecule, bound to its target molecule with a high degree of specificity but with a lower affinity than its linear counterpart. It was demonstrated that these "Y" branched molecules recognize their target molecules by having two binding domains - one involving only Watson-Crick base pairing and the other via triple helical formation. Once the reaction conditions for the branching step have been optimized, it is expected that this method for synthesizing branched nucleic acids will be both productive and effective - since virtually any sequence can be grown in any direction. The triplex-inducing capacity of these branched oligonucleotides has potentially important implications in the design of novel antisense and antigene strategies.

Employing the "silyl-phosphoramidite" method, an all 2',5'-linked oligoribonucleotide containing all four bases (Ad, Ur, Cy, and Gu) was synthesized and found to bind selectively to RNA relative to DNA. In terms of inhibiting one of the necessary steps in HIV viral inhibition *i.e.* DNA polymerization, it was found that the order of effective antisense inhibition *in vitro* was: 3',5'- linked RNA>DNA>2',5'-linked RNA. In addition this 2',5'-linked antisense oligomer was found to inhibit viral replication in a dose-dependent manner in HIV-1 infected MT-2 cells, as measured by a p24 assay.

The inability of 2',5'-linked oligoribonucleotides to form triple-helical complexes is discouraging for those wishing to use these compounds as "antigene agents". However, this conclusion will await further experimentation with other 2',5'-RNA sequences of longer sequences and with a greater cytidine composition.

To further improve their nuclease resistance a DNA oligomers containing four 3'-O-methyl adenosine residues was synthesized and found to possess the same type of RNA binding selectivity which is associated with 2',5'-linked oligomers.

Finally, pursuing our investigations on 2',5'-linked oligoribonucleotides, for the first time an enantio-L-2',5'-linked oligoadenylate was synthesized and its association properties studied. Unlike its D-enantiomer, the L-2',5'-linked oligoadenylate was found to hybridize to both poly (rU) and (dT) with a high affinity but with no selectivity. It is premature to conclude that these compounds have no selectivity and bind with a higher affinity than the natural D oligoadenylates (since only homopolymer interactions were studied). By investigating a L-2',5'-linked oligoribonucleotides containing all four bases one could clearly establish their hybridization, nuclease, and biological properties.

As a direct result of the studies described herein, the following publications have appeared or will be published in the near future.

A.) Publications/Invention Disclosures.

1.) Hudson, R.H.E.; Uddin, A.H.; Damha, M.J. "Assocation of Branched Nucleic Acids: Structural and Physiochemical Analysis of Antiparallel T·AT Triple-Helical DNA" Journal of American Chemical Society, **1995**, *117*, 12470-12477.

2.) Uddin, A.H.; Roman, M.A.; Anderson, J.R.; Damha, M.J. "A Novel N^3-Functionalized Thymidine Linker for the Stabilization of Triple Helical DNA" Journal of Chemical Society, Chemical Communications, **1996**, 171-172.

3.) Uddin, A.H.; Piunno, P.A.E.; Hudson, R.H.E; Krull, U.J.; Damha, M.J. "An Assay for the Detection of a T•AT Triplexes Using an Fibre Optic Biosensor"; (see Sections 2.33-2.45), Proceedings of the National Academy of Sciences, U.S.A., submitted.

4.) Piunno, P.A.E.; Uddin, A.H.; Hudson, R.H.E; Krull, U.J.; Damha, M.J. "An Assay for the Detection of a T•AT Triplexes Using an Fibre Optic Biosensor"; "; (see Sections 2.33-2.45), University of Toronto/McGill University Invention Disclosure Filed.

5.) Uddin, A.H.; Roman, M.A.; Damha, M.J. "Duplex/Triplex Forming Chimeric Molecules Branched with a Flexible Linker"; (see Chapter 3), Manuscript in preparation.

6.) Uddin, A.H.; Hudson, R.H.E; Damha, M.J. "Investigation of T•AT Antiparallel Triplexes Via: DNA-Binding Ligands and Molecular Modeling"; (see Sections 2.29-2.33), Manuscript in preparation.

7.) Borkow, G.; Arion, D.; Noronha, A.; Uddin, A.; Scartozzi, M.; Damha, M.J.; Parniak, M. "Probing Two Important Steps in the Replication of HIV-1 with Antisense Oligonucleotides: Priming and Template-Switching Reactions"; Manuscript in preparation.

Contributions to work:
Numbering corresponds to the publication list given above:
1.) Uddin contributed to work illustrated in Figures 2, 3, 6, 7, 8, 9, and 10 and Table 2.

2.) Uddin synthesized, purified and characterized the "V" oligomer having the flexible linker. Binding studies were also conducted by Uddin. Roman made the branching synthons.[126]

3.) Uddin synthesized and purified the "V" and "Y" compounds having the flexible linker. Binding studies were done by Uddin.

4 & 5.) Synthesis of the 5' phosphoramidite needed for reverse oligomer growth was done by Uddin. The "V" and dT_{10} were synthesized by Uddin and as well as running the native gel which was subsequently stained with ethidium bromide. Activation of the fibres, oligomer synthesis on the fibres and fluorescent studies were done with Piunno. Piunno developed the instrumentation and the protocols for oligomer synthesis in collaboration with Hudson and Damha.[62]

6.) The "V" and dT_{10} were synthesized by Uddin and as well as running the native gel which was subsequently stained with ethidium bromide. Binding studies involving ethidium bromide, Hoescht 33258, and BePI were all done by Uddin.

B.) Biotechnology Publications Not Included in Thesis.

1.) Uddin, A.H. "Canadian Biotechnology Companies form Alliances" Canadian Chemical News - Pharmaceutical Issue, April 1996, pp.11-12.

2.) Uddin, A.H. "Canadians also strong in alliances" BIO/TECHNOLOGY, January 1996, pp.22.

3.) Uddin, A.H. "Banking on Chemistry: A Chemist's Guide to Investing in Canadian Biotech's" Canadian Chemical News - Biotechnology Issue, September 1995, pp.19-20.

C.) Presentations Based upon Bio-Organic Research Endeavours.

1.) Uddin, A.H.; Hudson, R.H.E.; Damha, M.J. "Branched Nucleic Acids - Synthesis and Applications in Antisense Therapeutics" 78th Canadian Society for Chemistry Conference and Exhibition, Guelph. Ontario, 05/95

2.) Anderson, J.R., Uddin, A.H., Roman, M.A.; Damha, M.J. "Synthesis and Hybridization of Branched Oligonucleotides Containing Flexible Linkers: A Novel Class of Antisense Inhibitors" 78th Canadian Society for Chemistry Conference and Exhibition, Guelph. Ontario, 05/95

3.) M.J. Damha,; A. Noronha, A.; Scartozzi, Uddin, A.; Parniak, M.; Arion, D.; Borkow, G. "In Vitro Inhibition of HIV-1 Reverse Transcription by Antisense Oligonucleotides" 78th Canadian Society for Chemistry Conference and Exhibition, Guelph. Ontario, 05/95

4.) Uddin, A.H.; Hudson, R.H.E.; Damha, M.J. "Association of Branched Nucleic Acids - Evidence for Reverse-Hoogsteen Triplex Formation in the Purine (T·AT) Motif" 13th Annual Graduate Student Symposium, State University of New York at Buffalo, Buffalo, N.Y., 05/95.

5.) Piunno, P.A.E.; Uddin, A.H.; Hudson, R.H.E.; Damha, M.J.; Krull, U.J. "Fluorimetric Analysis of TAT Triple-Stranded Nucleic Acid Formation Using a Fiber-Optic Biosensor"; 14th Annual Graduate Student Symposium, State University of New York at Buffalo, Buffalo, N.Y., 05/96.

6.) Noronha, A.; Arion, D.; Borkow, G.; Uddin, A.; Scartozzi, M.; Parniak, M.; Damha, M.J. "Probing Two Important Steps in the Replication of HIV-1 with Antisense Oligonucleotides: Priming and Template-Switching Reactions"; 79th Canadian Society for Chemistry Conference and Exhibition, Saint Johns, Newfoundland, 06/96.

7.) Piunno, P.A.E.; Hudson, R.H.E.; Uddin, A.H.; Damha, M.J.; Krull, U.J. "Fluorometric Analysis of Double and Triple Stranded Nucleic Acid Sequences Using a Fibre-Optic Biosensor"; 79th Canadian Society for Chemistry Conference and Exhibition, Saint Johns, Newfoundland, 06/96.

Chapter 6- Experimental

6.1 General Methods.

6.1.1 Reagents.

Solvents were dried and fractionally distilled - under reduced pressure for high boiling point solvents. Nitromethane was stirred overnight with $CaCl_2$, then distilled. Pyridine (BDH, Toronto, ON) and collidine (BDH) were distilled from calcium hydride (BDH) and used without further purification. Methanol (BDH) was refluxed and then distilled over magnesium turnings (Fischer Scientific, Montreal, QC) to which a few crystals of iodine (BDH) were added. Dichloromethane (BDH) was distilled over P_2O_5 (Caledon, Georgetown, ON). Xylene (BDH) and toluene (BDH) were distilled over $CaCl_2$ (BDH). Water used for oligonucleotides was double distilled, treated with diethyl pyrocarbonate (Aldrich) and autoclaved. DMF (BDH) was dried by refluxing over calcium hydride (Aldrich), and then distilled. Ethyl acetate (Caledon) was shaken with a 5% aqueous solution of sodium bicarbonate (BDH) and dried over anhydrous sodium sulfate (BDH).

Analytical reagent grade acetic acid (BDH) was distilled over $KMnO_4$ (ACP Chemicals, Montreal, QC) to remove carbonyl impurities. Ammonium acetate (BDH), anhydrous sodium sulfate (Caledon), silver oxide Ag_2O (Aldrich), hydrazine hydrate (Aldrich), triethylamine tris(hydrogenfluoride) or TREAT HF (Aldrich) were all used without further purification. 98% or 60% sodium hydride dispersion in mineral oil (Aldrich) was "washed" with HPLC grade hexanes to remove the mineral oil prior to use.

Nucleosides, bis(4-methoxyphenyl)phenylmethyl chloride (dimethoxytrityl chloride or DMT-Cl), *t*-butyldimethlysilyl chloride (tBDMS-Cl), N,N-diisopropyl-2-cyano-ethylphosphonamic chloride were purchased from Dalton Chemical Laboratories (DCL, Toronto, ON). Chlorotrimethylsilane (TMS-Cl), 4-dimethylaminopyridine (4-DMAP), benzoyl chloride (Bz-Cl) and phenoxyacetyl chloride (PA-Cl) were obtained from Aldrich.

Hoescht 33258 and ethidium bromide (2, 7-diamino, 9-phenylphenanthridinium 10-ethyl bromide) were purchased from Aldrich Chemical Company. BePI was obtained as a gift from Dr. Claude Hélène.

Silica gel (Toronto Research Chemicals, Toronto, ON) derivatized with the optical fibres had a particle size of 30-70 microns. The optical fibres were obtained from 3M Canada (Toronto, ON).

Analytical grade magnesium chloride, sodium chloride, sodium dihydrogenphosphate, disodium hydrogenphosphate obtained from BDH were used for T_m buffers.

6.1.2 Chromatography.

Silica Gel Column Chromatography: Merck Kieselgel 60 (200-400 mesh) silica gel (VWR) was employed for gravity and flash columns.

Thin Layer Chromatography: R_f values were obtained by using Merck Kieselgel 60F 254 silica analytical sheets (0.2mm x 20cm x 20cm). Nucleosides and derivatives were detected by using a UV light source (mineralite, output ca. 254nm). Trityl containing compounds were detected by exposing the silica gel sheets over concentrated hydrochloric acid vapour.

6.1.3 Instruments.

NMR Spectra. All spectra were obtained at ambient temperature, either on a Varian XL-300 or XL-500 spectrophotometer, and the chemical shifts are reported in ppm downfield from tetramethylsilane (TMS). For the new compounds synthesized, all ^{13}C and ^{1}H assignments were made using 2-D n.m.r. experiments, including homonuclear correlated spectra (COSY), and ^{1}H-detected heteronuclear multiple quantum coherence spectra (HMQC). Deuterated solvents: D_2O, acetone-D6, and dimethylsulfoxide-D6 were obtained from Isotec, Inc. (Miamisburg, OH).

FAB-Mass Spectrometry. Fast atom bombardment mass spectra were collected using a Kratos MS25RFA high resolution mass spectrometer. Nitrobenzyl alcohol (NBA) matrix was used.

UV Spectra. UV-vis spectra were recorded with a Varian CARY I spectrophotometer (Varian: Mulgrave, Victoria, Australia). Absorbance versus temperature profiles of complexes were measured at 260 nm with a Varian Cary I UV-vis spectrophotometer equipped with a variable temperature cell holder controlled by an external variable temperature circulating bath. All data was collected using the manufacturer's supplied software (version: Cary 1.3e) and a personal computer.

Circular Dichroism. Circular dichroic spectra were collected on a Jasco J-710 spectropolarimeter. Hellma fused quartz (165-QS) cells were used, and the temperature was controlled by an external constant temperature Neslab RTE-111 circulating bath. The data were smoothed on a IBM/PC computer using Windows™ software supplied by Jasco, Inc. CD calculations were also performed with this software.

Electrospray Mass Spectrometer. The DNA sample was dissolved in a 0.5% aqueous ammonia solution The solution was injected into a VG Quattro II triple quadrupole mass spectrometer (acquired in negative mode) through a 20 μL loop attached to a Rheodyne model 7125 valve (which was interfaced through 60cm long 0.17mm id PEEK tubing). A Hewlett-Packard 1090 HPLC was used to pump the mobile phase (acetonitrile:water 1:1) with a rate of 10 μL/min.

6.2 Synthesis of Oligonucleotides.

6.2.1 General Considerations.

DNA synthesis reagents were purchased from Dalton Chemical Laboratories (Toronto, ON) and were used as received or were prepared as below. Anhydrous acetonitrile (Caledon) was predried by distillation from P_2O_5 and redistilled from calcium hydride under dry argon. Tetrahydrofuran (BDH) was predried over CaH_2, filtered and distilled immediately prior to use from sodium (Aldrich)/benzophenone (Aldrich). Detritylation was performed with 3% trichloroacetic acid in dichloroethane. Activation of phosphoramidites was achieved with 0.5M tetrazole in acetonitrile. Reagents for acetylation (capping) were prepared as follows: Cap A, 10% acetic anhydride and 10% collidine in THF; and Cap B, 16% N-methylimidazole in THF (w/v). Iodine, 0.1M, in THF/pyridine/water (25:20:2, v/v/v) was used for oxidations.

Long-chain alkylamine controlled-pore glass supports (LCAA-CPG, 500 Å pore size; density, Pierce Chemical Co., Rockford, IL or Dalton Chemicals) were derivatized according to previously described methods.[106,158] Nucleoside loadings were determined by spectrophotometric dimethoxytrityl cation assay.

Nucleoside-LCAA-CPG support was loaded into an empty column with replaced filters (ABI), crimped closed with aluminum seals (Pierce) and installed on the instrument. Prior to oligonucleotide assembly, the derivatized solid-support was treated with the acetic anhydride/N-methylimidazole capping reagent using the capping cycle provided by Richard Pon. Phosphoramidite reagents were dissolved in dry, freshly distilled acetonitrile. Final concentrations of 0.1M and 0.15 M for DNA and RNA, respectively. The 2' phosphoramidite reagents were used at 0.2M, and N^6-benzoyl-5'-O-dimethoxytrityl-2',3'-O-bis(2-cyanoethyl)N,N-diisopropylphosphoramidite was used at 0.03 M. All solutions were passed through a 0.45 μm pore Teflon® filter via a 'swinny'

filter apparatus (Millipore, Mississauga, ON) prior to DNA/RNA synthesis. The syntheses were evaluated by UV spectroscopic quantitation of trityl cation released during the trichloroacetic acid treatment step (504 nm for DMT+ ,ε = 76, 000 $L \cdot mol^{-1} \cdot cm^{-1}$).

6.2.2 Automated Synthesis of Branched "V" (2.1) and "Y" (2.2) Oligonucleotides.

All branched oligonucleotides were prepared according to the convergent synthesis protocols.[58] Branched sequences were synthesized on an Applied Biosystems 381A instrument on a 1-μmol-scale using β-cyanoethylphosphoramidite chemistry[7b, 159,160] The sequence 3'-$dT_{10}dC_4$5'-5'dT_{10}-3' was prepared by assembly of 3'-$dT_{10}dC_4$-5' on controlled-pore glass followed by "backward" 5'- to 3'-synthesis of the second dT_{10} segment. This necessitated a 5'-phosphoramidite 3'-dimethoxytritylated T monomer which was provided by Miguel Roman of the Damha laboratory.

6.2.3 Synthesis of Oligonucleotides on Optical Fibres.

The GOPS functionalized fibres were then placed in a 10-μmol scale synthesis column, with the "dead" volume being filled with polypropylene pieces. The fibres were then capped with Cap A and B solution (acetic anhydride/collidine) prior to DNA synthesis. The Cap A solution was replaced with the Millipore Cap A reagent (phenoxyacetyl anhydride/ collidine/THF) (Millipore, Mississauga, ON) for phenoxyacetyl amidites. Prior to oligonucleotide assembly, the optical fibres were treated with capping reagents to block undesired reactive sites[161] by use of the capping cycle. N^6-phenoxyacetyl-5'-O-DMT-2'-deoxyadenosine-3'-(2-cyanoethyl)phosphoramdite was obtained from Millipore, and N^6-phenoxyacetyl-3'-O-DMT-2'-deoxyadenosine-5'-O-(2-cyanoethyl)-phosphoramdite was prepared via standard protocols.[162] The amidites were dissolved in acetonitrile to a concentration of .1M and dA_{10} sequences were grown on a DNA synthesizer (Applied Biosytems 391 instrument) using β-cyanoethylphosphoramidite

chemistry. The DNA synthesizer's .2μmol scale cycle was modified to increase the coupling time to 10 minutes and the delivery of the solutions for a 10-μmol scale column. The syntheses were evaluated by spectrophotometric quantitation of trityl cation released during the trichloroacetic acid treatment step (504 nm for DMT+ ,ε = 76, 000 $L \cdot mol^{-1} \cdot cm^{-1}$). The oligomers were then deprotected with a solution of NH_3 /EtOH (3:1, v/v) for 2 hours at room temperature. Following deprotection, the ammonia solution was collected, the column was washed with autoclaved water and the eluent was also kept. Quantitation of the eluents at 260nm indicated that ca. 80% of oligomers were lost from the fibre surface.

6.2.4 Synthesis of Branched Oligonucleotides 3.3, 3.4 and 3.5.

The synthesis of these branched compounds involved first growing dT_{10} (1.0 μmol) with an automated DNA synthesizer, using standard phosphoramidite protocols and controlled-pore glass (23 μmol dT/g) as the solid support. The branching synthon (either 3.1 or 3.2) was introduced as a 0.15 M solution dissolved in THF-MeCN, CH_2Cl_2 (2:2:1), with an 80% and 38% efficiency (unoptimized), respectively, based upon the yield of the dimethoxytrityl cation released after coupling. Prior to branching the terminal 5'-hydroxyl was capped with the capping cycle. The synthesis of the branched oligonucleotides containing the flexible linker involved a manual deprotection step. The levulinyl protecting groups were removed with a solution of hydrazine hydrate using conditions which did not cause the cleavage of the oligomer from the support.[163] A 1 mL solution of 4:1 pyridine-acetic acid containing 50 μl of hydrazine hydrate solution should be made up in the following manner: add 800 μL of pyridine and 200μL of distilled acetic to the ependorf and mix thoroughly. Slowly add the hydrazine hydrate to the solution with thorough mixing until all 50 μL has been added. Wait approximately 10 minutes to ensure no precipitate forms prior to treatment of the column. Using a dual luer-type disposable syringe the hydrazine solution was run through the column containing the oligomer over a time period of 5 minutes. After thorough washing with

dry acetonitrile, the column was re-installed on the synthesizer, the column was re-installed on the synthesizer, and chain assembly of another dT_{10} strand was continued in the normal fashion. Quantitation of trityl cations released indicated that delevulination and subsequent coupling steps proceeded with *ca.* 98% yield.

6.2.5 Synthesis of D and L-2',5' Oligoribonucleotides.

All 2,'5'-linked oligonucleotides were prepared according the silyl-phosphoramidite approach. The purine 2'-phosphoramdites were introduced as a 0.20-0.25 M solution dissolved in MeCN, due to the poor coupling efficiency of these monomers. The pyrimidine 2'-amidites were introduced as a 0.15M solution dissolved in MeCN. Furthermore, the coupling time was extended to 15 minutes per nucleoside addition.

6.2.6 Deprotection of Oligonucleotides.

LCAA-CPG beads were treated with (3:1) 29% NH_3/EtOH at r.t. to liberate the oligonucleotides from the solid support and to remove the exocyclic amino protecting groups. Under these conditions, dT_{10} and rU_{10} oligomers were deprotected for 4 hours, all oligomers containing rG^{iBu}/dG^{iBu} were deprotected for 48 hours, and oligomers containing A/C/T/U were deprotected for 24 hours. The solution of oligonucleotides were removed from the control pore glass via micropipette, the sample then frozen in an ependorf using liquid nitrogen and further lyophilized to dryness. All ribooligonucleotides were desilylated by treatment with triethylamine tris(hydrogenfluoride) or TREAT HF[164] for 6 hours at room temperature.

Table 6.1 Synthetic Yields of Oligonucleotides.

Compound	scale (μmol)	crude yield‡ (OD units¶)	purification method†	yield OD, (%)
$A^{T10}{}_{T10}$ **1.1**	1	65	PAGE/SEC	12.6, (19.4)
5'mix-r$A^{T10}{}_{T10}$ **1.2**	1	75 : 20	PAGE/SEC	3.3, (16.5)
"Y" (linker n=2) **3.5**	1	26	PAGE/SEC	1.9, (7.3)
V (linker n=2) **3.4**	1	4.5	PAGE/SEC	0.21, (4.7)
V (linker n=5) **3.3**	1	63	PAGE/SEC	22, (35)
all 2',5'-linked 18mer	1	72	PAGE/SEC	1.7, (2.4)
18mer with 4x 3'-OMe-rA inserts **4.10**	1	61	OPC	1.5, (2.5)
2',5'-L-rA_9dT	0.2	8.4	PAGE/SEC	0.41, (4.9)
2',5'-D-rA_9dT	0.2	21:10	PAGE/SEC	1.7, (17)

‡ The crude yield is total number of optical density units, the number after the crude yield (:) represents the number of O.D.'s used for purification. ¶ An O.D. represents the number of absorbance units in 1mL of water as quantitated at 260nm. † PAGE represents polyacrylamide gel electrophoresis purification, and SEC, represents Sephadex size exclusion chromatography.

6.3 Purification of Oligonucleotides.

6.3.1 Polyacrylamide Gel Electrophoresis.

Crude oligomers obtained from deprotection were purified via polyacrylamide gel electrophoresis using Bio-Rad (Mississauga, ON) and Hoefer Scientific (San Francisco, CA) electrophoresis units. Molecular biology grade acrylamide, N,N'-methylene-bis(acrylamide) (BIS), ammonium persulphate (APS), N,N,N'N'-tetramethylethylenediamine (TEMED), bromophenol blue (BPB) and xylene cyanol (XC) were from Bio Rad (Mississauga, ON). Boric acid (BDH), formamide (BDH), disodium ethylenediaminetetracetate dihydrate (EDTA, BDH), tris(hydroxy-methylaminomethane)

(Tris), sucrose (Aldrich) and urea (Caledon) were used for gel electrophoresis experiments.

Analytical gels were cast using spacers have a thickness of 0.75 mm and preparative gels were cast with 1.5 mm thick spacers. Most common gels were composed of 25% (w/v) acrylamide and 5% (with respect to the mass of acrylamide) BIS, i.e. 19:1 acrylamide/BIS. Denaturing gels contained 7M urea and employed TBE buffer (89 mM TRIS/boric acid, 2.5 mM EDTA, pH = 8.3).[165] 100% formamide used as loading buffer was deionized by stirring over a mixed bed ion-exchange resin (Bio Rad AG 501-X8). All oligonucleotides were purified by denaturing PAGE (with the exception of dT_{10}), in order to prevent any self-association of the oligomers.

For the native gels, the solutions of oligonucleotides were lyophilized, incubated in 10μLs of 30% sucrose with 50 mM $MgCl_2$ at 75 °C for 15 min., and then cooled to room temperature slowly. After a 4 day incubation at 4 °C, the samples were loaded onto the gel. The running buffer contained 90mM Tris-borate buffer (TB) (pH 8.0). The nondenaturing 15% polyacrylamide gels contained 90mM tris-borate (TB) (pH 8.0) and 50mM $MgCl_2$. The native gels were run at 12.5mA for 12h. Following electrophoresis, the gels were covered with Saran Wrap and photographed with a Polaroid MP4 Land Camera over a fluorescent TLC plate (Merck, distributed by EM Science, Gibbstown, NJ) and illuminated by a UV lamp (Mineralight lamp, Model UVG-54, San Gabriel, CA). Instant Sheet Film (#52), medium contrast, ISO 400/21 °C was used; (f4.5, 1.5s) through a Kodak Wratten gelatin filter (#58). Subsequently, the gels were stained for 5 min in a 5μg/mL of ethidium bromide, destained in distilled water for 30s. The gels were then covered with Saran Wrap™, illuminated by a UV lamp and photographed (f4.5, 2s) through a Hoya orange filter over a white background.

6.3.2 Purification of "trityl-on" Oligonucleotides.

Following deprotection, oligomers bearing a terminal 5'-dimethoxytrityl protecting group were concomitantly detritylated and purified by reversed-phase column chromatography on "trityl-on oligonucleotide purification cartridges" (TOPC™) according to the supplier's specifications (Applied Biosystems, Inc.).

6.3.3 Desalting of oligonucleotides.

All oligonucleotides were separated from low molecular weight impurities and salts by size exclusion chromatography using sephadex G-25 fine SEC media (Pharmacia, Baie d'Urfé, QC). The sephadex was autoclaved (90 minutes, 120 °C, 5 atm) using an All American Electric Steam Sterilizer - Model No.25X (Wisonsin Aluminum Co., Inc., Manitowoc, WI) and allowed to hydrate overnight. SEC was run in sterile, 10mL disposable syringe barrels (Becton Dickinson & Co., Franklin Lakes, NJ) plugged with silanized glass wool (Chromatographic Specialties Inc., Brockville, ON). Double distilled, autoclaved water was used to hydrate the sephadex, pack the column and elute the oligonucleotides. Approximately 1mL fractions were collected and the amount of oligonucleotide in each was quantitated by UV absorbance spectrophotometry (both at 260nm and at λ_{max}) and stored at -20°C.

6.4 Characterization of Oligonucleotides.

6.4.1 Enzymatic Hydrolysis of Oligonucleotides and HPLC analyses.

Snake venom phosphodiesterase (SVPDE) from *Crotalus durissus* (Boehringer Mannheim, Dorval, QC) was obtained as a solution of 2 mg/mL in 50% (v/v) glycerol, pH 6.0. Alkaline phosphatase (AP) from calf intestine (Boehringer Mannheim) was

obtained as a suspension 2 mg/mL in $(NH_4)_2SO_4$ (3.2 M); $MgCl_2$ (1 mM); $ZnCl_2$ (0.1 mM), pH 7.0. The incubation buffers for the enzymatic digestions were prepared from autoclaved water and filtered through a sterile 0.2 mm membrane (Acrodisc®, Gelman Sciences Inc., Rexdale, ON). SVPDE/AP incubations were performed in 50 mM Tris-HCl, 10 mM $MgCl_2$, pH 8. Typically, 1.0 A_{260} units of oligonucleotide was dissolved in 10 μL of buffer to which the appropriate enzyme was added and incubated at 37°C. SVPDE/AP digests were done with 2 μL of SVPDE (2 μg, 0.002 U)/1 mL of AP (6 μg, 9 U) and were allowed to proceed for 24 hours at 37 °C.

Enzyme digested sample analyses were carried via a Waters HPLC instrument equipped with dual 501 pumps, UK6 injector, 480 UV detector governed by the 680 gradient controller being output through a 480 data module. The HPLC instrument was interfaced to a computer with a Water Bus LAC/E card running Millenium™ 2010 Chromatography Manager. A Whatman Partisil ODS-2 column (4.6 x 250 mm) with a linear gradient 0 - 50% in B was used over 30 minutes (solvent A: 20 mM KH_2PO_4, pH 5.5, solvent B: methanol) with a flow rate of 1.5 mL/minute at 30 °C.

Oligonucleotide/nucleoside samples were centrifuged at 12,000 x g for 1 minute prior to injection (this centrifuges the particulates to the bottom of the ependorf). Injections of 10 μL (0.5 A_{266}) were found to be suitable for the determinations. Components of the analyte solution were identified by comparison to an authentic sample of thymidine (Sigma Chemical Co., St. Louis). The 1.0 A_{266} linker synthon **3.1** (with a 3'-triisopropyl group) was treated with 5% trifluoroacetic acid in dichloromethane for 30min, followed by quenching of the TFA with 5% aqueous sodium bicarbonate and two subsequent extractions with 5% sodium bicarbonate. The organic layer was lypholized, treated with TREAT HF for 24 hours and then lypholized to a pellet. After desalting of the nucleoside, 0.5 A_{266} units were dissolved in 11uL, and then 10 uL was injected for HPLC analysis.

6.4.2 Capillary Electrophoresis (CE) Analysis.

Oligomers were characterized on a Beckman P/ACE System equipped with a eCAP ss DNA 100 Gel capillary, 100μm I.D. The elution buffer consisted of TRIS-Borate (44% Tris, 56% Borate) in 7M Urea. The samples were run at 30 °C, voltage 11.1V, wavelength 254nm. Injection time varied from 2 to 10 seconds depending on sample concentration, longer loading times being required for more dilute samples.

6.5 Spectroscopic Analysis.

6.5.1 UV-Thermal Denaturation Profiles.

Data were collected with the spectrophotometer set on dual beam optical mode to reduce optical drift. The data were collected at 260 and 284 nm at 0.5 °C intervals with an equilibration time of 60 s for each measurement point. Extinction coefficients of the branched molecules were assumed to be similar to their corresponding linear sequences and were calculated from those of mononucleotides and dinucleotides according to the nearest-neighbour approximation.[166] Samples for thermal denaturation analysis were prepared by mixing the oligomer with the target strand, lyophilizing the solution to dryness, and dissolving the oligomers in the appropriate buffer. The mixtures were then transferred to Hellma QS-1.000-104 cells. Solutions contained *ca.* 2μM of each oligomer in a buffer of (a) 10 mM Tris, 50 mM $MgCl_2$, pH 7.3 adjusted with HCl, or (b) 1 M NaCl, 10 mM Na_2HPO_4, pH 7.0 adjusted with HCl. Oligonucleotide solutions were heated to 80°C for 15 min and then slowly cooled to room temperature prior to melting experiments. Normalized plots were constructed according to the method of Kibler-Herzog *et al.*[167] ($\{A_t - A_0)/(A_f - A_0)\}$: where A_0 is the initial absorbance, A_f is the final absorbance and A_t is the absorbance at any temperature. Hyperchromicity values (%H) are reported as the percent increase in absorbance at the wavelength of interest with

respect to the final absorbance as described by Puglisi and Tinoco.[24] Precision in T_m values, determined from variance in repeated experiments, is no greater than ±0.5 °C.

Thermal denaturation studies involving DNA-binding ligands were performed by mixing the oligomer with the target strand, lyophilizing the solution to dryness, and dissolving the oligomers in magnesium buffer. The oligomers were then heated to 80 °C for 15 min, then slowly cooled to room temperature, and allowed to equilibrate at 4 °C for 48 hours. The lyophilized DNA ligand was dissolved in 10μL of buffer and added to oligonucleotide solution. The solution was then equilibrate for 48 hours, and degasssed briefly prior to running the melting experiment. All T_m runs were done in triplicate using separately prepared samples, and the average melting temperature calculated.

6.5.2 Circular Dichroism Spectroscopy.

All spectra were recorded between 200-350nm. The scan speed was 100 nm/min, sampling wavelength was 0.2 nm, and 15 repetitive scans were obtained and averaged for each sample. Solutions contained *ca.* 10 mM of each oligomer in a buffer of 10 mM Tris, 50 mM $MgCl_2$, pH 7.28 adjusted with HCl. Before data acquisition, samples were allowed to equilibrate for 10 min at the appropriate temperatures.

6.6 Biosensor Triplex Studies.

6.6.1 Activation of Optical Fibres.

The buffer coating was mechanically stripped from the pre-cut optical fibre pieces and the cladding was dissolved by treatment with acetone. The surface of the fibres were then cleaned via treatment with 25% ammonia/30% hydrogen peroxide/water (1:1:5, v/v/v) for 15 minutes at 80°C followed by rinsing with 30% hydrogen peroxide. The fibres were treated with a solution of conc. HCl/30% hydrogen peroxide/water (1:1:5, v/v/v) for 5

minutes at 80°C, followed by rinsing with methanol, dichloromethane, diethyl ether, respectively.

Optical Fibres and silica gel were activated by introduction into a solution of xylene/3-glycidoxypropylltrimethyl silane (GOPS)/diisopropylethylamine (100:30:1 v/v/v). The reaction was stirred under nitrogen at 80 °C for 24 hours. The fibres and silica gel were rinsed with methanol, dichloromethane, diethyl ether, respectively.

The solid supports were functionalized with mono-tritylated pentaethylene glycol (DMT-PEG) (4.83g, 8.93 mmol) in 30mL of xylene containing a catalytic amount of sodium hydride and stirred at 40 °C for 7 days. Silica gel samples were taken out of the reaction mixture to determine the loading of DMT-PEG on the activated fibres. The silica gel was washed with dichloromethane until the wash solution had no absorption at 504nm upon treatment with 5% trichloroacetic acid in dichloroethane. This analysis indicated that the reaction had finished within 7 days. The fibres were then washed with a solution of dichloromethane and dried overnight in the dessicator. The fibres were capped via treatment of a solution of chlorotrimethylsilane in pyridine (1:10, v/v) under argon at room temperature for 16 hours. The fibres were sequentially washed with pyridine, dichloromethane, methanol and diethyl ether.

6.6.2 Fluorescence Studies.

The fluorescent studies[2] were performed by the new optical fibre sensing unit developed by Piunno and Krull (unpublished results). First the fibre was aligned beneath the objective of a fluorescent microscope. Prior to the fluorescent measurements, the fibres were washed with ethanol, then with 10mM Tris, 50mM $MgCl_2$, pH7.3 (at 40 °C) and again with buffer containing 2.5 x 10^{-8} M ethidium bromide (at 40 °C). Fluorescent measurements were taken with the buffer solution containing and not containing ethidium

[2] Activation of the fibres and the fluorescent studies were conducted at the University of Toronto, all these experiments were done together with Piunno.

bromide solution to ensure the instrument was responding correctly. Lypholized dT_{10} or compound **2.1** were dissolved in a buffer of 10mM Tris, 50mM $MgCl_2$, pH7.3 to make a concentration of 2500ng/mL or 700ng/mL, respectively, in the presence of 2.5×10^{-8}M ethidium bromide. The oligomer solutions were delivered to the cell containing the fibres, the solutions were then heated to 80 °C, and cooled slowly. During the cooling process, fluorescent measurements were taken at various time intervals. The fluorescent response of the optical sensor was also measured with 2.5×10^{-8} M ethidium bromide at various temperatures to obtain the background fluorescent levels.

6.7 Inhibition of HIV-1 with 2',5'-Linked Antisense Oligonucleotides.

6.7.1 Inhibitory Potency of R-Region Specific Antisense Oligonucleotides Against *in vitro* DNA Polymerization catalyzed by HIV-1 Reverse Transcriptase.

Note: All HIV-1 antisense studies were conducted at the McGill AIDS Centre, the experimental was performed by Dr. Gadi Borkow.

Materials. Recombinant heteropolymeric p51/p66 HIV-1 RT was purified from lysates of *E.coli* JM-105 transformed with expression plasmids pRT66 and pRT51. The "donor" and "acceptor" RNA templates used in reverse transcription reactions were prepared by *in vitro* transcription from plasmids pHIV-PBS and pHIV-R/U3, respectively, using T7 polymerase. Ultrapure dNTPs, T7 RNA polymerase and *E.coli* RNase H were obtained from Pharmacia. [α-^{32}P]-dCTP was purchased from Amersham.

Method. The effect of the various AON on reverse transciptase RNA-dependent DNA polymerase (RDDP) activity of HIV-1 RT was examined in fixed time assays by using the 496 nt pHIV-PBS donor RNA template primed with a synthetic 18 nt DNA oligonucleotide complementary to the HIV-1 primer binding sequence (PBS) in the donor RNA template. Template/primer was prepared by mixing pHIV-PBS RNA (50pmol)

with 18nt (500pmol) and antisense oligonucleotides (250-2500 pmol) in a final volume of 100 µL of 50mM Tris-HCl (pH 8, 37 °C). Reaction mixtures (50µL total volume) for (-) strong stop DNA synthesis typically contained 50pmol performed template primer, 20µM of the four dNTPs and tracer [α-^{32}P]-dCTP in 50mM Tris-HCl (pH 7.8, 37 °C) containing 10mM dithiothreitol, 60mM KCl and 4mM $MgCl_2$. Reactions were initiated by the addition of 25-50ng p51/p66 R, followed by incubation at 37 °C. After a 24 hour incubation period, an aliquot was placed on ice, and the polymerization products were extracted with phenol/chloroform, followed by precipitation with sodium acetate/ethanol, and centrifugation at 12,000xg for 10 minutes. The resulting pellet was washed with 70% ethanol then dissolved in 25µL loading buffer (TBE buffer containing 98% deionized formamide, 10mM EDTA, 1mg/mL bromophenol blue and 1mg/mL xylene cyanol) and heated at 100 °C for 5 minutes. Polymerization reaction products were resolved on a 10% sequencing gel containing 7M urea in TBE buffer and visualized by autoradiography (Kodak X-OMAT film).

6.7.2 Inhibition of HIV-1 (strain 3B) Infected Cells using Antisense Oligonucleotides

MT-2 cells were adjusted to a concentration of 10^5 cells/mL and cultured. The cells were then incubated for 2 hours with various concentrations of the AONs. Subsequently the cells were then infected with HIV-1B virus and cultured for three days. The HIV-specific antigen (p24) was measured by an Enzyme Immuno Assay.

6.8 Monomer Preparation for Synthesis of Oligonucleotides.

6.8.1 Synthesis of 5' phosphoramidite used in Optical Fibre Studies.

5',3'-O-Bis(dimethoxytrityl)-N^6-benzoyl-2'-deoxyadenosine. (2.4)

To pure 5'-O-dimethoxytrityladenosine N^6-benzoyl-2'-deoxyadenosine (2.3) (7.2mmol, 4.7g) was added (14.2mmol, 4.84g) DMT-Cl and dry pyridine with a catalytic amount of 4-DMAP in a oven dried (purged with nitrogen) 500mL round-bottom flask with a stirring bar. The reaction mixture was stirred at 35°C for 48 hours and TLC analysis R_f= 0.56 (5% methanol in dichloromethane) showed that the reaction to have proceeded quantitatively. The reaction was then stopped by the addition of 50mL of 5% $NaHCO_3$, and the solvent was removed by rotary evaporation. The mixture was then dissolved with 250mL of dichloromethane and extracted 3x with 250mL of $NaHCO_3$. The organic layer was removed via evaporation, followed by subsequent co-evaporations with 2x 100mL of dry toulene, until a yellow foam was obtained, 9.75g of crude material. The crude product (2.4) was used for the next step without further purification.

3'-O-Dimethoxytrityl-N^6-benzoyl-2'-deoxyadenosine. (2.5)

Crude nucleoside (2.4) (7.22g, assume 95% yield) was placed in a dessiccator over P_2O_5 overnight and was added to a saturated solution of $ZnBr_2$ in anhydrous nitromethane (.1M, containing some solid $ZnBr_2$) in a dry 250 mL round-bottom flask with a stirring bar. The solution turned bright orange. After stirring for 25 minutes at 0 °C, the reaction was worked up by adding the mixture to 200mL of a 1M NH_4OAc. The mixture was extracted with dichloromethane. The organic layer was then extracted with 200mL of 1M NH_4OAc followed by a subsequent extraction with brine solution. The organic layer was dried over Na_2SO_4, filtered and the solvent removed by rotary evaporation. The gum was further co-evaporated with toulene to remove nitromethane. Silica gel column (30 g of silica gel/g of nucleoside with a gradient of hexanes: dichloromethane 1:4, to 0-5%

methanol in dichloromethane) gave 2.55g (73%, two steps) of compound (2.5) as a light beige foam after being concentrated.

TLC R_f=.62 (ethyl acetate:dichloromethane, 19:1). UV (95% ethanol) λmax=280nm, λmin=256nm. ^{1}H NMR (DMSO-D6) 500Hz, δ=1.90 (m, 1H, H2'), 2.41 (m, 1H, H2''), 3.17-3.21 (m, 2H, H5' & H5''), 3.72 (s, 6H, 2x PhOC$\underline{H}_3$ of DMT), 4.00 (m, 1H, H4'), 4.38 (m, 1H, H3'), 4.98 (m, 1H, 5'OH)*, 6.48 (dd, 1H, H1'), 8.56 (s, 1H, H2), 8.70 (s, 1H, H8), 11.18 (s, 1H, N$^6\underline{H}$). *Note: Upon addition of a drop of D_2O, the proton peak at 4.98 disappeared confirming the presence of a free 5' hydroxyl group. ^{13}C NMR (DMSO-D6) 500Hz, δ= 38.1 (C2'), 54.9 (PhO$\underline{C}H_3$ of DMT), 75.0 (C3'), 84.7 (C1'). MS (FAB - nitrobenzyl alcohol calc. M^+: 657), found: MH^+: 658, DMT^+: 303, (MH-DMT^+): 355.

3'-O-dimethoxytrityl-2'-deoxyadenosine. (2.6)

To pure 3'-O-dimethoxytrityl-N^6-benzoyl deoxyadenosine (2.5) (3.64 mmol, 2.5 g) was added a mixture of 350 mL of NH_3/EtOH (3:1, v/v) in a 500mL round bottom flask with a stirring bar. After stirring for 48 hours at room temperature, TLC analysis R_f=0.28 (ethyl acetate: dichloromethane, 19:1) indicated the reaction had proceeded to completion, the solvent was then removed by rotary evaporation. The crude product (2.6) was used for the next step without further purification.

3'-O-dimethoxytrityl-N^6-phenoxyacetyl-2'-deoxyadenosine. (2.7)

Nucleoside (2.6) (3.26 mmol, calculated from the crude mixture) was dissolved in 60 mL of dry pyridine in an oven-dried 100mL round bottom flask containing a stir bar, and to this trimethylsilyl chloride (16.3mmol, 2.1mL, 5eq.) was added. The reaction was stirred for 1 hour at room temperature, cooled to 0 °C for 15 minutes and a solution of 1-hydroxybenzotriazole hydrate (5.13mmol, .69g, 1.5eq.), phenoxyacetyl chloride (4.89mmol, 0.67mL) with dry acetontrile (1.33mL) was added dropwise with a 10mL oven-dried addition funnel. The reaction was stirred for 6 hours at 0 °C and stirred at

room temperature for 24 hours. The reaction was stopped with 10mL of 5% $NaHCO_3$. The solvent was concentrated to yield an oil, and then dissolved in 100mL of dichloromethane, and extracted 2x with 5% $NaHCO_3$. After drying the organic layer over Na_2SO_4 and rotovaping the mixture (in a 100mL round bottom flask) it was kept in a dessiccator over P_2O_5 for 12 hours. 15mL of 1M TBAF was added to the round bottom flask and stirred for 6 hours. The orange colored reaction was stopped by the addition of 50mL of 5% aqueous $NaHCO_3$. The mixture was extracted with 100mL of dichloromethane and washed with 2 x 5% $NaHCO_3$ and 2x brine solution 100mL. The organic layer was dried over Na_2SO_4, filtered, and rotovapped to yield a dark oil. The compound was purified by column chromatography (30g silica gel/g of nucleoside) by elution with a gradient of 0-65% ethyl acetate in dichloromethane to yield 0.96g of **2.7** (43%, two steps).

TLC R_f=.67 (ethyl acetate:dichloromethane, 1:1). UV (95% ethanol) λmax =273, λmin=252. ^{1}H NMR (DMSO-D6) 500Hz, δ=1.87 (m, 1H, H2'), 2.36 (m, 1H, H2''), 3.10-3.14 (m, 2H, H5'& H5''), 3.72 (s, 6H, 2x $PhOCH_3$ of DMT) 3.84 (m, 1H, H4'), 4.37 (m, 1H, H3'), 4.96 (m, 1H, 5'-OH)*, 6.45 (dd, 1H, H1'), 8.58 (s, 1H, H2), 8.63 (s, 1H, H8), 10.91 (s, 1H, N^6H of Ad). *Note: Upon addition of a drop of D_20, the peak at 4.96 disappeared confirming the presence of a free 5' hydroxyl group. ^{13}C NMR (DMSO-D6) 500Hz, δ= 56.1 ($PhOCH_3$ of DMT), 57.7 (C5'), 75.9 (C3'), 84.3 (C1'), 87.2 (C4'). MS (FAB - nitrobenzyl alcohol, calc. M^+: 687), found: MH^+= 688, DMT^+= 303.

3'-O-dimethoxytrityl-N^6-phenoxyacetyl-2'-deoxyadenosine 5'-O-N,N-diisopropylamino-2-cyanoethylphosphoramidite. (2.8)

To 3'-O-dimethoxytrityl-N^6-phenoxyacetyl-2'-deoxyadenosine (**2.7**) (.27 mmol, .184g) previously dried in a dessicator containing P_2O_5, was added 1.5mL of dry distilled THF in a nitrogen purged, oven dried, septum sealed 10mL hypovial containing a stir bar. To the stirring solution, a catalytic amount of 4-DMAP and N,N'-diisopropylethylamine (2.6 mmol, .24mL) was added, followed by the dropwise addition of N,N'-diisopropyl(2-

cyanoethyl)phosphonamidic chloride (.76 mmol, 100μL). After 4 hours of stirring, TLC analysis (acetone:dichloromethane, 3:7) showed complete consumption of starting material. The reaction mixture was added to ethyl acetate (50mL, prewashed with 5% $NaHCO_3$) and washed with 2x 50mL of 5% $NaHCO_3$, and then 5x 50mL of brine solution. The ethyl acetate layer was dried over Na_2SO_4, filtered and concentrated *in vacuo*, the product was coevaporated with dichloromethane and diethyl ether to yield a light yellow foam of compound **2.8** (.231g, 97%).

TLC R_f=0.58, 0.64 (dichloromethane:ether, 1:1). UV (95% ethanol, λ) λmax =273, λmin=252. ^{31}P NMR (ppm, acetone-D6) 500Hz δ=:148.80, 148.85 (two diastereomers).

6.8.2 Synthesis of monomers for 3',5' and 2',5' linked oligonucleotides.

Standard silylated ribonucleoside 3'-(2-cyanoethyl)phosphoramidite monomers were prepared according to the detailed protocols,[160] and were used in the synthesis of 3',5'-linked oligo-RNA. 3'-O-*t*-butyldimethylsilyl ribonucleoside monomers (U, C^{bz}, A^{bz}, G^{ibu}) were prepared according to literature protocols[168,169]. The isomeric purity of these monomers was established by comparison with the known 2'-silylated ribonucleoside 3'-phosphoramidite regioisomers using TLC analysis, ^{1}H and ^{31}P-NMR. Table 6.2, compares the ^{31}P NMR data for 2'-silylated nucleoside 3'-phosphoramidites and 3'-silylated nucleoside 2'-phosphoramidites isomers.

Table 6.2. ^{31}P NMR[¶] data of D-Ribonucleoside 2'- and 3'-O-Phosphoramidites.

	DMT-Cy-Bz	DMT-Ad-Bz	DMT-U	DMT-G-iBu
2'-amidite	150.98	150.79	155.22	150.39
	148.55	150.12	155.15	150.25
3'-amidite	146.09	150.92	150.15	151.13
	145.98	149.00	149.52	149.37

[¶](ppm, acetone-D6)

6.8.3 Synthesis of 3'-O-Methyl adenosine monomer.

5'-O-Dimethoxytrityl-3'-O-methyl-N^6-benzoyladenosine [4.3].

The mineral oil of the 80% sodium hydride/oil dispersion was removed by washing the hydride with HPLC grade hexanes in a hypovial (under Argon). The sodium hydride (7.54 mmol, 1.3eq.) was added in 30mL of dry DMF containing methyl iodide (7.54 mmol, 1.07g, 0.47mL, 1.3 eq.) and cooled to 0 °C in an oven dried 100mL round bottom flask containing a stir bar. 5'-O-dimethoxyltrityl-2'-O-t-butyldimethylsilyl-N^6-benzoyl adenosine [4.1] (4.57g, 5.8 mmol) was then dissolved in 15mL of DMF, cooled to 0 °C and added dropwise to the stirring reaction mixture. The reaction was stirred at 0 °C for 1 hour, and then stopped by the dropwise addition of 20mL of 5% $NaHCO_3$. The reaction mixture was added to 100mL of dichloromethane and extracted with 2x 100 mL of 5% $NaHCO_3$. The organic layer was dried over Na_2SO_4, filtered, and concentrated. The mixture of methylated/silylated compounds **4.2a** and **4.2b** having the same mobility [TLC R_f=.50 (ether:dichloromethane, 1:3)] were isolated as a mixture, using 30g of silica gel/g of nucleoside with a gradient of (ether:dichloromethane, 1:7 to 1:3). The products were then concentrated to yield 3.20g (65%) of a 4:1 mixture. The 4:1 ratios of compounds **4.2a** and **4.2b** were determined via ^1H NMR (acetone-d6) 500Hz by comparing the integration of the dimethyl shifts (δ = 0.13 and .08 : 0.00 and -0.13) and tert-butyl groups (δ = 0.88 : 0.78). The mixture of compounds (3.93mmol, 3.15g) was treated with 10 mL of 1 M TBAF in THF and stirred for 2 hours at room temperature. The reaction mixture was added to 50mL of dichloromethane and extracted with 5 x 30mL of brine solution. The organic layer was dried over Na_2SO_4, filtered, and concentrated *in vacuo*. The crude material was purified on a silica gel column using 70g of silica gel/g of nucleoside, employing a gradient of 1:1 ethyl acetate:dichloromethane to 5:2 ethyl acetate:dichloromethane, then from 5:2:1 ethyl acetate:dichloromethane:acetone to 5:2:3 ethyl acetate:dichloromethane:acetone. After evaporating the desired pooled fractions, the pure 3'-O-methyl isomer [4.3] was obtained with a yield of 0.54g (20%).

UV λ_{max} (95% EtOH) =280nm. TLC (acetone:dichloromethane, 3:7, R_f =.23). ^{1}H NMR (DMSO-D6) 500Hz, δ= 11.18 (s, 1H, N^6H), 8.36 (s, 1H, H8), 8.04 (s, 1H, H2), 5.93 (d, 1H, H1'), 5.28 (d, 1H, 2'OH)*, 4.27 (m, 1H, H2'), 4.01 (dd, 1H, H3'), 3.43 (s, 3H, OCH_3), 3.21 (m, 1H, H4'), 3.05 (m, 2H, H5' & H5''). Coupling constants (Hertz), $J_{H1'-H2'}$= 4.39, $J_{H3'-H4'}$=6.84. *Note: upon addition of drop of D_2O, the proton peak at 5.28 disappeared confirming the presence of a free 3' hydroxyl group. ^{13}C NMR (acetone D6) 500Hz: 87.08 (C1'), 85.08 (C4'), 83.83 (C2'), 70.51, (C3'), 64.54 (C5').

5'-O-dimethoxytrityl-3'-O-methyl-N^6-benzoyl-adenosine-2'-O-N,N-diisopropylamino-2-cyanoethylphosphoramidite [4.4].

To 5'-O-dimethoxytrityl-3'-O-methyl-N^6-benzoyl-adenosine [4.3] (.76 mmol, .50 g) - dried in a dessicator containing P_2O_5, was added 3mL of dry distilled THF in a nitrogen purged, oven dried, septum sealed 10mL hypovial containing a stir bar. To the sitrring solution, a catalytic amount of 4-DMAP (11mg) and N,N'-diisopropylethylamine (3.10mmol, .54mL) was added, followed by the dropwise addition of N,N'-diisopropyl(β-cyanoethyl)phosphonamidic chloride (0.90 mmol, 200μL). After 4hours of stirring, TLC analysis (acetone:dichloromethane, 3:7) showed complete consumption of starting material. The reaction mixture was added to ethyl acetate (50mL, prewashed with 5% $NaHCO_3$) and washed with 2x 50mL of 5% $NaHCO_3$, and then 5x 50mL of brine solution. The ethyl acetate layer was dried over Na_2SO_4, filtered and concentrated *in vacuo*, the product was coevaporated with dichloromethane and diethyl ether to yield 95% (0.72mmol, .49g) of a light yellow foam, compound [4.4].

TLC R_f=.68 and .75(acetone:dichloromethane, 3:7). UV λ_{max} (95% EtOH) =281nm. ^{31}P NMR (ppm, acetone-D6) 300Hz, δ= 148.1 and 148.8 (two diastereomers). ^{1}H NMR (acetone-D6) 500Hz, diastereomer 1: δ= 8.03 (s, 1H, H2), 8.38 (s, 1H, H8), 6.01 (d, 1H, H1'), 4.64 (m, 1H, H3'), 4.60 (m, 1H, H2'), 4.32 (m, 1H, H4'), 3.78 (s, 6H, PhOCH_3), 3.40 (m, 2H, H5' & H5''); diastereomer 2: δ=8.04 (s, 1H, H2), 8.39 (s, 1H, H8), 6.04 (d, 1H, H1'), 4.66 (m, 1H, H3'), 4.62 (m, 1H, H2').

6.8.4 Synthesis of SEM monomers.

3-N-(trimethylsilyl)ethoxymethyl-5'-O-dimethoxytrityl-2'-O-(trimethylsilyl)ethoxymethyl uridine [4.6a].

To pure 5'-O-dimethoxytrityl uridine [4.5] (3.00g, 5.50 mmol) dissolved in 65mL of distilled dichloromethane was added (55mmol, 7.11g, 9.58mL, 10 eq.) diisopropylethyl amine, in an oven dried 250 mL round bottom flask. The reaction was stirred under nitrogen, cooled to 0 °C and (12.65mmol, 2.11g, 2.24mL, 2.3 eq.) SEM-Cl was added dropwise. The reaction was allowed to proceed for 14 hours and then the dichloromethane and diisopropylethyamine were removed to yield a thick orange oil. The compound was purified by column chromatography (40 g of silica gel/g of nucleoside), where the mixture itself was dissolved in dichloromethane and then loaded onto the column a gradient of hexanes to 1:1 hexanes/ethyl acetate was used to elute the compounds. The compounds were eluted in the order of 3-N-(trimethylsilyl)ethoxymethyl-5'-O-dimethoxytrityl-2',3'-O-bis (trimethylsilyl)ethoxymethyl uridine, 3-N-(trimethylsilyl)ethoxymethyl-5'-O-dimethoxytrityl-2'-O-(trimethylsilyl)ethoxymethyl uridine, 3-N-(trimethylsilyl)ethoxymethyl-5'-O-dimethoxytrityl-3'-O-(trimethylsilyl)ethoxymethyl uridine, 3-N-(trimethylsilyl)ethoxymethyl-5'-O-uridine. Compounds 2'SEM [4.6a] and 3'SEM [4.6b] were isolated as white gummy foams in yields of 1.71g (38%) and 1.62g (36%), respectively.

Compound 4.6a:

TLC Rf= 0.60 (1:1, ethyl acetate/ hexanes). UV λ_{max} (95% EtOH) =266. ^{1}H NMR (DMSO-D6) 500Hz, δ= 7.78 (dd, 1, H6), 5.86 (d, 1H, H1'), 5.42 (d, 1, H5), 5.30 (d, 1, 3'-O<u>H</u>)*, 4.24 (m, 1, H2'), 4.20 (m, 1, H3'), 3.98 (m, 1, H4'), 3.72 (s, 6, 2x PhOC<u>H</u>$_3$ of DMT), 0.83 (t, 4H, 2x C<u>H</u>$_2$Si(CH$_3$)$_3$), -0.063(s, 18H, 2x Si(C<u>H</u>$_3$)$_3$). *Note: upon addition of drop of D_2O, the proton peak at 5.30 disappeared confirming the presence of a free 3' hydroxyl group.

Compound 4.6b:

TLC Rf= 0.47 (1:1, ethyl acetate/ hexanes). UV λ_{max} (95% EtOH) =266. ^{1}H NMR (DMSO-D6) 500Hz, δ=7.78 (dd, 1, H6), 5.73 (d, 1H, H1'), 5.58 (d, 1H, 2'-OH), 5.42 (d, 1H, H5), 4.24 (m, 1H, H2'), 4.14 (m, 1H, H3'), 4.07 (m, 1H, H4') 3.71 (s, 6H, 2x PhOC$\underline{H}_3$ of DMT), 0.81 (t, 4H, 2x C$\underline{H}_2$Si(CH$_3$)$_3$), -0.063, -0.085(s, 18H, 2x Si(C$\underline{H}_3$)$_3$).

3-N-(trimethylsilyl)ethoxymethyl-5'-O-dimethoxytrityl-3'-O-methyl-2'-O-(trimethylsilyl)ethoxymethyl uridine [4.7].

To pure 3-N-(trimethylsilyl)ethoxymethyl-5'-O-dimethoxytrityl-2'-O-(trimethylsilyl)ethoxymethyl uridine [4.6a] (1.86 mmol, 1.52g) dissolved in 35mL of distilled dry toulene was added 3 equivalents (1.29g, 5.58 mmol) of Ag_2O and an excess of iodomethane (25 eq., 6.60g, 2.89 mL, 46.5 mmol), in an oven dried 100 mL round bottom flask. The reaction was stirred under nitrogen at 35 °C for 13 hours, where TLC analysis showed the reaction went to completion. The compound was filtered to removed the AgI and dried to yield 1.51g (98%) of a white gummy compound [4.7].

TLC Rf=0.71 (1:1, ethyl acetate/hexanes). UV λ_{max} (95% EtOH) =266. ^{1}H NMR (DMSO-D6) 500Hz, δ=5.82 (d, 1H, H1'), 5.42 (d, 1H, H5), 4.45 (m, 1H, H2'), 4.07 (m, 1H, H4'), 4.06 (m, 1H, H3'), 3.72 (s, 6, 2x PhOC$\underline{H}_3$ of DMT), 3.55 (t, 2H, C$\underline{H}_2$CH$_2$Si(CH$_3$)$_3$), 3.31 (s, 3H, CH$_3$O), 3.25 (m, 2H, H5' & H5''), 0.83, 0.81 (t, 4H, 2x C$\underline{H}_2$Si(CH$_3$)$_3$), -0.045, -0.055(s, 18H, 2x Si(C$\underline{H}_3$)$_3$). ^{13}C NMR (acetone D6) 500Hz: δ= 88.4 (C1'), 75.3 (C2'), 80.9 (C4'), 77.5 (C3'), 57.7 (PhO$\underline{C}$H$_3$ of DMT), 62.1 (C5').

6.8.5 Synthesis of L-riboadenosine 2'-phosphoramidite.

L-5'-O-dimethoxytrityl-3'-O-t-butyldimethylsilyl-N^6-benzoyl-adenosine-2'-O-N,N-diisopropylamino-2-cyanoethylphosphoramidite [4.12].

L-5'-O-dimethoxytrityl-3'-O-t-butyldimethylsilyl-N^6-benzoyladenosine (>95% pure) was obtained from Dr. Anna Garbesi (Bologna, Italy). This monomer was further purified via column chromatography using 20g of silica gel/g of product with a gradient of dichloromethane to ether (7:1 to 3:1). To pure L-5'-O-dimethoxytrityl-3'-O-t-butyldimethylsilyl-N^6-benzoyl-adenosine (.43 mmol, .340g), was added to 1.5mL of THF, N,N'-diisopropylethylamine (2.26mmol, 4mL) and a catalytic amount of 4-DMAP. N,N-diisopropyl(2-cyanoethyl)phosphonamidic chloride (.66mmol, 150μL) was added dropwise. After stirring for 4 hours at room temperature, TLC (dichloromethane : diethyl ether, 3:1). analysis indicated that the reaction had proceeded to completion. The reaction mixture was added to 30mL of ethyl acetate (pre-washed with 5% $NaHCO_3$) and extracted with 30mL of 5% aqueous $NaHCO_3$, and 4x 30mL of saturated brine solution. The organic layer was dried over Na_2SO_4, filtered, concentrated and foamed by co-evaporation with dichloromethane and diethyl ether to yield .416 g (98%) of a white foam [5.8]. TLC: Rf= 0.43, 0.54 (3:1, DCM : diethyl ether). UV λ_{max} (95% EtOH)=280, λ_{min}=256. ^{31}P NMR (ppm, acetone-D6) 500Hz δ=: 150.81, 150.14 (two diastereomers).

References

[1] Watson, J.D.; Crick, F.H.C. *Nature*, **1953**, *171*, 737.

[2] (a) Crick, F.H.C. *Symp. Soc. Exp. Biol.*, **1958**, *12*, 138. (b) Crick, F.H.C. *Nature*, **1970**, *227*, 562.

[3] (a) Felsenfeld, G.; Davies, D.R.; Rich, A.J. *J. Am. Chem. Soc.*, **1957**, *79*, 2023. (b) Riley,M.; Mailing, B.; Chamberlin, M.J. *J.Mol.Biol.* **1966**, *20*, 359. (c) Michelson, A.M.; Massoulie, J.; Gushchelbauer, W. *Prog. Nucleic Acid Res. Mol. Biol.* **1967**, *6*, 83. (d) Morgan, A.R.; Wells, R.D. *J. Mol. Biol.* **1968**, *37*, 63.

[4] (a) Moser, H.E.; Dervan, P.B. *Science* **1987**, *238*, 645. (b) Le Doan, T.; Perrouault.; Praseuth, D.; Habhoub, N.; Decout, J.L.; Thoung, N.T.; Lhomme, J.; Hélène, C. *Nucleic Acids Res.* **1987**, *15*, 7749.

[5] (a) Mirkin, S.M.; Lyamichev, V.I.; Drushlyak, K.N.; Dobrynin, V.N.; Filipov, S.A.; Frank-Kamenetskii, M.D. *Nature* **1987**, *330*, 495. (b) For a review, see: Wells, R.D.; Collier, D.A.; Hanvey, J.C. Shimizu, M.; Wohlrab, F. *FASEB J.* **1988**, *2*, 2939.

[6] (a) Plum, G.E.; Pilch, D.S.; Singleton, S.F.; Breslauer, K.J. *Annu. Rev. Biophys. Biomol. Struct.* **1995**, *24*, 319, and references therein. (b) Sekharudu, C.Y.; Yathindra, N.; Sundaralingam, M. In *Structural Biology: The State of the Art*; Sarma, R.H.; Sarma, M.H., Eds.: Adenine Press, 1994, pp. 113.

[7] (a) Letsinger, R.L.; Lunsford, W.B. *J. Am. Chem. Soc.* **1976**, *98*, 3655. (b) Beaucage, S.; Caruthers, M.H. *Tetrahedron Lett.* **1981**, *22*, 1859. (c) Alvaredo-Urbina, G.; Sathe, G.M.; Liu, W.-C.; Gillen, M.F.; Duck, P.D.; Bender, R.; Ogilvie, K.K. *Science* **1981**, *214*, 270.

[8] For recent reviews see: (a) Radhakrishnan, I.; Patel, F.J.; *Structure* **1994**, *2*, 395. (b) Maher III, L.J. *BioEssays* **1992**, *14*, 807. (c) Cheng, Y.-K.; Pettitt, B.M.; *Prog. Biophys. Mol.Biol.* **1992**, *58*, 225. (d) Hélène, C. *Eur. J. Cancer* **1991**, *27*, 1466.

[9] (a) Xodo, L.E.; Manzini, G.; Quadrifoglio, F. *Nucleic Acids Res.* **1990**, *18*, 3557. (b) Kool, E.T. *J. Am. Chem. Soc.* **1991**, *113*, 6265. (c) Prakash, G.; Kool, E.T. *J. Chem.Soc. Chem. Commun.* **1991**, 1161. (d) Giovannangeli, C.; Monteney-Garestier, T.; Rougée, M.; Chassignol, M.; Thuong, N.T.; Hélène, C. *J. Am. Chem. Soc.* **1991**, *113*, 7775. (e) Salunkhe, M; Wu, T.; Letsinger, R.L. *J. Am. Chem. Soc.* **1992**, *114*, 8768. (f) D'Souza,D.J.; Kool, E.T. *J. Biomol. Str. & Dyn.* **1992**, *10*, 141. (g) Trapane, T.L.; Ts'o P.O.P. *J. Am. Chem. Soc.* **1994**, *116*, 10437. (h) Noll, D.M.; O'Rear, J.L.; Cushman, C.D.; Miller, P.S. *Nucleosides & Nucleotides* **1994**, *13*, 997.

[10] (a) Wang, S.; Kool, E.T. *J. Am. Chem. Soc.* **1994**, *116*, 8857. (b) Reynolds, M.A.; Arnold, L.J.; Almazan, M.T.; Beck, T.A.; Hogrefe, R.I.; Metzler, M.D.; Stoughto, S.R.;

Tseng, B.Y.;Trapane, T.L.; Ts'o, P.O.P. *Proc. Natl. Acad. Sci. U.S.A.* **1994**, *91*, 2433. (c) Wang, S.; Kool, E.T. *Nucleic Acids Res.* **1994**, *22*, 2326.

[11] Radhakrishnan, I.; Patel, D.J. *Biochemistry* **1994**, *33*, 11405.

[12] (a) Miller, J.H.; Sobell, H.M.; *Proc. Natl. Acad. Sci. U.S.A.* **1966**, *55*, 1201. (b) Morgan, A.R., Wells, R.D. *J. Mol. Biol.* **1968**, *37*, 63. (c) Lee, J.S.; Johnson, D.A.; Moran, A.R. *Nucleic Acids Res.* **1979**, *6*, 30731. (d) Meervelt, L.V.; Vlieghe, D.; Dautant, A.; Gallois, B; Précigoux, G.; Kennard, O. *Nature* **1995**, *374*, 742.

[13] Hoogsteen, K. *Acta Crystallogr.* **1963**, *16*, 907-916.

[14] (a) Cooney, M.; Czernuszewicz, G.; Postel, E.H.; Flint, S.J.; Hogan, M.E. *Science* **1988**, *241*, 456. (b) Beal, P.A.; Dervan, P.B. *Science* **1991**, *251*, 1360. (c) Durland, R. H.; Kessler, D. J.; Gunnell, S.; Duvic, M.; Pettit, B. M.; Hogan, M. E.; *Biochemistry* **1991**, *30*, 9246. (d) Chen, F.-M. *Biochemistry* **1991**, *30*, 4472. (e) Pilch, D.S.; Levenson, C. & Shafer, R.H. *Biochemistry* **1991**, *30*, 6081.

[15] Jiang, S.-P.; Jernigan, R.L.; Ting, K.-L.; Syi, J.-L.; Raghunathan, G. *J. Biomol. Str. & Dyn.* **1994**, *12*, 383.

[16] Escudé, C.; François, J.-C.; Sun, J.; Ott, G.; Sprinzl, M.; Garestier, T.; Hélène, C. *Nucleic Acids Res.* **1993**, *21*, 5547.

[17] Pilch, D.; Levenson, C.; Shafer, R.; *Proc. Natl. Acad. Sci. USA* **1990**, *87*, 1942.

[18] (a) Fox, K.R. *Nucleic Acids Res.* **1994**, 22, 2016. (b) Cassidy, S.A.; Strekowski, L.; Wilson, W.D.; Fox, K.R. *Biochemistry* **1994**, *33*, 15338. (c) Washbrook, E.; Fox, K.R. *Nucleic Acids Res.* **1994**, *19*, 3977. (d) Chandler, S.P.; Strekowski, L.; Wilson, W.D.; Fox, K.R. *Biochemistry* **1995**, *34*, 7234.

[19] (a) Clarenc, J.-P., Lebleu, B.; Leonetti, J.-P. *Nucleosides & Nucleotides* **1994**, *13*, 799. (b) Durland, R.H.; Rao, T.S.; Jayaraman, K.; Revankar, G.R. *Bioconjugate Chem.* **1995**, *6*, 278.

[20] (a) Milligan, J.F.; Krawczyk, S.H.; Wadwani, S.; Matteucci, M.D. *Nucleic Acids Res.* **1993**, *21*, 327. (b) Cheng, A.-J.; Van Dyke, M.W. *Nucleic Acids Res.* **1993**, *21*, 5630. (c) Musso, M.; Van Dyke, M.W. *Nucleic Acids Res.* **1995**, *23*, 2320.

[21] (a) Tener, G.M. *J. Am. Chem. Soc.*, **1961**, *83*, 159. (b) Letsinger, R.L.; Finnan, J.L.; Heavner, G.A.; Lunsford, W.B. *J. Amer. Chem. Soc.*, **1975**, *97*, 3278.

[22] Ralph, R.K.; Khorana, H.G. *J. Am. Chem. Soc.*, **1961**, *83*, 2926.

[23] Smith, M.; Rammler, D.H.; Goldberg, I.H.; Khorana, H.G. *J. Am. Chem. Soc.*, **1962**, *84*, 430.

[24] Corey, E.J.; Venkateswarlu, *J. Am. Chem. Soc.*, **1972**, *94*, 6190.

[25] (a) Ogilvie, K.K.; Sadana, K.L.; Thompson, E.A.; Quilliam, M.A.; Westmore, J.B. *Tetrahedron Lett.*, **1974**, *33*, 2861. (b) Ogilvie, K.K.; Beaucage, S.L.; Schifman, A.L.; Theriault, N.Y. Sadana, K.L. *Can. J. Chem.*, **1978**, *56*, 2768. (c) Ogilvie, K.K.; Theriault, N.Y. *Can. J. Chem.*, **1979**, *57*, 3140. (d) Ogilvie, K.K.; Theriault, N.Y.; Seifert, J.M.; Pon, R.T.; Nemer, M.J. *Can. J. Chem.*, **1980**, *58*, 2686. (e) Hakimelahi, G.H.; Proba, Z.A.; Ogilvie, K.K.; Entwistle, D.W. *Carbohydrate Res.*, **1981**, *89*, 203. (f) Ogilvie, K.K. *Can. J. Chem.*, **1982**, *60*, 1106.

[26] Beaucage, S.L.; Caruthers, M.H. *Tetrahedron Lett.*, **1981**, *22*, 1859.

[27] (a) Letsinger, R.L.; Hamilton, S.B. *J. Amer. Chem. Soc.* **1959**, *81*, 3009. (b) Lestinger, R.L.; Finnan, J.L.; Heavner, G.A.; Lunsford, W.B. *J. Am. Chem. Soc.* **1975**, *97*, 3278.

[28] *BioWorld Today - The Daily Biotechnology Newspaper*, February 22, 1996, pp.4.

[29] For a review see: Stull, R.A.; Szoka, Jr.; F.C. *Pharmaceutical Res.*, **1995**, *12*, 465.

[30] For reviews see: (a) Pyle, A.M.; *Science*, **1993**, *261*, 709. Ahsen, U.V.; (b) Schroeder, R.; *BioEssays*, **1993**, *15*, 299. (c) Symons, R.H.; *Current Biology*, **1994**, *4*, 322. (d) Breaker, R.R.; Joyce, G.F.; *TIBTECH*, **1994**, *12*, 268. (e) Burgstaller, P.; Famulok, M. *Angew. Chem. Int. Ed. Engl.*, **1995**, *34*, 1189.

[31] For reviews and articles of a general interest see see: (a) Werner, R.G. *Meth. Find. Exp. Clin. Pharmacol.*, **1994**, *16*, 525. (b) The Economist, April 9th 1994, 89. (c) Marshall, E. *Science*, **1995**, *269*, 1050.

[32] For an update on the Human Genome Project see: Bearsley, T. *Scientific American*, **March 1996**, 100.

[33] Zamecnik, P.C.; Stephenson, M.L. *Proc. Natl. Acad. Sci. U.S.A.*, **1978**, *75*, 280.

[34] Matsukura, M.; Shinozuka, K.; Zon, G.; Mitsuya, H.; Reitz, M.; Cohen, J.S.; Broder, S. *Proc. Natl. Acad. Sci. U.S.A.*, **1987**, *84*, 7706.

[35] Miller, P.S.; Yano, J.; Yano, E.; Carroll, C.; Jayaraman, K.; Ts'o, P.O.P. *Biochemistry*, **1979**, *18*, 5134.

[36] Letsinger, R.L.; Singman, C.N.; Histand, G.; Salunkhe, M. *J. Am. Chem. Soc.*, **1988**, *110*, 4470.

[37] For a recent review of the problems of antisense therapy see: Stein, C.A.; Krieg, A.M. *Antisense Research & Development*, **1994**, *4*, 67.

[38] Gura, T. *Science*, **1995**, *270*, 575.

[39] Letsinger, R.L.; Zhang, G.; Sun, D.K.; Ikeuchi, T.; Sarin, P.S.; *Proc. Natl. Acad. Sci. USA*, **1989**, *86*, 6553.

[40] Juliano, R.L.; Akhtar, S., *Antisense Res. Dev.*, **1992**, *2*, 165.

[41] For a recent review of gene transfer using synthetic amphiphiles see: Behr, J.P.; *Bioconjugate Chem.*, **1994**, *5*, 382.

[42] Godard, G.; Boutorine, A.S.; Saison-Behmoaras, E.; Hélène, C. *Eur. J. Biochem.*, **1995**, *232*, 404.

[43] For reviews see: (a) Cohen, J.S. *Pharmac. Ther.*, **1991**, *52*, 211. (b) Agrawal, S., *In Prospects for Antisense Nucleic Acid Therapy of Cancer and AIDS*, Wiley-Liss, Inc., 1991, pp. 143. (c) Agrawal, S. *TIBTech*, **1992**, *10*, 312. (d) Tonkinson, J.L.; Stein, C.A. *Antiviral Chem. & Chemotherapy*, **1993**, *4*, 193. (e) Wright, J.A.; Anazodo, M. *The Cancer Journal*, **1995**, *8*, 185.

[44] Sharma, O.K.; Goswami, B.B. *Proc. Natl. Acad. Sci. USA*, **1981**, *78*, 2221.

[45] (a)Torrence, P.F.; Maitra, R.K.; Lesiak, K.; Khamnei, S.; Zhou, A.; Silverman, R.H. *Proc. Natl. Acad. Sci. USA*, **1993**, *90*, 1300. (b) Maitra, R.K.; Li, G.; Xiao, W.; Dong, B.; Torrence, P.F.; Silverman, R.H. *J. Biol. Chem.*, **1995**, *270*, 15071.

[46] For reviews of Dervan's Triple-Helix Work see: (a) Maher III, L.M.; Wold, B.; Dervan, P.B. *Antisense Research and Development*, **1991**, *1*, 277. (b)) Maher III, L.M.; Wold, B.; Dervan, P.B. *Prospects for Antisense Nucleic Acid Therapy of Cancer and AIDs*, **1991**, 227.

[47] For reviews of Hélène's Triple-Helix Work see: Hélène, C. *Biochim. Biophys. Acta*, **1990**, *1049*, 99. Hélène, C. *Anti-Cancer Drug Design*, **1991**, *6*, 569. Thoung, N.T.; Hélène, C. *Angew. Chem. Int. Ed Engl.*, 1993, *32*, 666.

[48] Postel, E.H.; Flint, S.J.; Kessler, D.J.; Hogan, M.E. *Proc. Natl. Acad. Sci. U.S.A.*, **1991**, *88*, 8227.

[49] Griffin, L.C.; Kiessling, L.L.; Beal, P.A.; Gillespie, P.; Dervan, P.B. *J. Am. Chem. Soc.*, **1992**, *114*, 7976.

[50] Hunziker, J.; Priestley, S.; Brunar, H.; Dervan, P.B. *J. Am. Chem. Soc.*, **1995**, *117*, 2661.

[51] Wang, G.; Seidman, M.M.; Glazer, P.M. *Science*, **1996**, *271*, 802.

[52] Spence, J.H. In *The Physics and Chemistry of DNA and RNA No.9*, W.B. Saunders and Co., Toronto, 1972, 128-129.

[53] (a) Rich, A.; Tinoco, I. Jr. *J. Am. Chem. Soc.*, **1960**, *82*, 6409. (b) Weissbluth, M. *Quaterly Rev. Biophys.*, **1971**, *1*, 1.

[54] Harada, N.; Nakanishi, K. In *Circular Dichroic Spectroscopy: Exciton Coupling in Organic Stereochemistry*, University Science Books, New York, New York, 1983, 1-31.

[55] Steely, J.R., H.T.; Gray, D.M.; Ratliff, R.L. *Nucleic Acids. Res.*, **1986**, *14*, 10071.

[56] Cantor, C.R.; Warshaw, M.M. *Biopolymers*, **1970**, *9*, 1059.

[57] Skoog, D.A.; West, D.M.; In *Principles of Instrument Analysis*, Saunders College, Philadelphia, 1980, 280.

[58] (a) Hudson, R.H.E.; Damha, M.J.; *J. Am. Chem. Soc.*, **1993**, *115*, 2119. (b) Damha, M.J., Ganeshan, K., Hudson, R.H.E.; Zabarylo, S.V. *Nucleic Acids Res.* **1992**, *20*, 6565. (c) Damha, M.J.; Zabarylo, S.V. *Tetrahedron Lett.* **1989**, *46*, 6295. (d) Damha, M.J.; Ogilvie, K.K. *Biochemistry* **1988**, *27*, 6403. (e) Damha, M.J.; Ogilvie, K.K. *J. Org. Chem.* **1988**, *53*, 3710. (f) Damha, M.J.; Pon, R.T.; Ogilvie, K.K. *Tetrahedron Lett.* **1985**, *26*, 4839.

[59] (a) Hudson, R.H.E.; Damha, M.J. *Nucleic Acids Res. Symp. Ser.* **1993**, *29*, 97. (b) Hudson, R.H.E.; Ganeshan, K.; Damha, M.J. *In Carbohydrate Modifications in Antisense Research*; Sanghvi, Y.S.; Cook, P.D., Eds.: ACS Symposium Series, 1994, Vol. 580, pp. 133.

[60] (a) Azhayeva, E; Azhayev, A.; Guzaev, A.; Hovinen J.; Lonnberg, H. *Nucleic Acids Res.* **1995**, *23*, 1170. (b) Wengel, J. *Bioorg. Med. Chem. Lett.* **1995**, *8*, 791.

[61] Hudson, R.H.E. *University of Toronto Ph.D. Thesis*, **1995**.

[62] (a) Piunno, P.A.E.; Krull, U.J.; Hudson, R.H.E.; Damha, M.J.; Cohen, H. *Analytica Chimica Acta*, **1994**, *288*, 205. (b) Piunno, P.A.E.; Krull, U.J.; Hudson, R.H.E.; Damha, M.J.; Cohen, H. *Anal. Chem.*, **1995**, *67*, 2635.

[63] Sund, C.; Agback, P.; Koole, L.H.; Sandstrom, A.; Chattopadhyaya, J. *Tetrahedron* **1992**, *48*, 695.

[64] (a) Kondo, N.S.; Holmes, H.M.; Stempel, L.M.; Ts'o, P.O.P. *Biochemistry* **1970**, *9*, 3479. (b) Doornbos, J.; Den Hartog, J.A.J.; van Boom, J.H.; Altona, C. *Eur. J. Biochem.* **1981**, *116*, 403.

[65] Job, P. *Ann. Chim. (Paris)* **1928**, *9*, 113.

[66] Riley, M.; Maling, B.; Chamberlin, M.J. *J. Mol. Biol.* **1966**, *20*, 359.

[67] Blake, R.D.; Massoulie. J.; Fresco, J.R. *J. Mol. Biol.* **1967**, *30*, 291.

[68] Pilch, D.S.; Brousseau, R.; Shafer, R.H. *Nucleic Acids Res.* **1990**, *18*, 5743.

[69] Durland, M.; Peloille, N.T.; Thuong, N.T.; Maurizot, J.C. *Biochemistry* **1992**, *31*, 9197.

[70] Fossella, J.A.; Kim, Y.J.; Shih, H.; Richards, E.G.; Fresco, J.R. *Nucleic Acids Res.* **1993**, *21*, 4511.

[71] Rumney, S.; Kool, E.T. *J. Am. Chem. Soc.* **1995**, *117*, 5635.

[72] (a) Craig, M.E.; Crothers, D.M.; Doty, P. *J. Mol. Biol.* **1971**, *62*, 383. (b) Rougée, M; Fauçon, B.; Mergny, J.L.; Barcelo, F.; Giovannangeli, C.; Garestier, T.; Hélène, C. *Biochemistry* **1992**, *31*, 9269.

[73] Uddin, A.H.; Roman, M.A.; Anderson, J.R.; Damha, M.J., *J. Chem. Soc. Chem. Commun.*, **1996**, 171.

[74] Xodo, L.; Alunni-Fabbroni, M.; Manzini, G.; Quadrifoglio, F. *Nucleic Acids Res.* **1994**, *22*, 3322.

[75] Alberts, B. *In Molecular Biology of the Cell*, Garland, New York, 1989, pp.304.

[76] Leijon, M.; Graslund, A. *Nucleic Acids Res.* **1992**, *20*, 5339.

[77] (a) Strobel, S.A.; Dervan, P.B. *J. Am. Chem. Soc.* **1989**, *111*, 6956. (b) Colocci, N.; Distefano; M.D.; Dervan, P.B. *J. Am. Chem. Soc.* **1993**, *115*, 4468. (c) Colocci, N.; Dervan, P.B. *J. Am. Chem. Soc.*, **1995**, *117*, 4781.

[78] Naylor, R.; Gilham, P.T. *Biochemistry* **1966**, *5*, 2722.

[79] Noll, D.M.; O'Rear, J.L.; Cushman, C.D.; Miller, P.S. *Nucleosides & Nucleotides* **1994**, *13*, 997.

[80] (a) Horne, D.A.; Dervan, P.B. *J. Am. Chem. Soc.* **1990**, *112*, 2435. (b) Jayasena, S.D.; Johnston, B.H. *Nucl. Acids Res.* **1992**, *20*, 5279.

[81] François, J.C.; Hélène, C. *Biochemistry*, **1995**, *34*, 65.

[82] Long, E.C.; Barton, J.K. *Acc. Chem. Res.* **1990**, *23*, 273.

[83] Fox, K.R.; Polucci, P.; Jenkins, T.C.; Neidle, S. *Proc. Natl. Acad. Sci. USA*, **1995**, *92*, 7887.

[84] Escudé, C.; Mohammadi, S.; Sun, J.S.; Nguyen, C.H.; Bisagni, E.; Liquier, J.; Taillandier, E.; Garestier, T.; Hélène, C. *Chemistry and Biology*, *1996*, *3*, 57.

[85] (a) Mergny, J.L.; Duval-Valentin, G.; Nguyen, C.H.; Perrouault, L.; Faucon, B.; Rougée, M.; Montenay-Garestier, T.; Bisagni, E.; Hélène, C. *Science* **1992**, *256*, 1681. (b) Pilch, D.S.; Waring, M.J.; Sun, J.S.; Rougee, M.; Nguyen, C.H.; Bisagni, E.; Garestier, T.; Helene, C. *J. Mol. Biol.* **1993**, *232*, 926. (c) Pilch, D.S.; Martin, M.T.; Nguyen, C.H.; Sun, J.S.; Bisagni, E.; Garestier, T.; Hélène, C. *J. Am. Chem. Soc.* **1993**, *115*, 9942. (d) Duval-Valentin; G.; de Bizemont, T.; Takasugi, M.; Mergny, J.L., Bisagni, E.; Hélène, C. *J. Mol. Biol.* **1995**, *247*, 847.

[86] Bizemont, T.; Duval-Valentin, G.; Sun, J.S.; Bisagni, E.; Garestier, T.; Hélène, C. *Nucleic Acids Res.*, **1996**, *24*, 1136.

[87] (a) Scaria, P.V.; Shafer, R.H. *J. Biol. Chem.* **1991**, *266*, 5417. (b) Ye, F.; Chun-Li, B.; Zhang, P.C.; Cao, E.H.; He, Y.J.; Tang, Y.Q. *Science In China (Series B)* **1994**, *37*, 1306.

[88] (a) Mergny, J.L.; Collier, D.; Rougée, M.; Montenaaay-Garestier, T.; Hélène, C. *Nucl. Acids Res.* **1991**, *19*, 1521. (b) Sun, J.S.; Lavery, R.; Chomilier, J.; Zakrzewska, K.; Montenay-Garestier, T.; Hélène, C. *J. Biomol. Struct. Dynam.* **1991**, *9*, 425.

[89] Krugh, T.R. *Curr. Opin. Struct. Biol.* **1994**, *4*, 351.

[90] Durland, M.; Thuong, N.T., Maurizot, J.C. *Biochimie* **1994**, *76*, 181.

[91] (a) Breslauer, K.J.; Park, Y.W. *Proc. Natl. Acad. Sci. USA* **1992**, 89, 6653. (b) Durand, M.; Thoung, N.T.; Maurizot, J.C. *J. Biol. Chem.* **1992**, *267*, 25394. (c) Chalikian, T.V.; Plum, G.E.; Sarvazyan, A.P.; Breslauer, K.J. *Biochemistry* **1994**, *33*, 8629. (d) Rentzeperis, D.; Marky, L.A. *J. Am. Chem. Soc.* **1995**, *117*, 5423.

[92] Pilch, D.S.; Breslauer, K.J. *Proc. Natl. Acad. Sci. USA* **1994**, *91*, 9332.

[93] (a) Washbrook, E.; Fox, K.R. *Nucleic Acids Res.*, **1994**, *22*, 3977. (b) Howard, F.B.; Miles, H.T.; Ross, P.D. *Biochemistry*, **1995**, *34*, 7135.

[94] Lim, C.S. *BioTechniques*, **1994**, *17*, 626.

[95] (a) Moser, H.E.; Dervan, P.B. *Science*, **1987**, 238, 645. (b) Strobel, S.A.; Doucettestamm, L.A.; Riba, L.; Housman, D.E.; Dervan, P.B. *Science*, **1991**, *254*, 1639.

[96] (a) Durland, R.H.; Kessler, D.J., Gunnel, S., Duvic, M.; Pettit, B.M.; Hogan, M.E.; *Biochem.*, **1991**, *30*, 9246. (b) Maher, L.J.; Dervan, P.B.; Wold, B.; *Biochemistry*, **1992**, *31*, 70. (c) Maher, L.J. *BioEssays*, **1992**, 14, 807.(d) Maher, L.J. *Biochemistry*, **1992**, 31, 7587. (e) Duvalvalentin, G.; Thoung, N.T.; Hélène, C. *Proc. Nat. Acad. Sci. USA*, **1992**, 89, 504. (f) Lu, G.; Ferl, R.J. *Int. J. Biochem.*, **1993**, *25*, 1529.

[97] For a recent review see: Stull, R.A.; Szoka, Jr., F.C.; *Pharmceutical Research*, **1995**, **12**, 465.

[98] (a) Ito, T., Smith, C.L.; Cantor, C.R. *Proc. Natl. Acad. Sci. U.S.A.*, **1992**, *89*, 495. (b) Ito, T., Smith, C.L.; Cantor, C.R. *Nucleic Acids Res.* **1992**, *20*, 3524.

[99] (a) Pilch, D.S.; Levenson, C.; Shafer, R.H. *Proc. Natl. Acad. Sci. USA*, **1990**, *87*, 1942. (b) Radhakrishnan, I.; Patel, D.J.; Gao, X. *J. Mol. Biol., 1991, 221*, 1403. (c) Radhakrishnan, I.; de los Santos, C.; Patel, D.J., *J. Mol. Biol.*, **1993**, *234*, 188.

[100] (a) Geselowitx, D.A.; Neumann, R.D. *Bioconjugate Chem.*, **1995**, *6*, 502. (b) Bates, P.J., Dosanjh, H.S.; Kumar, S.; Jenkins, T.C.; Laughton, C.A.; Neidle, S. *Nucleic Acids Res.*, **1995**, 23, 3627.

[101] Bauer, G.J.; McCaskill, J.S.; Otten, H. *Proc. Natl. Acad. Sci. USA*, **1989**, *86*, 7937.

[102] Waring, M.J. *Biochim. Biophys. Acta*, **1966**, *114*, 234.

[103] LePecq, J.B.; Paoletti, C. *J. Mol. Biol.*, **1967**, *27*, 87.

[104] Scaria, P.V.; Shafer, R.H. *J. Biol. Chem.*, **1991**, *266*, 5417.

[105] LePecq, J.B.; Paoletti, C. *C. R. Acad. Sc. Paris* **1965**, *260*, 7033.

[106] Mergny, J.L.; Collier, D.; Rougée, M.; Montenay-Garestier, T.; Hélène, C. *Nucleic Acids Res.*, **1991**, *19*, 1521.

[107] Sun, J.S.; Lavery, R.; Chomilier, J.; Zakrzewska, K.; Montenay-Garestier, T.; Hélène, C. *J. Biomol. Struct. Dynam.*, **1991**, *9*, 425.

[108] Salunkhe, M.; Wu, T.; Letsinger, R.L. *J. Am. Chem. Soc.*, **1992**, *114*, 8768.

[109] Fang, Y.; Bai, C.L.; Zhang, P.C.; Cao, E.H.; Tang, Y.Q. *Science In China (Ser. B)*, **1994**, *37*, 1306.

[110] Maskos, U.; Southern, E.M. *Nucleic Acids Res.*, **1992**, *20*, 1679.

[111] (a) Matteucci, M.D.; Caruthers, M.H. *Tetrahedron Lett.*, **1980**, *21*, 3243. (b) Cormier, J. *McGill University Ph.D. Thesis*, **1987**, 70.

[112] Hudson, R.H.E.; Uddin, A.H.; Damha, M.J. *J. Am. Chem. Soc.*, **1995**, *117*, 12470.

[113] (a) Craig, M.E.; Crothers, D.M.; Doty, P.J. *J. Mol. Biol.* **1971**, *62*, 383. (b) Rougée, M.; Fauçon, B.; Mergny, J.L.; Barcelo, F.; Giovannangeli, C.; Garesyier, T.; Hélène, C. Biochemistry, 1992, 31, 9269.

[114] Wagner, R.W. *Nature Medicine* **1995**, *1*, 1116.

[115] Thomas, D.; *Bio/Technology*, **1995**, *13*, 439.

[116] (a) Rumney IV, S.; Kool, E.T. *Angew. Chem. Int. Ed. Engl.* **1992**, *21*, 1617. (b) Prakash, G.; Kool, E.T. *J. Am. Chem. Soc.* **1992**, *114*, 3523. (c) Rubin, E.; McKee, T.L.; Kool, E.T.; *J. Am. Chem. Soc.* **1993**, *115*, 360. (d) Wang, S.; Kool, E.T. *Nucleic Acids Res.*, **1994**, *22*, 2326. (e) D'Souza, D.J.; Kool, E.T. *Bioorganic & Medicinal Chemistry Letters*, **1994**, *4*, 965. (f) Gao, H.; Yang, M.; Patel, R.; Cook, A.F. *Nucleic Acids Res.*, **1995**, *23*, 2025.

[117] (a) Chen, G.; Seeman, N.C. *Nature*, **1991**, *350*, 631. (b) Zhang, Y.; Seeman, N.C. *J. Am. Chem. Soc.*, **1994**, *116*, 1661. (c) Hoffman, R. *American Scientist*, **1994**, *82*, 308.

[118] (a) Ray, R.A.; Cooper, P.J.; Wakefield, A.J. *Bio/Technology*, **1995**, *13*, 445. (b) McGown, L.B.; Joseph, M.J.; Pitner, J.B.; Vonk, G.P.; Linn, C.P. *Anal. Chem.*, **1995**, November 1, 663A.

[119] Musso, M.; Van Dyke, M.W. *Nucleic Acids Res.* **1995**, *23*, 2320.

[120] Lown, J.W. *ChemTracts - Organic Chemistry*, **1993**, *6*, 205.

[121] (a) Duval-Valentin, G.; Bizemont, T.; Takasugi, M.; Mergny, J.; Bisagni, E.; Helene, C. *J. Mol. Biol.*, **1995**, *247*, 847. (b) Cassidy, S.A.; Strekowski, L.; Wilson, W.D.; Fox, K.R. *Biochemistry*, **1994**, *33*, 15338.

[122] Letsinger, R.L.; Wu, T. *J. Am. Chem. Soc.* **1995**, *117*, 7323. (b) Hunziker, J.; Priestly, S.; Brunar, H.; Dervan, P.B. *J. Am. Chem. Soc.* **1995**, *117*, 2661.

[123] (a) Ma, M.Y.-X.; McCallum, K.; Climie, S.C.; Kuperman, R.; Lin, W.C.; Sumner-Smith, M.; Barnett, R.W. *Nucleic Acids Res.*, **1993**, *21*, 2568; (b) Ma, M.Y.-X.; Reid, L.S.; Climie, S.C.; Lin, W.C.; Kuperman, R.; Sumner-Smith, M.; Barnett, R.W. *Biochemistry*, **1993**, *32*, 1751; (c) Gao, H.; Chidambaram, N.; Chen, B.C.; Pelham, D.E.; Patel, R.; Yang, M.; Zhou, L.; Cook, A.; Cohen, J.S. *Bioconjugate Chemistry*, **1994**, *5*, 445; (d) Gao, H.; Yang, M.; Cook, A.F.; *Nucleic Acids Res.*, **1995**, *23*, 285.

[124] Urdea, M.S. *BIO/TECHNOLOGY*, **1994**, *12*, 926.

[125] (a) Dolinnaya, N.; Gryaznov, S.; Ahle, D.; Chang, C.A.; Shabarova, Z.A.; Urdea, M.S.; Horn, T. *Bioorganic & Medicinal Chemistry Letters*, **1994**, *4*, 1011. (b) Sproat, B.S.; Beijer, B.; Grotli, M.; Ryder, U.; Morand, K.L.; Lamond, A.I. *J. Chem. Soc. Perkin Trans.*, **1994**, 422. (c) Brandenburg, G.; Petersen, G.V.; Rasmussen, K.; Wengel, J. *Bioorganic & Medicinal Chemistry Letters*, **1995**, *5*, 791. (d) Grotli, M.; Sproat, B.S.; *J. Chem. Soc., Chem. Commun.*, **1995**, 495.

[126] Roman, M.A. *McGill University Master's Thesis*, 1995.

[127] Ogilvie, K.K., Nemer, M.J.; Hakimelahi, G.H.; Proba, Z.A.; Lucas, M. *Tet. Lett.*, **1982**, *23*, 2615.

[128] Manoharan, M., Johnson, L.K., Tivel, K.L., Springer, R.H., Cook, P.D. *Bioorg. Med. Chem. Lett.*, **1993**, *3*, 2765.

[129] Jung, K.E.; Switzer, C. *J. Am. Chem. Soc.*, **1994**, *116*, 6059.

[130] (a) Dougherty, J.P.; Rizzo, C.J.; Breslow, R. *J. Am. Chem. Soc.*, **1992**, *114*, 6254. (b) Hasimoto, S.; Switzer, C. *J. Am. Chem. Soc.*, **1992**, *114*, 6255.

[131] Jin, R.; Chapman, W.H. Jr.; Srinivasan, A.R.; Olson, W.K.; Breslow, R.; Breslauer, K.J. *Proc. Natl. Acad. Sci. USA.*, **1993**, *90*, 10568.

[132] (a) Giannaris, P.A.; Damha, M.J. In Herron, W.; Miller, A.C.; McFarland, J (eds), Proceedings of Tenth Annual Graduate Students Symposium. pp.23-31; (b) Kierzek, R.; He, L.; Turner, D.H. *Nucleic Acids Res.*, **1992**, *20*, 1685.

[133] Seki, J.; Kuroda, K.; Ozaki, H.; Sawai, H. *Nucleic Acids Symposium Series*, **1993**, *29*, 71.

[134] Giannaris, P.A.; Damha, M.J.; *Nucleic Acids Res.*, **1993**, *21*, 4742.

[135] (a) Pudlo, J.S.; Cao, X.; Swaminathan, S.; Matteucci, M.D. *Tetrahedron Lett.*, **1994**, *35*, 9315. (b) Matteucci, M.D.; Cao, X. *U.S. Patent 5,4324, 257*, **July 18, 1995**.

[136] Zou, R.; Matteucci, M.D. *Tetrahedron Lett.*, **1996**, *37*, 941.

[137] (a) Lamond, A.I.; Sproat, B.; Ryder, U.; Hamm, J. *Cell*, **1989**, *58*, 383. (b) Lamond, A.I.; Barabino, S.; Blencowe, B.J.; Sproat, B.; Ryder, U. *Molecular Biology Reports*, **1990**, *14*, 201. (c) Cotten, M.; Oberhauser, B.; Brunar, H.; Holzner, A.; Issakides, G.; Noe, C.R.; Schaffner, G.; Wagner, E.; Birnstiel, M.L. *Nucleic Acids Res.*, **1991**, *19*, 2629. Monia, B.P.; Lesnik, E.A.; Gonzalez, C.; Lima, W.F.; McGee, D.; Gionosso, C.J.; Kawasaki, A.M.; Cook, P.D.; Freier, S.M. *J. Biol. Chem.*, **1993**, *268*, 14514. (d) Lamond, A.I.; Sproat, B.S. *FEBS Lett.*, **1993**, *325*, 123. (e) Johansson, H.E.; Belsham, G.J.; Sproat, B.S.; Hentze, M.W. *Nucleic Acids Res.*, **1994**, *22*, 4591. (e) Boiziau, C.; Larrouy, B.; Sproat, B.S.; Toulmé, J.J. *Nucleic Acids Res.*, **1995**, *23*, 64. (f) Larrouy, B.; Boiziau, C.; Sproat, B.; Toulmé, J.J. *Nucleic Acids Res.*, **1995**, *23*, 3434.

[138] (a) Inoue, H.; Hayase, Y.; Asaka, M.; Imura, A.; Iwai, S.; Miura, K.; Ohtsuka, E. *Nucleic Acids Symp. Ser.*, **1985**, *16*, 165. (b) Inoue, H.; Hayase, Y.; Iwai, S.; Ohtsuka, E. *FEBS Lett.*, **1987**, *215*, 327. (c) Inoue, H.; Hayase, Y.; Iwai, S.; Ohtsuka, E. *Nucleic Acids Symp. Ser.*, **1988**, *19*, 135. (d) Sproat, B.S.; Lamond, A.I.; Garcia, G.; Beijer, B.; Pieles, U.; Douglas, M.; Bohman, K.; Carmo-Foseco, M.; Weston, S.; O'Loughlin, S. *Nucleic Acids Symp. Ser.*, **1991**, *24*, 59.

[139] (a) Inoue, H.; Hayase, Y.; Imura, A.; Iwai, S.; Miura, K.; Ohtsuka, E. *Nucleic Acids Res.*, **1987**, *15*, 6131. (b) Sproat, B.S.; Lamond, A.I.; Beijer, B.; Neuner, P. Ryder, U. *Nucleic Acids Res.*, **1989**, *17*, 3373.

[140] (a) Lesnik, E.A.; Guinosso, C.J.; Kawasaki, A.M.; Sasmor, H.; Zounes, M.; Cummins, L.L.; Ecker, D.J.; Cook, P.D.; Freier, S.M. *Biochem.*, **1993**, *32*, 7832. (b) Damha, M.J.; Meng, B.; Wang, D.; Yannopoulos, C.G.; Just, G. *Nucleic Acids Res.*, **1995**, *23*, 3967.

[141] Yano, J.; Jan, L.S.; Ts'o, P.O.P. *Biochim. Biophys. Acta*, **1980**, *629*, 178.

[142] Corey, E.J.; Yi, K.Y. *Tetrahedron Lett.*, **1992**, *33*, 2289.

[143] Damha, M.J. *McGill University Ph.D.Thesis.*, **1987**.

[144] Plavec, J.; Thibaudeau, C.; Chattopahyaya, J. *J. Am. Chem. Soc.*, **1994**, *116*, 6558.

[145] (a) Uesugi, S.; Miki, H.; Ikehara, M.; Iwahasi, H.; Kyogoku, Y. *Tetrahedron Lett.*, **1979**, *42*, 4073, (b) Ikehara, M. *Heterocycles*, **1984**, *21*, 75.

[146] Fujimori, S.; Shudo, K., Hashimoto, Y. *J. Am. Chem. Soc.*, **1990**, *112*, 7436.

[147] Asseline, U.; Hau, J.F.; Czernecki, S.; Le Diguarher, T.; Perlat, M.C.; Valery, J.M.; Thoung, N.T. *Nucleic Acids Res.*, **1991**, *19*, 4067.

[148] (a) Anderson, D.J.; Reischer, R.J.; Taylor, A.J.; Wechter, W.J. *Nucleosides & Nucleotides*, **1982**, *3*, 499. (b) Morvan, F.; Genu, C.; Rayner, B.; Gosselin, G.; Imbach, J.L. *Biochem. Biophys. Res. Com.*, **1990**, *172*, 537.

[149] Ashley, G.W. *J. Am. Chem. Soc.*, **1992**, *114*, 9731.

[150] Tazawa, I.; Tazawa, S.; Stempel, L.M.; Ts'o, P.O.P. *Biochemistry*, **1971**, *9*, 3499.
[151] Garbessi, A.; Capobianco, M.L.; Colonna, F.P.; Tondelli, L.; Arcamone, F.; Manzini, G.; Hilbers, C.W.; Aelen, J.M.E.; Blommers, M.J.J. *Nucleic Acids Res.*, **1993**, *21*, 4159.

[152] (a) Damha, M.J.; Giannaris, P.A.; Marfey, P.; Reid, L.S. *Tetrahedron Lett.*, **1991**, *32*, 2573. (b)Damha, M.J.; Giannaris, P.A.; Marfey, P. *Biochemistry*, **1994**, *33*, 7877.

[153] Arts, E.J.; Li, X.; Gu, Z.; Kleiman, L.; Parniak, M.A.; Wainberg, M.A. *J. Biol. Chem.*, **1994**, *269*, 14672.

[154] Mouscadet, J.F.; Carteau, S.; Goulaouic, H.; Subra, F.; Auclair, C. *J. Biol. Chem.*, **1994**, *269*, 21635.

[155] Peliska, J.A.; Balasubramanian, S.; Giedroc, D.P., Benkovic, S.J. *Biochemistry*, **1994**, *33*, 13817.

[156] Stryer, L. in *Biochemistry*, **1988**, W.H. Freeman and Co., New York, , pp.875.

[157] Flores-Rozas, H.; Hurwitz, J. *J. Biol. Chem.*, **1993**, *268*, 21372.

[158] Pon, R.T.; Usman, N.; Ogilvie, K.K. *BioTechniques* **1988**, *6*, 768.

[159] Sinha, N.D.; Biernat, J.; McManus, J.; Koster, H. *Nucleic Acids Res.* **1984**, *12*, 4539-4557.

[160] Damha, M.J.; Ogilvie, K.K. In *Methods in Molecular Biology, Vol. 20: Protocols for Oligol-nucleotides and Analogs*; Agrawal, S. Ed.: Humana Press, Inc.: Totowa, N.J., U.S.A. 1993, pp 81-114.

[161] Pon, R.T.; Usman, N.; Ogilvie, K.K. *BioTechniques*, **1988**, *6*, 768.

[162] (a) Van de Sande, J.H.; Ramsing, N.B.; Germann, M.W.; Elhorst, W.; Kalisch, B.W.; Kitzing, E.V.;; Pon, R.T.; Clegg, R.C.; Jovin, T.M. Science, 1988, 241, 551. (b) Sinha, N.D.; Davis, P.; Usman, N.; Perez, J.; Hodge, R.; Kremsky, J.; Casale, R. *Biochimie*, **1993**, *75*, 13.

[163] Ogilvie, K.K., Nemer, M.J.; Hakimelahi, G.H.; Proba, Z.A.; Lucas, M. *Tetrahedron Lett.*, 1982, **23**, 2615.

[164] McClinton, M.A.; *Aldrichimica Acta*, **1995**, *28*, 31.

[165] Grierson, D. In *Electrophoresis of Nucleic Acids, A Practical Approach* D. Rickwood and B.D. Hanes, Ed.'s; IRL press Ltd.: Oxford, England, 1982, p. 15.

[166] Puglisi, J.D.; Tinoco, Jr. I.; In *Methods in Enzymology*; Dahlberg; J.E.; Abelson, J.N., Eds.: Academic Press, Inc.: San Diego, U.S.A. 1989; Vol. 180, pp. 304.

[167] Kibler-Herzog, L.; Zon, G.; Whittierm, G.; Shaikh, M.; Wilson, W.D. *Anti-Cancer Drug Des.* **1993**, *8*, 65.

[168] Usman, N.; Ogilvie, K.K.; Jiang, M.Y.; Cedergren, R.J. *J. Am. Chem. Soc.* **1987**, *109*, 7845.

[169] Wu, T.; Ogilvie, K.K. J. *Org. Chem.*, **1990**, *55*, 4714.